

K⁺ Catalyzed Diels-Alder Reaction by Macrocyclic Bis(crown ether) Boronic Ester

Kosuke Ono, Morikazu Niibe and Nobuharu Iwasawa^{*,†}

Department of Chemistry, Tokyo Institute of Technology, O-okayama, Meguro-ku, Tokyo 152-8551, Japan

*e-mail: niwasawa@chem.titech.ac.jp

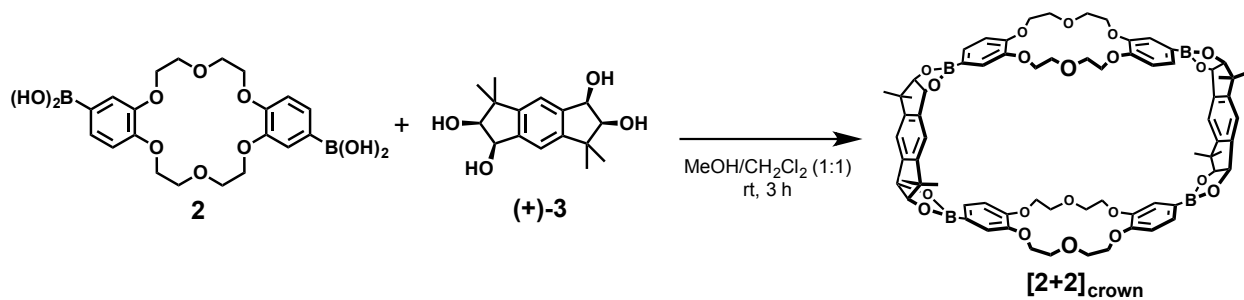
Table of Contents

1. General Methods	S2
2. Self-assembly of [2+2] _{crown}	S3
3. Complexation of [2+2] _{crown} with 1,4,9,10-Anthraquinone 1 in the Presence of 2 equiv. KOTf.....	S5
3-1. NMR Study of the Complexation of [2+2] _{crown} with 1 in the Presence of 2 equiv. of KOTf.....	S5
3-2. ITC Study of the Complexation of [2+2] _{crown} with 1 in the Presence of 2 equiv. of KOTf.....	S5
3-3. Control Experiments of the Complexation of [2+2] _{crown} with 1	S6
4. The Diels-Alder Reaction of 1 with Various Dienes	S8
4-1. The Diels-Alder Reaction of 1 with Anthracene 4 Under Various Conditions.....	S8
4-2-1. The Diels-Alder Reaction of 1 with 2-Mono and 2,3-Di-substituted 1,3-Butadienes.....	S15
4-2-2. The Enantioselective Diels-Alder Reaction of 1 with 2-Substituted 1,3-Butadienes.....	S41
4-3. The Diels-Alder Reaction of 1 with 1-Mono and 1,4-Di-substituted 1,3-Butadienes... ..	S43
5. Experimental Procedure and Characterization of New Compounds.....	S49
6. ¹ H and ¹³ C NMR Spectra of New Compounds.....	S53
7. X-ray Crystallographic Analysis of a Racemic Crystal of [2+2] _{crown}	S59
8. References.....	S62

1. General Methods

All operations were performed under air unless otherwise noted. ^1H and ^{13}C NMR spectra were recorded on a JEOL ECX-500, a Bruker DRX-500 (500 MHz for ^1H and 125 MHz for ^{13}C), or a JEOL ECX-400, a JEOL AL-400, a JEOL Lambda-400 (400 MHz for ^1H and 100 MHz for ^{13}C), or a JEOL AL-300 (300 MHz for ^1H and 75 MHz for ^{13}C) spectrometer using CDCl_3 [residual CHCl_3 (7.26 ppm) served as an internal standard in ^1H NMR and CDCl_3 (77.0 ppm) in ^{13}C NMR], dimethylsulfoxide (DMSO)- d_6 [residual DMSO (2.49 ppm) served as an internal standard in ^1H NMR and $\text{DMSO}-d_6$ (39.73 ppm) in ^{13}C NMR] as a solvent. Chemical shifts are expressed in parts per million (ppm). High- or low-resolution mass analyses (FAB^+) were performed on a JEOL JMS-700 mass spectrometer. High- or low-resolution mass analyses (FD^+) were performed on a JEOL T-GCV mass spectrometer. IR spectra were recorded on a JASCO FT/IR-460 plus spectrometer. Gel permeation chromatography (GPC) was performed using LC-9130NEXT series (Japan Analytical Industry Co., Ltd.). ITC (Isothermal Titration Calorimetry) experiments were performed on a Microcal iTC200 at 298 K. GPC (Gel Permeation Chromatography) experiments were performed on a JAIGEL-1H and JAIGEL-2H columns. The single crystal X-ray diffraction data were collected on a Rigaku R-Axis II with IP area detector system using $\text{CuK}\alpha$ radiation ($\alpha = 1.54186 \text{ \AA}$). Dehydrated dichloromethane, DMF, Et_2O , acetonitrile, toluene and benzene was purchased from Kanto Chemical Co., Inc. and all other solvents were distilled before using. Tetrahydrofuran (THF) was purified by solvent purification system of Glass-Contour. Other solvents were distilled according to the usual procedures and stored over molecular sieves. 1,4,9,10-Anthradiquinone **1**,^{S1} enantiopure tetrol (+)-**3** and (-)-**3**,^{S2} bis[2-(methylsulfonyl)oxyethyl]ether,^{S3} 2-substituted-1,3-butadiene (**7**, **9**, **10**, **12**)^{S4} were prepared according to the literature procedures.

2. Self-assembly of [2+2]_{crow}



The (+)-tetrol **(+)-3** (17.7 mg, 0.064 mmol) was added to a methanol/ CH₂Cl₂ (1:1) solution (3.6 mL) of **2** (30 mg, 0.067 mmol). The reaction mixture became homogeneous in a few minutes. After the mixture was stirred at room temperature for 24 hours, solvent was removed under reduced pressure. The residue was purified by GPC to afford the desired product **[2+2]_{crow}** (37 mg, 88 %).

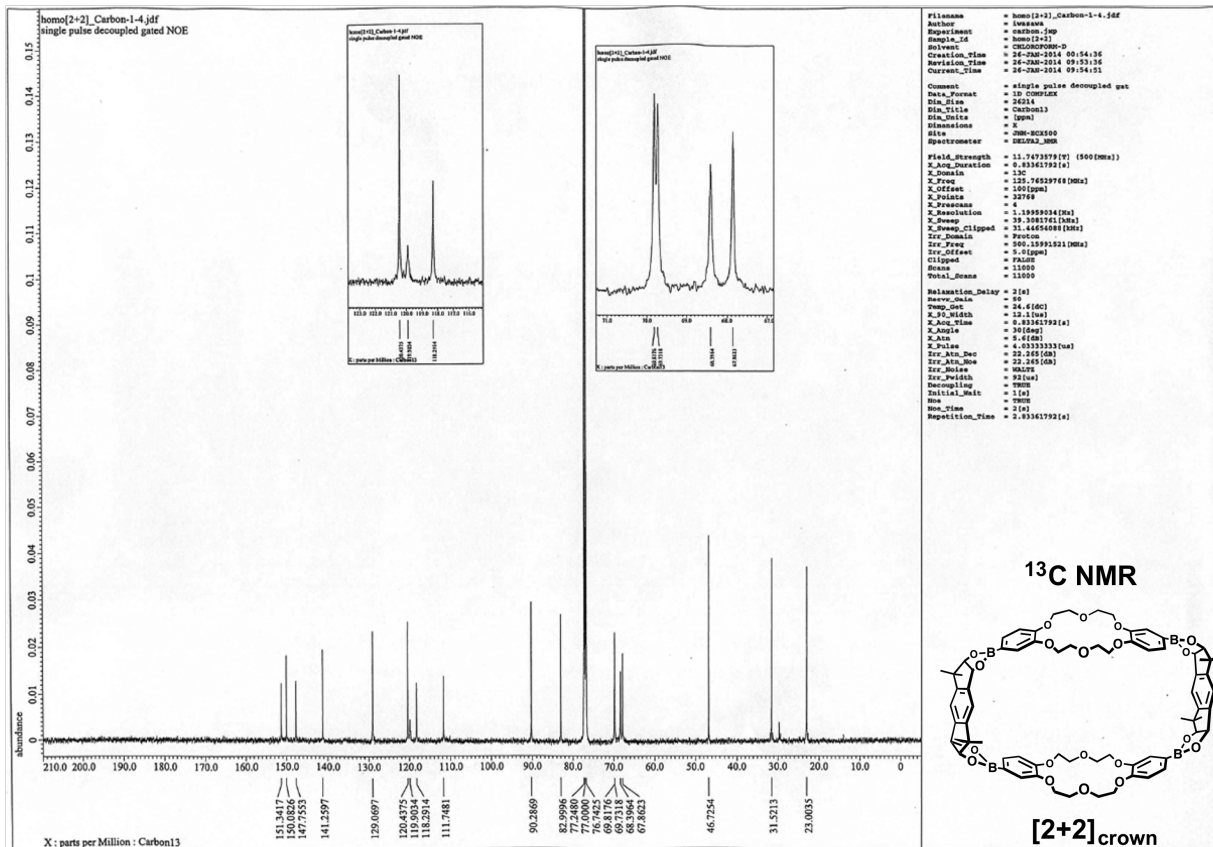
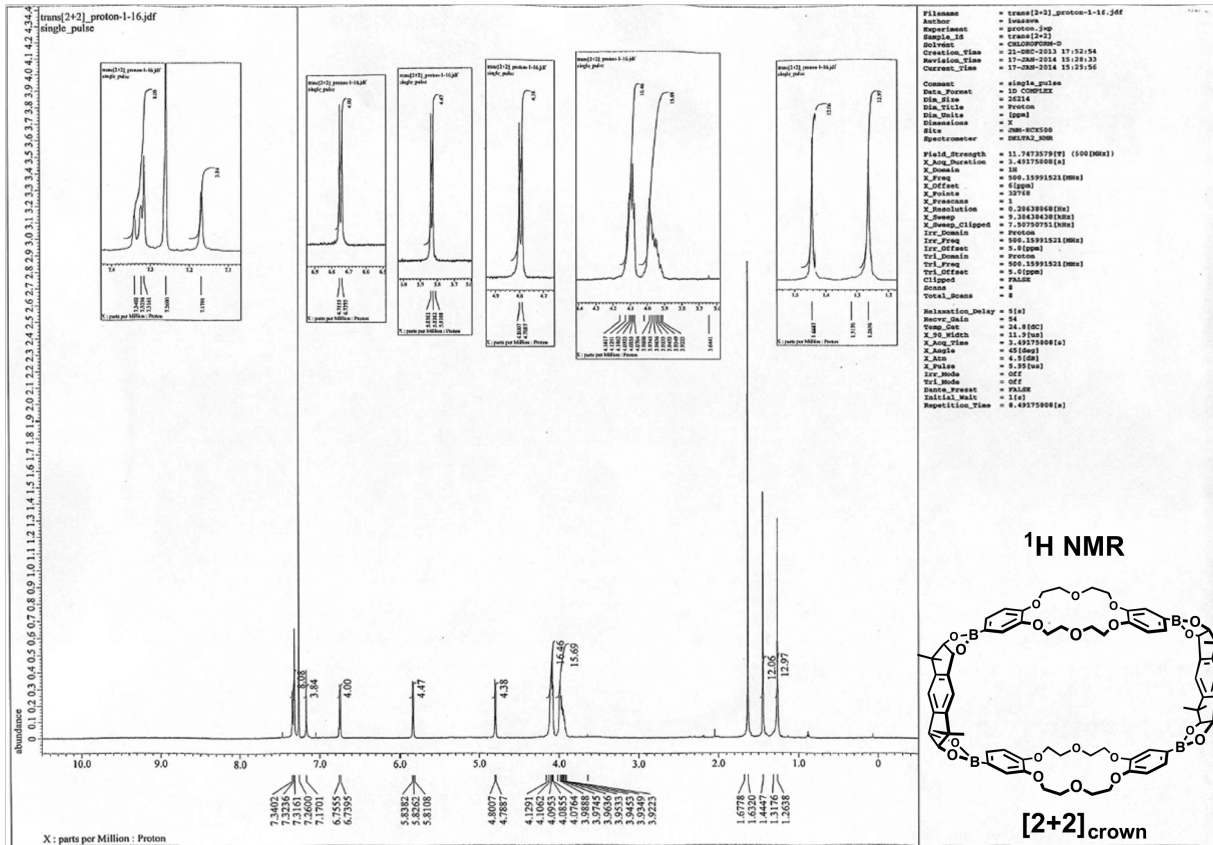
Physical data of **[2+2]_{crow}**

¹H NMR (500 MHz, CDCl₃): δ 7.34-7.32 (m, 8H), 7.17 (s, 4H), 6.75 (d, *J* = 8.8 Hz, 4H), 5.83 (d, *J* = 6.2 Hz, 4H), 4.80 (d, *J* = 6.2 Hz, 4H), 4.11 (br, 16H), 3.98 (br, 16H), 1.44 (s, 12H), 1.26 (s, 12H).

¹³C NMR (125 MHz, CDCl₃): δ 151.3, 150.1, 147.8, 141.3, 129.1, 120.4, 119.9, 118.3, 111.7, 90.3, 83.0, 69.8, 69.7, 68.4, 67.9, 46.7, 31.5, 23.0.

HRMS (FAB⁺, NBA): *m/z* Calcd. for C₇₂H₈₀O₂₀B₄K: 1346.5289., Found: 1346.5299 [M]⁺.

IR (ATR): 1601, 1518, 1419, 1356, 1310, 1260, 1213, 1142, 1093, 1055, 953 cm⁻¹.



3. Complexation of $[2+2]_{\text{crown}}$ with 1,4,9,10-Anthraquinone **1** in the Presence of 2equiv. KOTf

3-1. NMR Study of the Complexation of $[2+2]_{\text{crown}}$ with **1** in the Presence of 2 equiv. of KOTf

The binding behavior of $[2+2]_{\text{crown}}$ containing alkaline metal salts with 1,4,9,10-anthraquinone **1** was examined (Fig. S1a). When $[2+2]_{\text{crown}}$ (6.5 mM), 2 equivalents of KOTf (13.0 mM), and 1 equivalent of **1** (6.5 mM) were mixed in $\text{CDCl}_3/\text{CD}_3\text{CN}$ (0.8 mL, 1:1), a large up-field shift of protons of the guest molecule **1** was observed as shown in Fig. S1b,c. Almost the same degree of upfield shifts of *A*, *B* and *C* of **1** as shown in Fig. S1b,c was due to the shielding effect of the benzene ring of the host framework, suggesting that **1** was included just inside the host molecule with its π -face facing outside as shown in Fig. S1a. This speculation suggests that **1** included in this $[2+2]_{\text{crown}} \cdot 2\text{K}^+$ could react with appropriate substrates on its π -face, where the reaction might be accelerated by coordination of four carbonyl oxygens of **1** to two K^+ ions. By the addition of another 1 equivalent of **1** to the solution, the peaks derived from **1** in the host shifted downfield and came closer to the peaks of free guest **1** (Fig. S1d). This ^1H NMR study suggested 1:1 complexation of $[2+2]_{\text{crown}}$ with **1** in the presence of 2 equiv. K^+ .

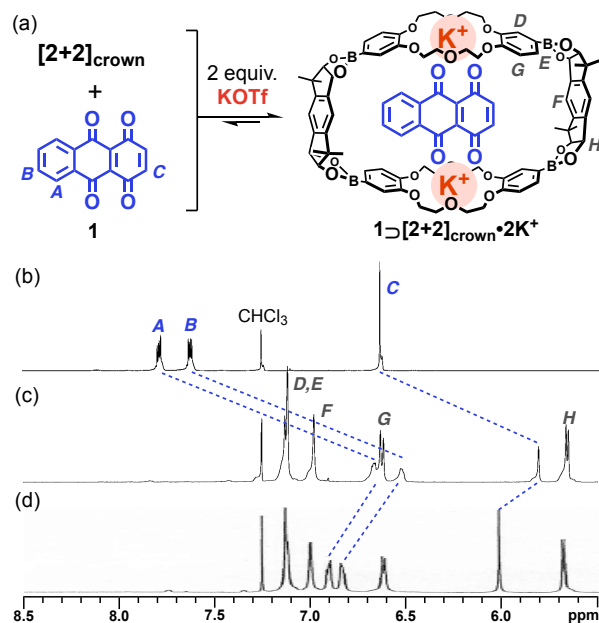


Fig. S1 (a) Complexation of $[2+2]_{\text{crown}}$ with diquinone **1** in the presence of K^+ . Partial ^1H NMR spectra (500 MHz, $\text{CDCl}_3/\text{CD}_3\text{CN}$ (1:1), 298 K) of (b) **1**, (c) a mixture of $[2+2]_{\text{crown}}$ (6.5 mM), **1** (6.5 mM), and KOTf (13mM), and (d) a mixture of $[2+2]_{\text{crown}}$ (6.5 mM), **1** (13 mM), and KOTf (13mM).

3-2. ITC Study of the Complexation of with $[2+2]_{\text{crown}}$ with **1** in the Presence of 2 Equiv. of KOTf

A 1 mM $\text{CHCl}_3/\text{CH}_3\text{CN}$ (1:1) solution of $[2+2]_{\text{crown}} \cdot 2\text{K}^+$ was prepared. Titration of this solution with 60 mM solution of **1** was operated. The titration curve was fitted with a simple 1:1 model and the thermodynamic parameters $K_a = 3.54 \times 10^3 \text{ M}^{-1}$, $\Delta H = -1284 \text{ cal/mol}$, and $\Delta S = 11.9 \text{ cal/mol/deg}$ were

obtained for the association of $[2+2]_{\text{crown}} \cdot 2\text{K}^+$ with **1** (Fig. S2b). The value of binding constant indicated that ca. 80% of the guest **1** was included in 6.5 mM each of $[2+2]_{\text{crown}} \cdot 2\text{K}^+$ and **1** in $\text{CHCl}_3/\text{CH}_3\text{CN}$ (1:1).

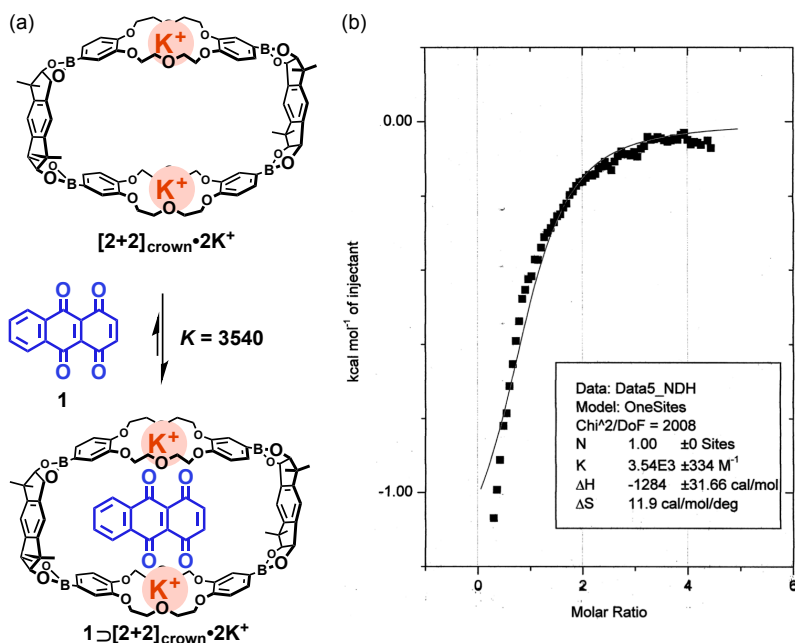


Fig. S2. (a) Complexation of $[2+2]_{\text{crown}} \cdot 2\text{K}^+$ with diquinone **1**. (b) Titration curve of the addition of 60 mM solution of **1** charged with 1 mM $[2+2]_{\text{crown}} \cdot 2\text{K}^+$ in $\text{CHCl}_3/\text{CH}_3\text{CN}$ (1:1) at 25°C. The line represents the curve fitting analysis with the one set of sites model. Thermodynamic parameters are also shown.

3-3. Control Experiments of the Complexation of $[2+2]_{\text{crown}}$ with **1**

The binding behavior of $[2+2]_{\text{crown}}$ containing other alkaline metal salts with 1,4,9,10-anthradiquinone **1** was examined (Fig. 3a). When $[2+2]_{\text{crown}}$ (6.5 mM), 2 equivalents of MOTf ($M = \text{Li}, \text{Na}; 13.0 \text{ mM}$), and 1 equivalent of **1** (6.5 mM) were mixed in $\text{CDCl}_3/\text{CD}_3\text{CN}$ (0.8 mL, 1:1), no shift of the signals of the guest molecule **1** was observed as shown in Fig. S3b-d. A mixture of monomeric pinacol ester of dibenzo-18-crown-6 diboronic acid **2_{pin}**, KOTf, and **1** was also examined. When **2_{pin}** (13.0 mM), 1 equivalent of KOTf (13.0 mM) and 0.5 equivalent of **1** (6.5 mM) were mixed in $\text{CDCl}_3/\text{CD}_3\text{CN}$ (0.8 mL, 1:1), no shift of the signals of the guest molecule **1** was observed as shown in Fig. S4b,c. These ^1H NMR studies suggested that the macrocyclic structure of $[2+2]_{\text{crown}}$ and K^+ ion was essential for the efficient binding of **1**.

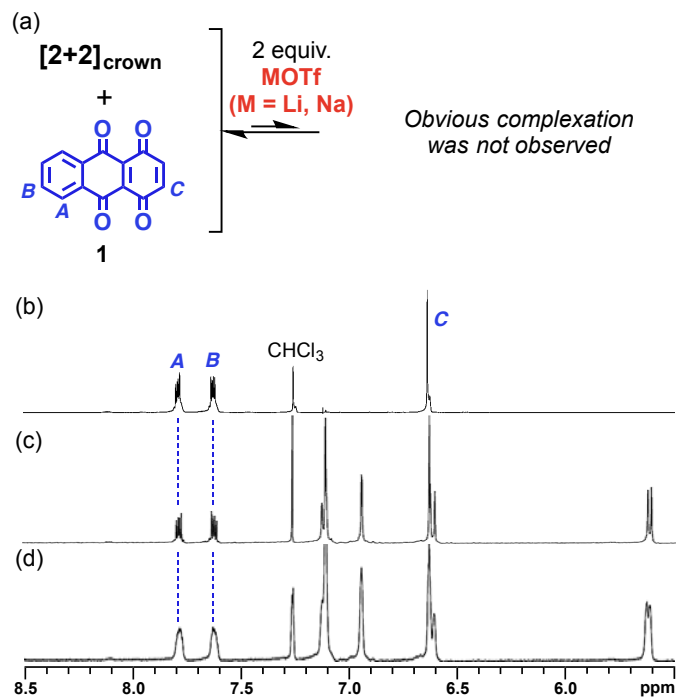


Fig. S3 (a) Examination of complexation of $[2+2]_{\text{crown}}$ with diquinone **1** in the presence of MOTf ($M = \text{Li, Na}$). Partial ^1H NMR spectra (400 MHz, $\text{CDCl}_3/\text{CD}_3\text{CN}$ (1:1), 298 K) of (b) **1**, (c) a mixture of $[2+2]_{\text{crown}}$ (6.5 mM), **1** (6.5 mM), and LiOTf (13mM), and (d) a mixture of $[2+2]_{\text{crown}}$ (6.5 mM), **1** (6.5 mM), and NaOTf (13mM).

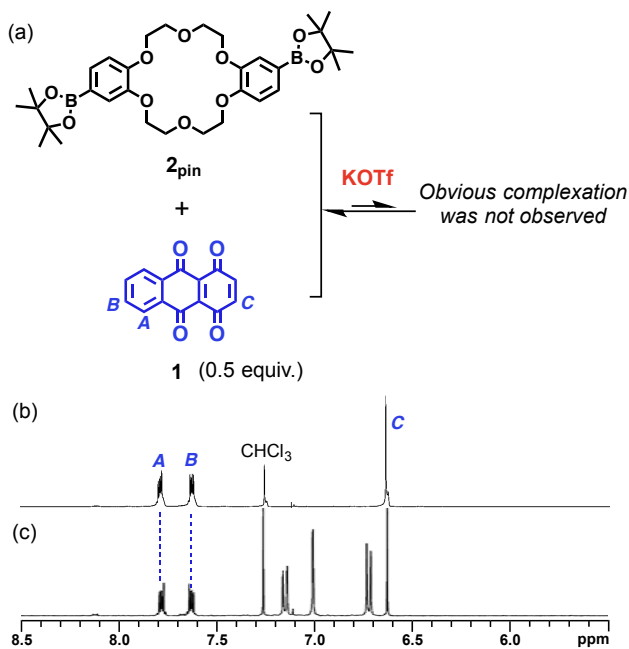


Fig. S4 (a) Examination of complexation of 2_{pin} with diquinone **1** in the presence of KOTf. Partial ^1H NMR spectra (400 MHz, $\text{CDCl}_3/\text{CD}_3\text{CN}$ (1:1), 298 K) of (b) **1**, and (c) a mixture of 2_{pin} (13 mM), **1** (6.5 mM), and KOTf (13mM).

4. The Diels-Alder Reaction of **1** with Various Dienes

Typical experiment: **1** (5.2 μmol , 6.5 mM), diene (7.8 μmol , 9.8 mM), **[2+2]_{crow}** (5.2 μmol , 6.5 mM), and KOTf (10.4 μmol , 13 mM) were dissolved in 0.8 mL of $\text{CDCl}_3/\text{CD}_3\text{CN}$ (1:1) in an NMR tube. The sample was kept at 27 °C and NMR spectrum was periodically recorded. Concentrations of **1**, products (internal and terminal adduct) and diene were monitored by using 1,4-dinitrobenzene as standard. The second-order rate constants were evaluated using a least-squares computer program (Excel program) from the plot ($1/([\text{diene}]_0 - [\mathbf{1}]_0) \ln([\text{diene}][\mathbf{1}]_0 / [\mathbf{1}][\text{diene}]_0) / \text{M}^{-1}$ vs. t/min). Control experiments (no cat.) were carried out under the same conditions but in the absence of **[2+2]_{crow}** and KOTf. The purification of the products was performed as follows. To the reaction mixture was added water and the organic material was extracted with dichloromethane. Organic layer was dried over MgSO_4 , filtered, and concentrated under reduced pressure. The residue was purified by GPC to afford the products.

4-1. The Diels-Alder Reaction of **1** with Anthracene **4** Under Various Conditions

$$A = 1/([\text{diene}]_0 - [\mathbf{1}]_0) \ln([\text{diene}][\mathbf{1}]_0 / [\mathbf{1}][\text{diene}]_0)$$

Condition: Table 1 entry 1

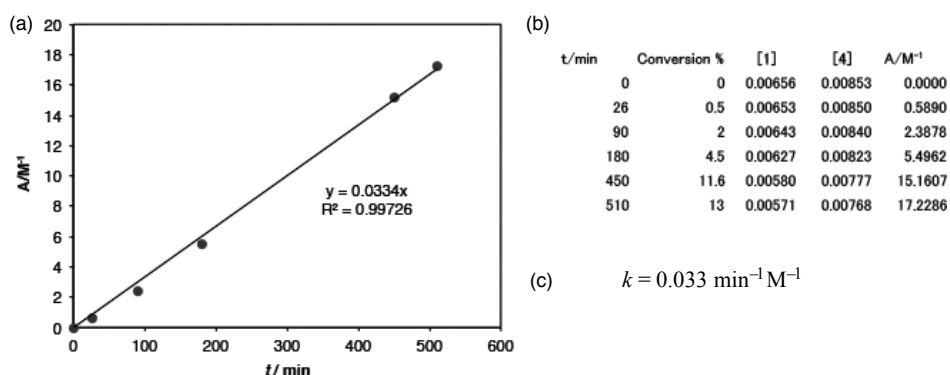


Fig. S5 (a) Second-order plot (A / M^{-1} vs. t / min) (b) table of time dependence of conversion, [1], [4] and A and (c) reaction rate

Condition: Table 1 entry 2

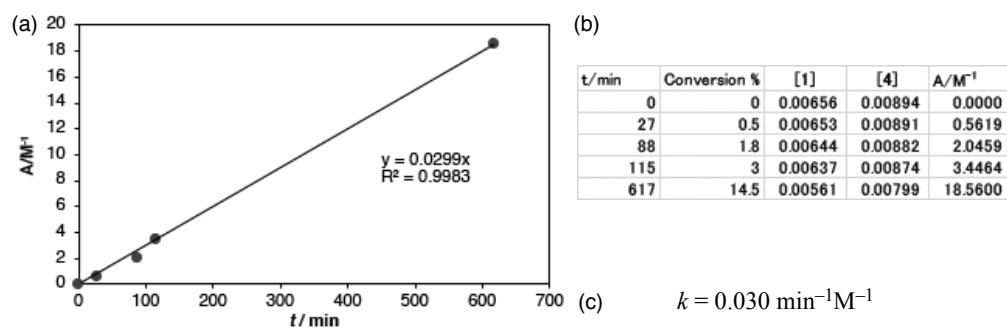


Fig. S6 (a) Second-order plot (A / M^{-1} vs. t / min) (b) table of time dependence of conversion, [1], [4] and A and (c) reaction rate

Condition: Table 1 entry 3

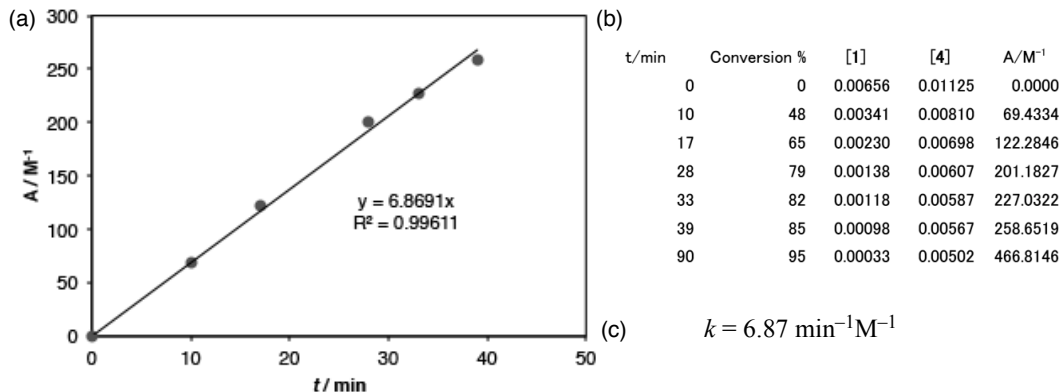


Fig. S7 (a) Second-order plot (A / M^{-1} vs. t / min) (b) table of time dependence of conversion, [1], [4] and A and (c) reaction rate

Condition: Table 1 entry 4

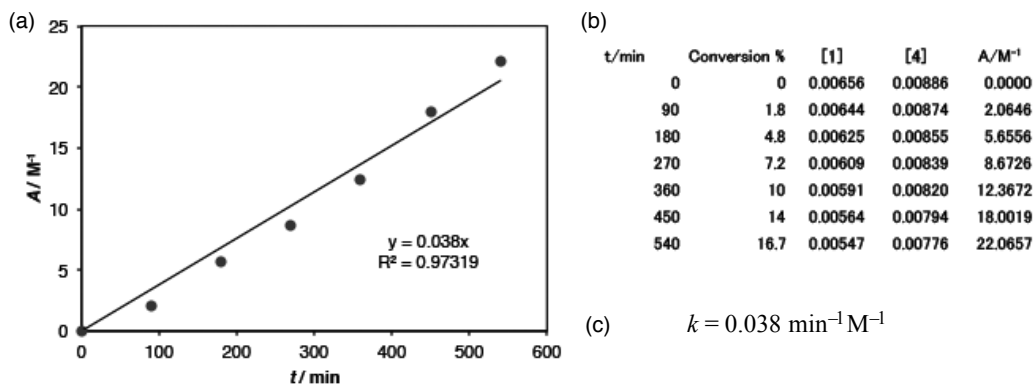


Fig. S8 (a) Second-order plot (A / M^{-1} vs. t / min) (b) table of time dependence of conversion, [1], [4] and A and (c) reaction rate

Condition: Table 1 entry 5

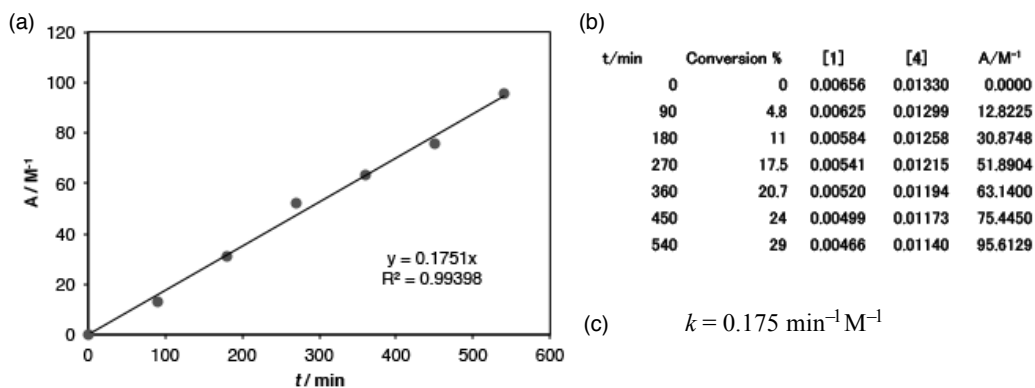


Fig. S9 (a) Second-order plot (A / M^{-1} vs. t / min) (b) table of time dependence of conversion, [1], [4] and A and (c) reaction rate

In the reaction of anthracene (Table 1, entry 3), the signal of the anthracene slightly up-field shifted compared to free anthracene in ^1H NMR spectra, suggesting the formation of a weak Michaelis complex $\mathbf{1}\cdot\mathbf{4}@[2+2]_{\text{crown}}\cdot 2\text{K}^+$ (Fig. S10a,b).

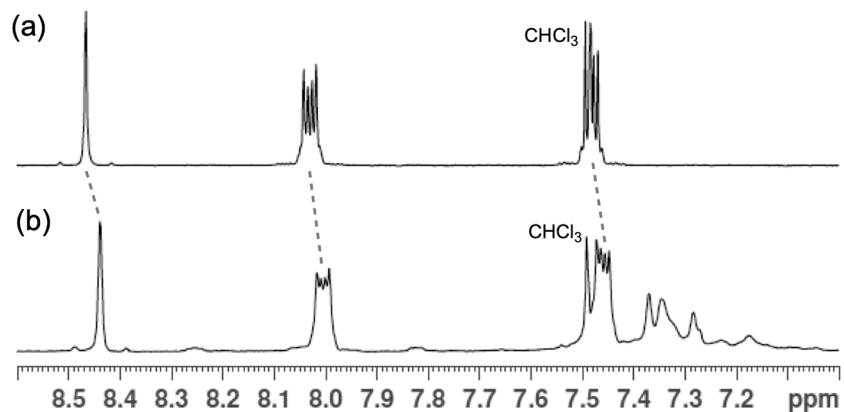


Fig. S10 Partial ^1H NMR spectra (400 MHz, $\text{CDCl}_3/\text{CD}_3\text{CN}$ (1:1)) of (a) **4** and (b) a mixture of $[2+2]_{\text{crown}}$ (6.5 mM), **1** (6.5 mM), **4** (9.8 mM), and KOTf (13.0 mM). (Residual TMS was set at 0 ppm.)

When **1** (0.65 mM) and **4** (0.65 mM) were mixed in $\text{CDCl}_3/\text{CD}_3\text{CN}$ (1:1), no shift of the signals was observed (Fig. S11).

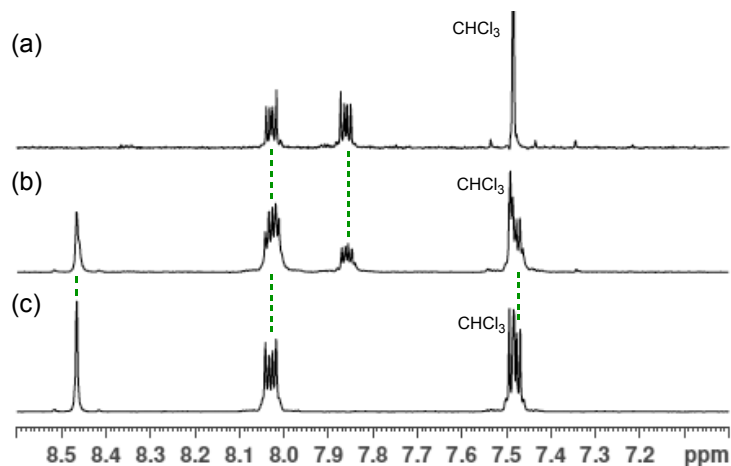


Fig. S11 Partial ^1H NMR spectra (400 MHz, $\text{CDCl}_3/\text{CD}_3\text{CN}$ (1:1)) of (a) **1**, (b) a mixture of **1** (6.5 mM), and **4** (6.5 mM) and (c) **4**. (Residual TMS was set at 0 ppm.)

The binding behavior of $[2+2]_{\text{crown}}$ containing K^+ with 5_{int} was examined (Fig. S12a). $[2+2]_{\text{crown}}$ (6.5 mM), 2 equivalents of KOTf (13.0 mM), and 1 equivalent of 5_{int} (6.5 mM) were mixed in $\text{CDCl}_3/\text{CD}_3\text{CN}$ (0.8 mL, 1:1) and ^1H NMR spectra were measured at 303 K and 323 K (Fig. S12c,d). Upfield shift and broadening of proton signals of 5_{int} was observed (Fig. 12b,c). These signals also became diastereotopic and the separation of signals was observed due to the chirality of the $[2+2]_{\text{crown}}$, suggesting 5_{int} was included in the host. From the ITC study, association constant of 5_{int} with $[2+2]_{\text{crown}} \cdot 2\text{K}^+$ was measured. A 1 mM $\text{CHCl}_3/\text{CH}_3\text{CN}$ (1:1) solution of $[2+2]_{\text{crown}} \cdot 2\text{K}^+$ was titrated with 30 mM solution of 5_{int} . The titration curve was fitted with a simple 1:1 model and the thermodynamic parameters $K_a = 1.08 \times 10^3 \text{ M}^{-1}$, $\Delta H = -3463 \text{ cal/mol}$, and $\Delta S = 2.76 \text{ cal/mol/deg}$ were obtained for the association of $[2+2]_{\text{crown}} \cdot 2\text{K}^+$ with 5_{int} (Fig. S12e).

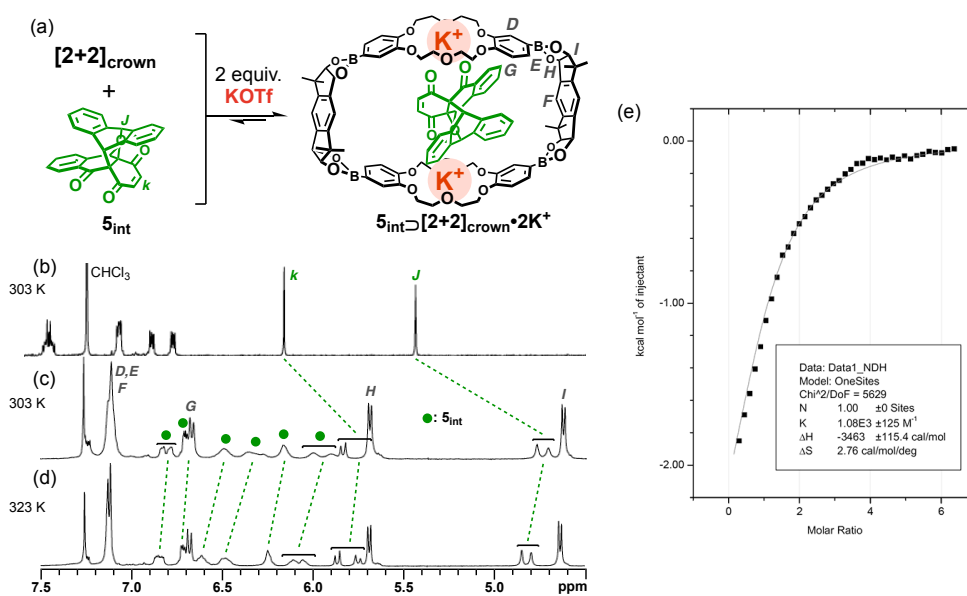
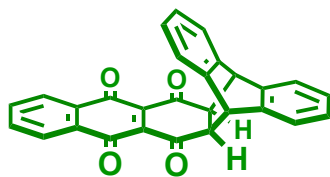


Fig. S12 (a) Complexation of $[2+2]_{\text{crown}}$ with 5_{int} in the presence of K^+ . Partial ^1H NMR spectra (400 MHz, $\text{CDCl}_3/\text{CD}_3\text{CN}$ (1:1)) of (b) 5_{int} at 303 K, (c) a mixture of $[2+2]_{\text{crown}}$ (6.5 mM), 5_{int} (6.5 mM), and KOTf (13 mM) at 303 K, and (d) the same sample at 323 K. (e) Titration curve of $[2+2]_{\text{crown}} \cdot 2\text{K}^+$ with 5_{int} in $\text{CHCl}_3/\text{CH}_3\text{CN}$ (1:1) at 25°C. The line represents the curve fitting analysis with the one set of sites model. Thermodynamic parameters are also shown.



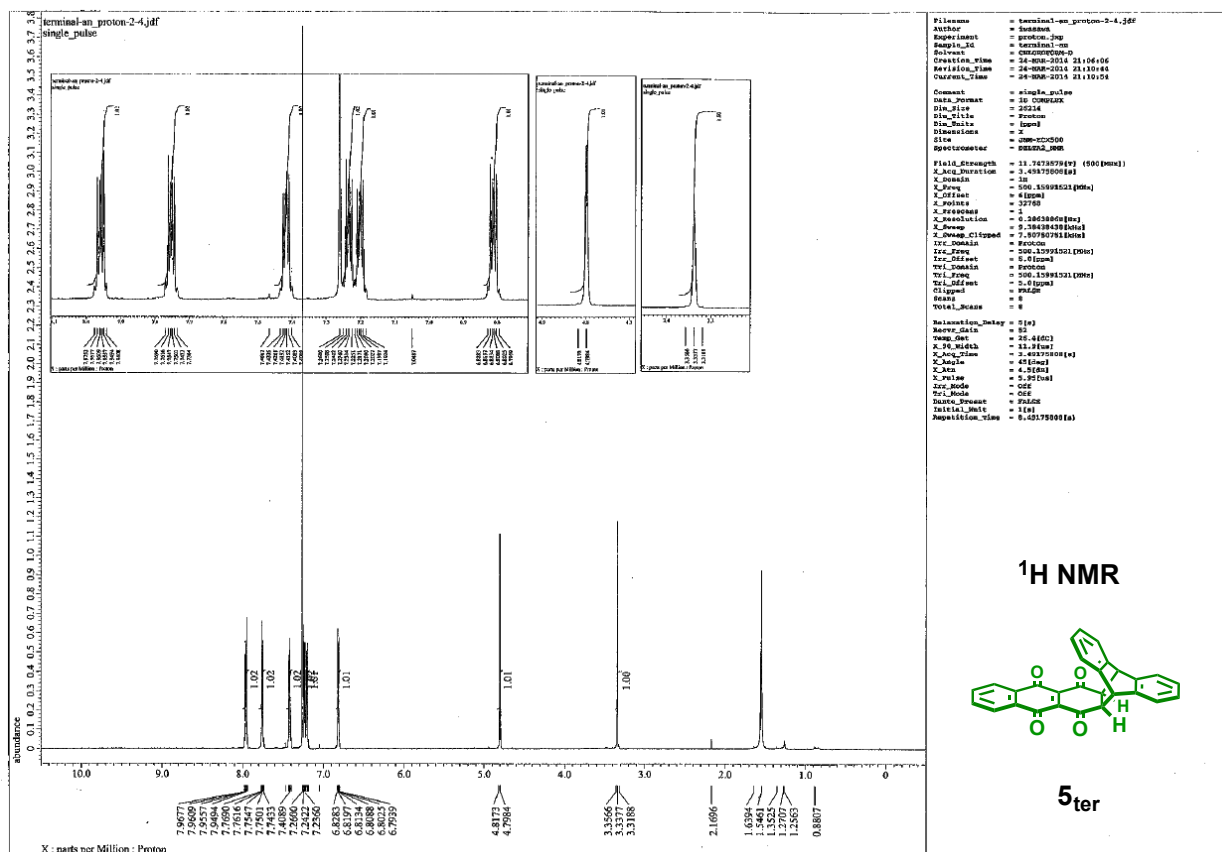
Physical data of **5_{ter}**

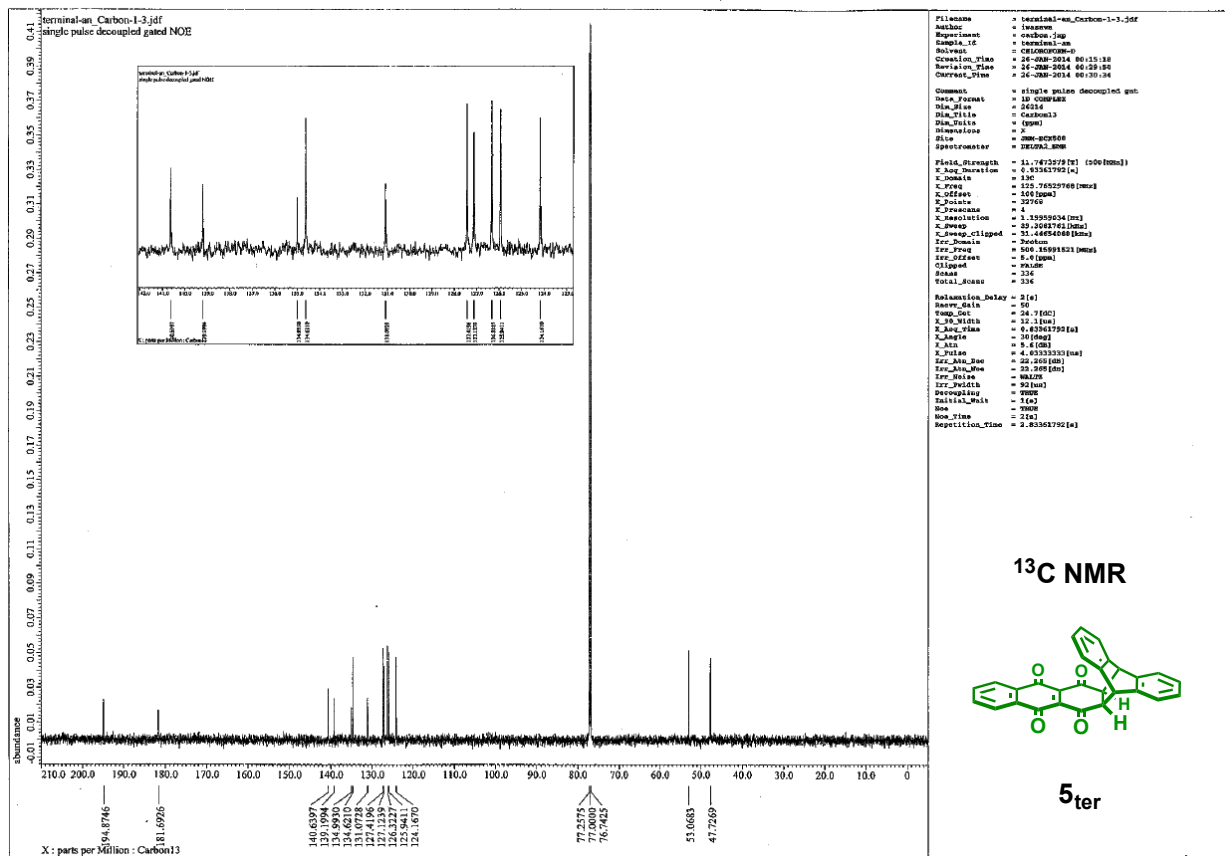
¹H NMR (500 MHz, CDCl₃): δ 7.97-7.94 (m, 2H), 7.77-7.74 (m, 2H), 7.42-7.40 (m, 2H), 7.24-7.22 (m, 4H), 7.21-7.19 (m, 2H), 6.83-6.79 (m, 2H), 4.80 (s, 2H), 3.34 (s, 2H).

¹³C NMR (125 MHz, CDCl₃): δ 194.9, 181.7, 140.6, 139.2, 135.0, 134.6, 131.1, 127.4, 127.1, 126.3, 125.9, 124.2, 53.1, 47.7.

HRMS (FAB⁺, NBA): *m/z* Calcd. for C₂₈H₁₇O₄: 417.1127., Found: 417.1109 [M+H]⁺.

IR (ATR): 1705, 1607, 1593, 1274, 1244, 1087, 1045, 1003 cm⁻¹.





4-2-1. The Diels-Alder Reaction of **1** with 2-Mono and 2,3-Di-substituted 1,3-Butadienes

$$A = 1/([diene]_0 - [1]_0) \ln([diene][1]_0 / [1][diene]_0)$$

Condition: Table 2 entry 1

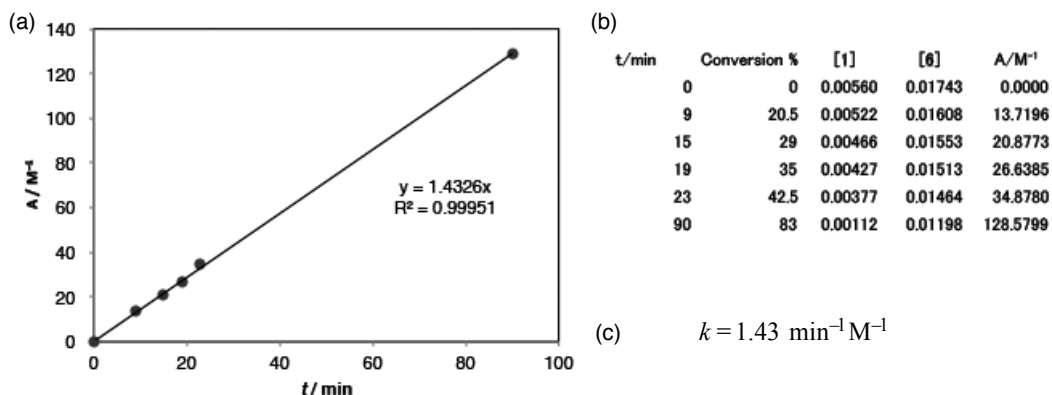
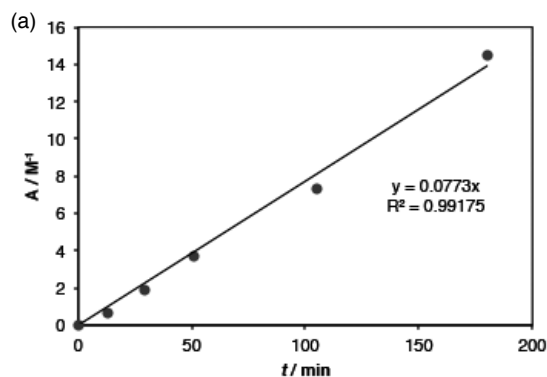


Fig. S13 (a) Second-order plot (A / M^{-1} vs. t / min) (b) table of time dependence of conversion, [1], [6] and A and (c) reaction rate

Condition: Table 2 entry 2

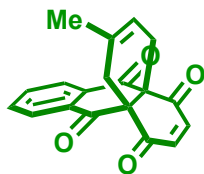


(b)

t/min	Conversion %	[1]	[6]	A/M ⁻¹
0	0	0.01500	0.04500	0.0000
13	3	0.01455	0.04455	0.6803
29	8	0.01380	0.04380	1.8784
51	15	0.01275	0.04275	3.7075
105	27	0.01095	0.04095	7.3467
180	45	0.00825	0.03825	14.5106

(c) $k = 0.077 \text{ min}^{-1} \text{ M}^{-1}$

Fig. S14 (a) Second-order plot (A / M^{-1} vs. t / min) (b) table of time dependence of conversion, [1], [6] and A and (c) reaction rate



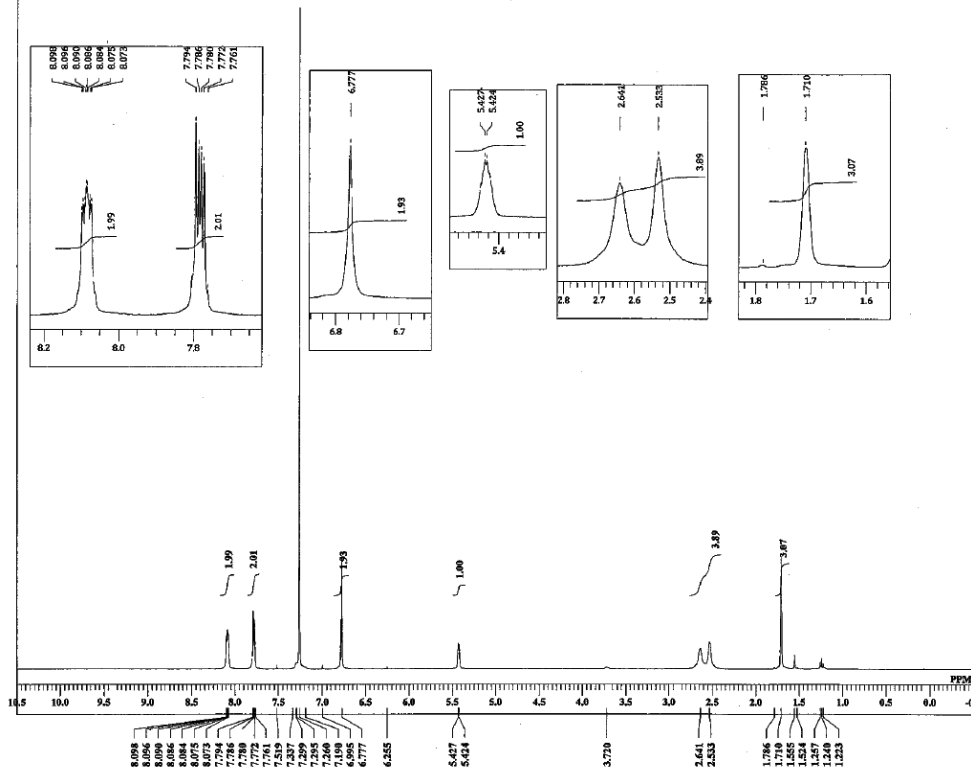
Physical data of **S1_{int}**

¹H NMR (500 MHz, CDCl₃): δ 8.10-8.07 (m, 2H), 7.79-7.76 (m, 2H), 6.78 (br, 4H), 5.42 (br, 1H), 2.64 (br, 2H), 2.53 (br, 2H), 1.71 (s, 3H).

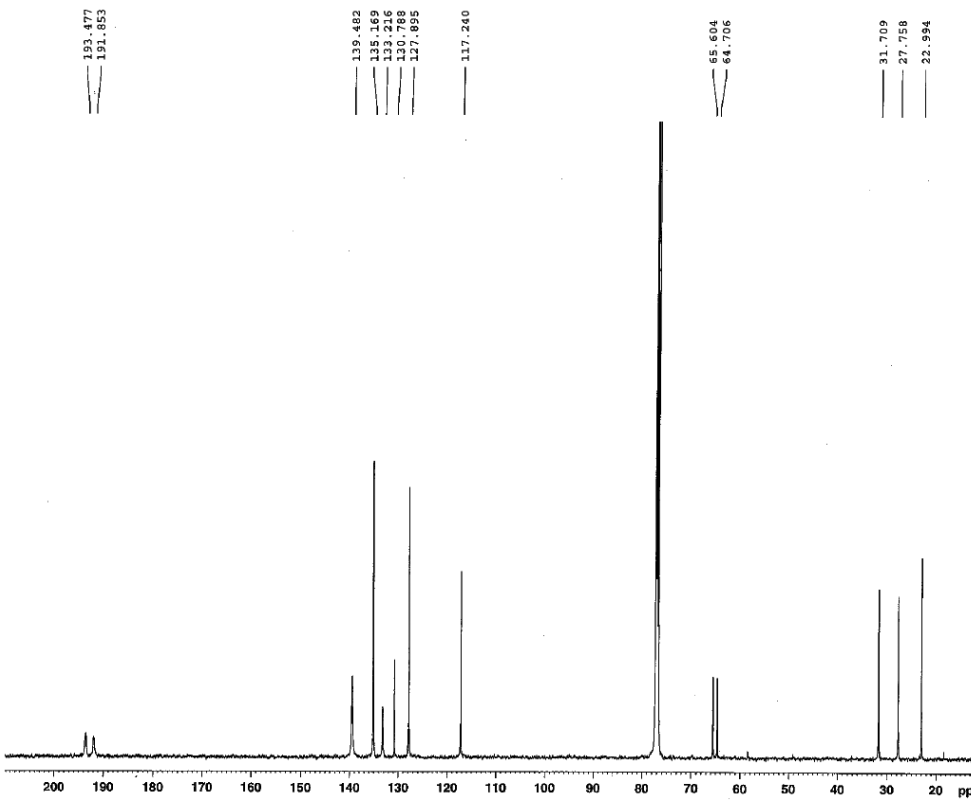
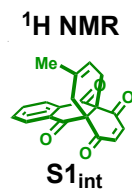
¹³C NMR (125 MHz, CDCl₃): δ 193.5, 191.9, 139.5, 135.2, 133.2, 130.8, 127.9, 117.2, 65.6, 64.7, 31.7, 27.8, 23.0.

HRMS (FAB⁺, NBA): m/z Calcd. for C₁₉H₁₅O₄: 307.0971., Found: 307.0944 [M+H]⁺.

IR (ATR): 1710, 1679, 1592, 1259, 1234 cm⁻¹.



DFILE _DEFAULTALS
 COMNT The Jan 09 21:50:39 2014
 OBNUC 1H
 EXMOD NON
 OBVRO 399.65 MHz
 OBSET 124.00 kHz
 OBFIN 16590.00 Hz
 POINT 16384
 FREQU 7592.01 Hz
 SCANS 16
 ACQTM 2.0500 sec
 TD 3.0000 sec
 FW1 5.00 sec
 ERNUC 1H
 CTEMP 6348.5 c
 SINTV CDC13
 EXREF 7.26 ppm
 BF 0.12 Hz
 RGAIN 18



BRUKER

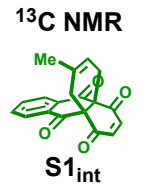
Current Data Parameters
 NAME MN_internal-Me
 EXPNO 2
 PROCNO 1

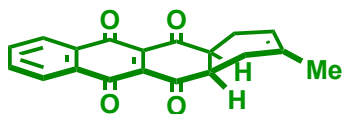
F2 - Acquisition Parameters
 Date 20140110
 Time 9:43
 INSTRUM spect
 PROBHD 5 mm Multinucl
 PULPROG zgpg
 TD 65536
 SOLVENT CDC13
 NS 12160
 DS 2
 SWH 30303.031 Hz
 FIDRES 0.462388 Hz
 AQ 1.0814105 sec
 RG 2298.8
 DW 16.560 use
 DE 6.00 use
 TE 300.0 K
 D1 2.0000000 sec
 d11 0.0300000 sec
 DELTA 1.8999998 sec
 WCRET 0.0000000 sec
 MCNEX 0.0150000 sec

===== CHANNEL f1 =====
 NUC1 13C
 P1 4.30 use
 PL1 3.00 dB
 SFO1 125.7715723 MHz

===== CHANNEL f2 =====
 CDEPRG2 waltz16
 MUX 1H
 PCPD2 90.00 use
 PL2 120.00 dB
 PL12 19.70 dB
 PL13 18.70 dB
 SFO2 500.1320005 MHz

F2 - Processing parameters
 SI 65536
 SF 125.757913 MHz
 WDW EM
 SSB 0
 LB 5.00 Hz
 GB 0
 FC 1.40





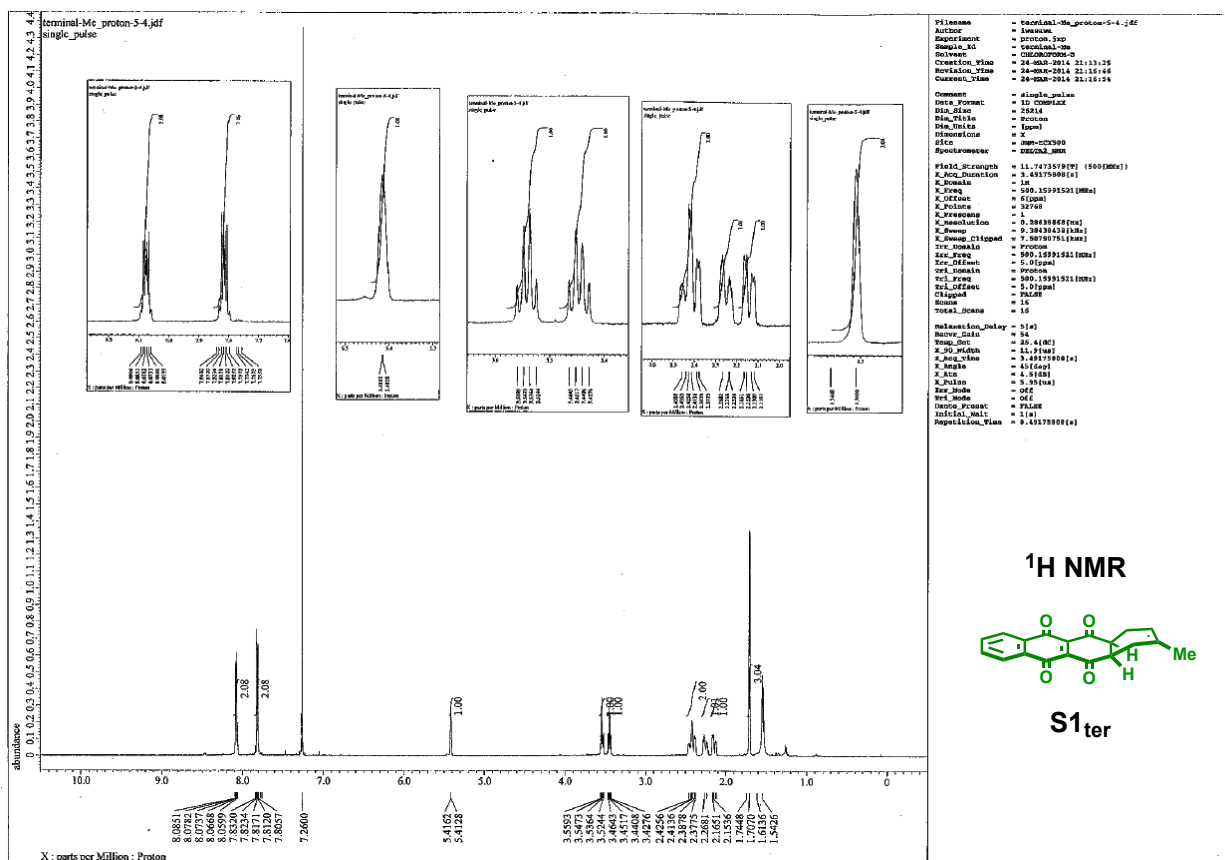
Physical data of **S1_{ter}**

¹H NMR (500 MHz, CDCl₃): δ 8.07-8.05 (m, 2H), 7.83-7.80 (m, 2H), 5.41 (br, 1H), 3.55 (q, *J* = 5.4 Hz, 1H), 3.45 (q, *J* = 5.4 Hz, 1H), 2.41 (td, *J* = 18.1, 5.0 Hz, 2H), 2.26-2.23 (m, 1H), 2.14 (dd, *J* = 17.5, 5.0 Hz, 1H), 1.70 (s, 3H).

¹³C NMR (125 MHz, CDCl₃): δ 196.8, 196.4, 183.4, 183.3, 134.8, 133.8, 133.5, 131.9, 131.8, 131.3, 126.5, 117.8, 49.8, 49.1, 28.2, 24.1, 23.3.

HRMS (FD⁺): *m/z* Calcd. for C₁₉H₁₄O₄: 306.0892., Found: 306.0868 [M]⁺.

IR (ATR): 1708, 1665, 1591, 1284, 1179 cm⁻¹.



Condition: Table 2 entry 4

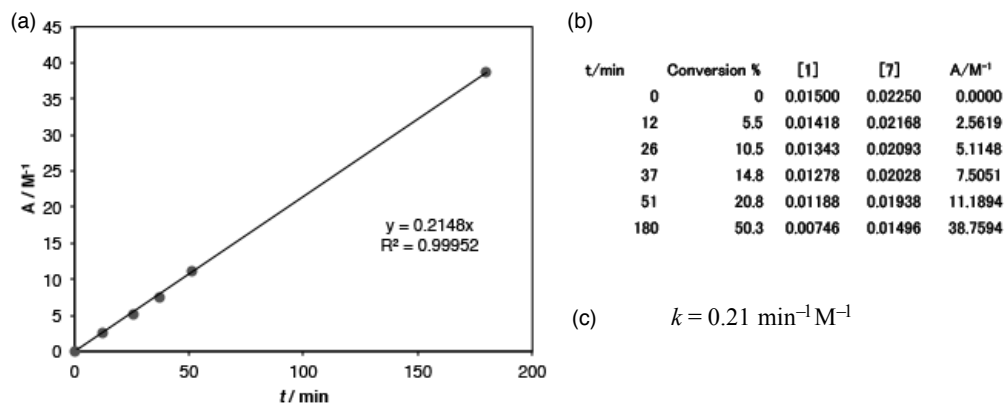
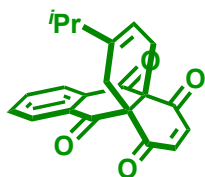


Fig. S16 (a) Second-order plot (A / M^{-1} vs. t / min) (b) table of time dependence of conversion, [1], [7] and A and (c) reaction rate



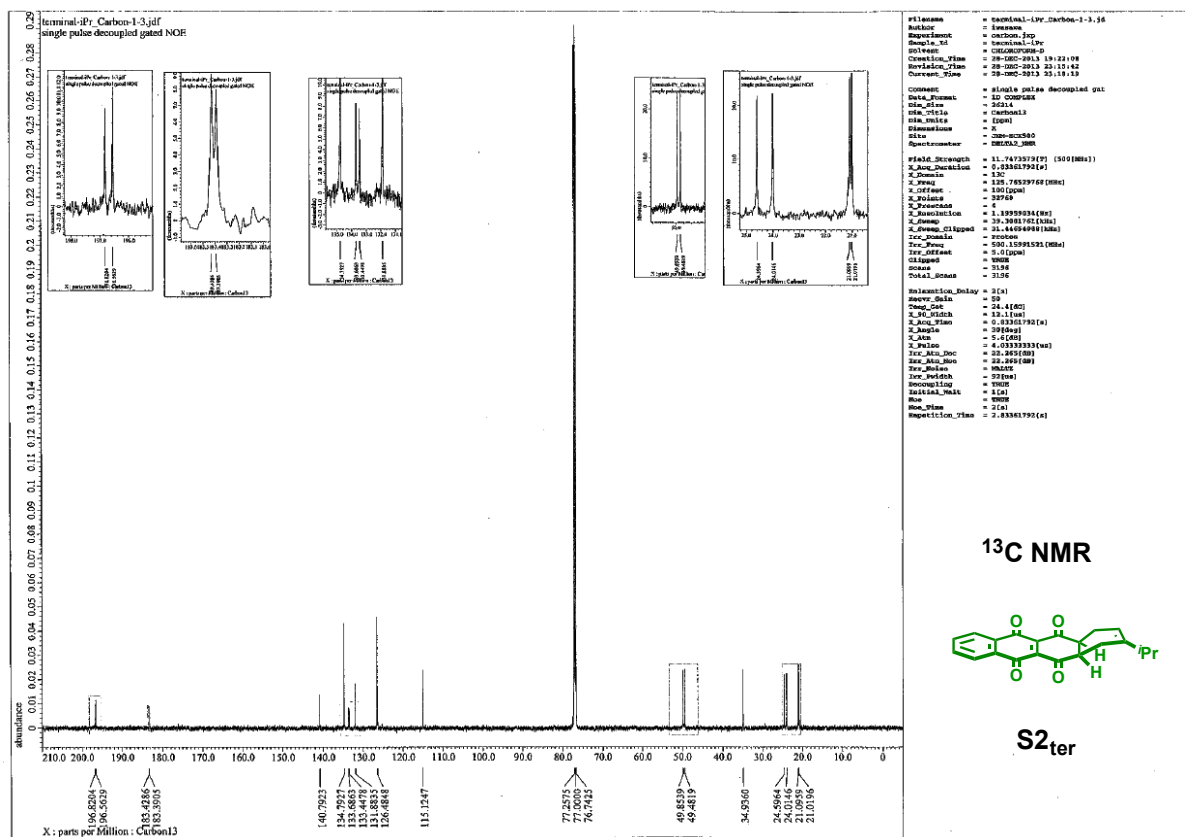
Physical data of $S2_{\text{int}}$

^1H NMR (500 MHz, CDCl_3): δ 8.10-8.07 (m, 2H), 7.80-7.77 (m, 2H), 6.80-6.75 (m, 2H), 5.42 (br, 1H), 2.66 (br, 2H), 2.54 (br, 2H), 2.23 (sep, $J = 6.9$ Hz, 1H), 1.01 (d, $J = 6.9$ Hz, 6H).

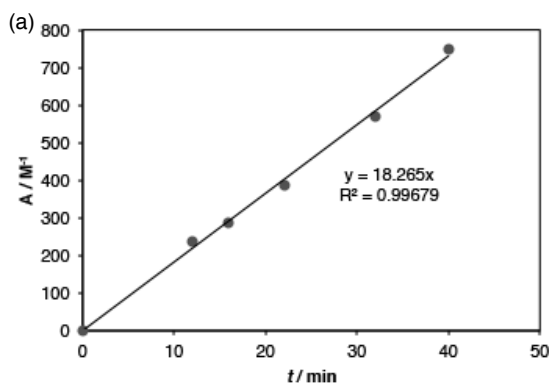
^{13}C NMR (125 MHz, CDCl_3): δ 193.6, 192.1, 191.7, 140.2, 139.6, 139.3, 135.1, 133.2, 127.9, 114.5, 65.5, 64.9, 34.7, 28.6, 27.6, 20.8.

HRMS (FAB^+ , NBA): m/z Calcd. for $\text{C}_{21}\text{H}_{19}\text{O}_4$: 334.1283., Found: 335.1279 $[\text{M}+\text{H}]^+$.

IR (ATR): 2961, 2927, 1710, 1683, 1592, 1465, 1424, 1363, 1259, 1235, 1083 cm^{-1} .



Condition: Table 2 entry 5



t/min	Conversion %	[1]	[8]	A/M ⁻¹
0	0	0.00656	0.00938	0.0000
12	76	0.00158	0.00439	237.2985
16	80.6	0.00127	0.00409	287.5593
22	86.7	0.00087	0.00369	385.0140
32	93	0.00046	0.00328	570.6877
40	96	0.00026	0.00308	747.3511

(c) $k = 18.27 \text{ min}^{-1} \text{M}^{-1}$

Fig. S17 (a) Second-order plot (A / M^{-1} vs. t / min) (b) table of time dependence of conversion, [1], [8] and A and (c) reaction rate

Condition: Table 2 entry 6

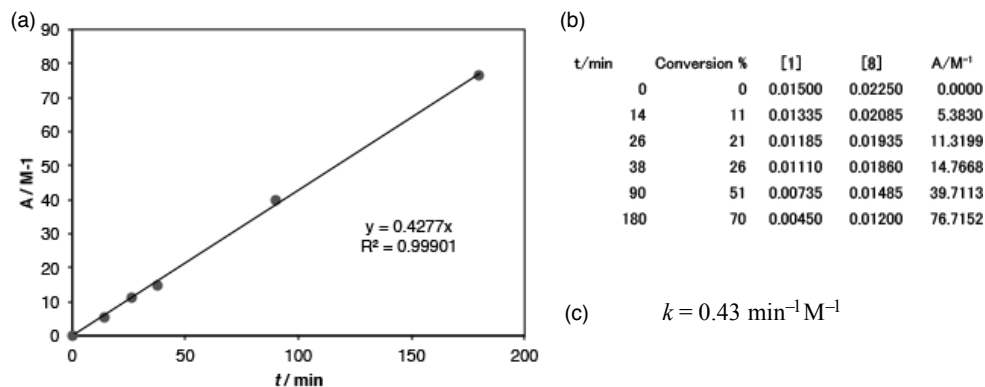
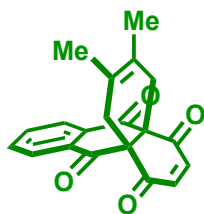


Fig. S18 (a) Second-order plot (A / M^{-1} vs. t / min) (b) table of time dependence of conversion, [1], [8] and A and (c) reaction rate



Physical data of **S3_{int}**

¹H NMR (500 MHz, CDCl₃): δ 8.09-8.07 (m, 2H), 7.79-7.77 (m, 2H), 6.77 (s, 2H), 2.55 (br, 4H), 1.64 (s, 6H).

¹³C NMR (125 MHz, CDCl₃): δ 193.6, 191.9, 139.5, 135.1, 133.2, 127.8, 122.5, 65.6, 33.2, 18.6.

HRMS (FAB⁺, NBA): m/z Calcd. for C₂₀H₁₆O₄: 320.1049., Found: 320.1079 [M]⁺.

IR (ATR): 2915, 2873, 1712, 1678, 1592, 1425, 1259, 1240, 1081, 1066, 859 cm⁻¹.

Condition: Table 2 entry 7

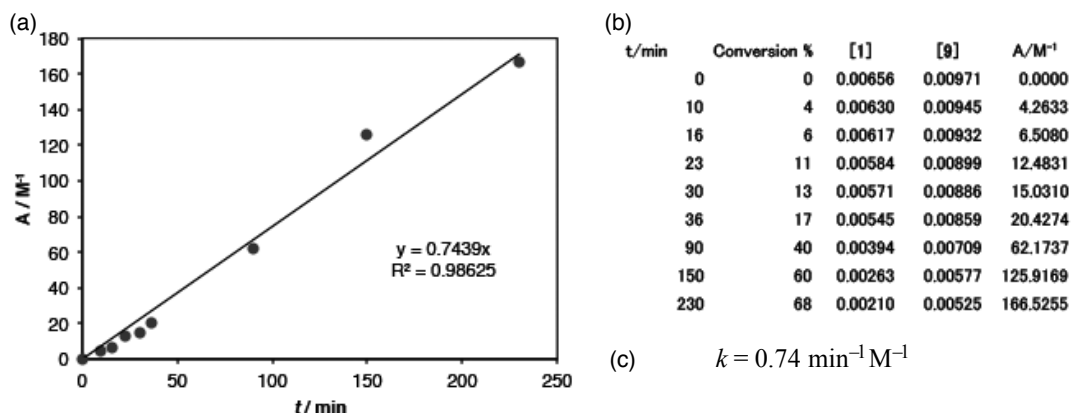


Fig. S19 (a) Second-order plot (A / M^{-1} vs. t / min) (b) table of time dependence of conversion, [1], [9] and A and (c) reaction rate

Condition: Table 2 entry 8

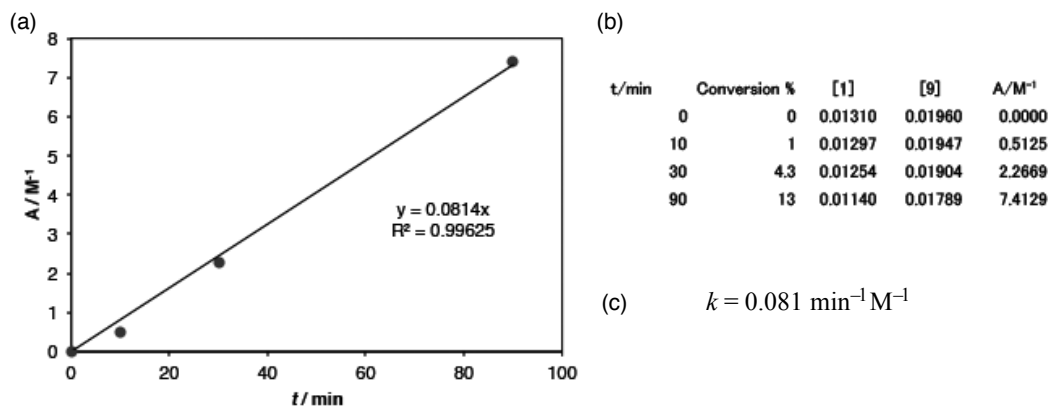
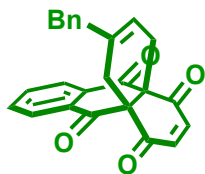


Fig. S20 (a) Second-order plot (A / M^{-1} vs. t / min) (b) table of time dependence of conversion, [1], [9] and A and (c) reaction rate



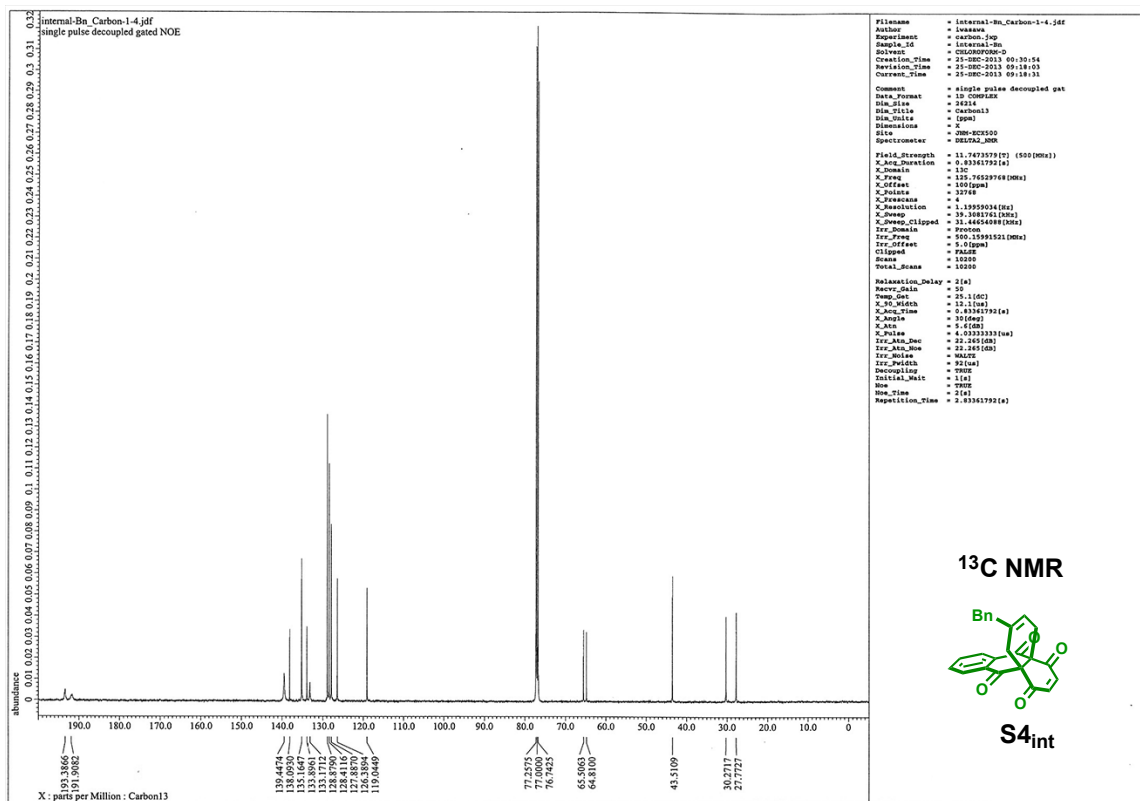
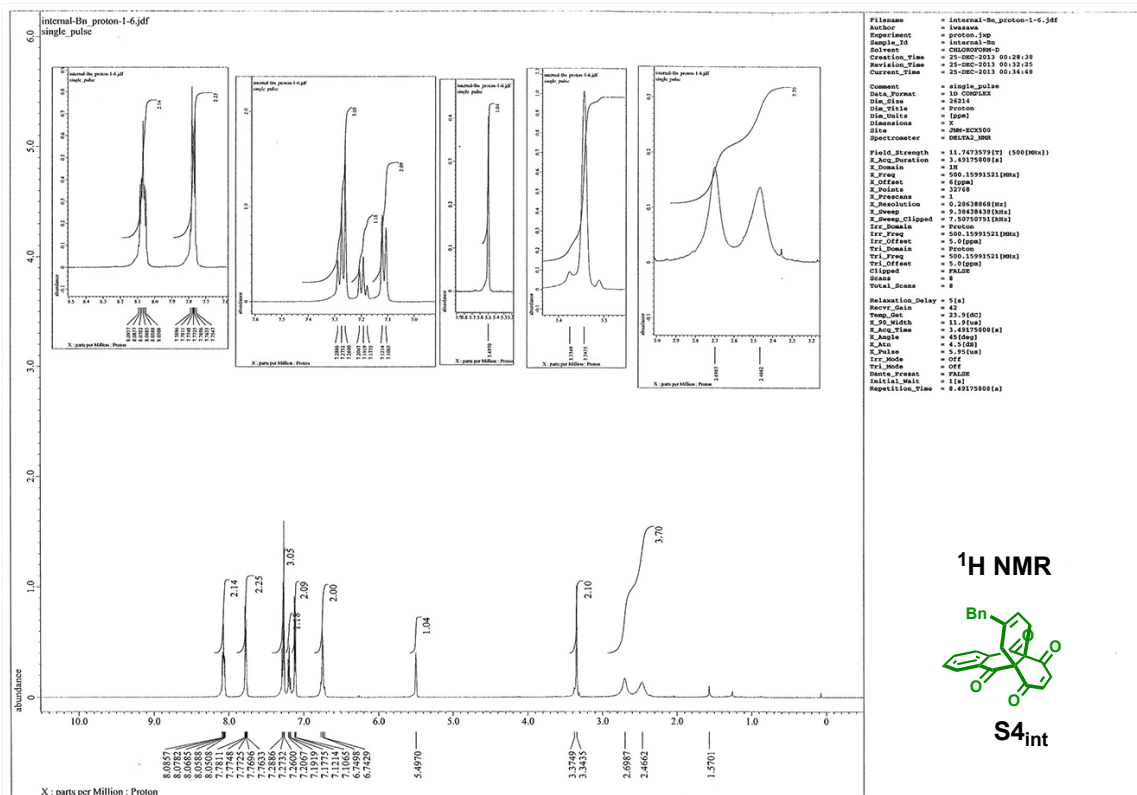
Physical data of **S4_{int}**

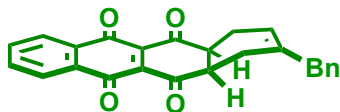
¹H NMR (500 MHz, CDCl₃): δ 8.09-8.05 (m, 2H), 7.79-7.75 (m, 2H), 7.28 (d, $J = 7.6$ Hz, 2H), 7.19 (t, $J = 7.2$ Hz, 1H), 7.11 (d, $J = 7.6$ Hz, 2H), 6.75 (m, 2H), 5.50 (br, 1H), 3.37-3.34 (m, 2H), 2.70 (br, 2H), 2.47 (br, 2H).

¹³C NMR (125 MHz, CDCl₃): δ 193.4, 191.9, 139.4, 138.1, 135.2, 133.9, 133.2, 128.9, 128.4, 127.9, 126.4, 119.0, 65.5, 64.8, 43.5, 30.3, 27.8.

HRMS (FAB⁺, NBA): m/z Calcd. for C₂₅H₁₈O₄: 382.1205., Found: 382.1213 [M]⁺.

IR (ATR): 2893, 1710, 1681, 1592, 1494, 1453, 1423, 1258, 1234, 1070 cm^{-1} .





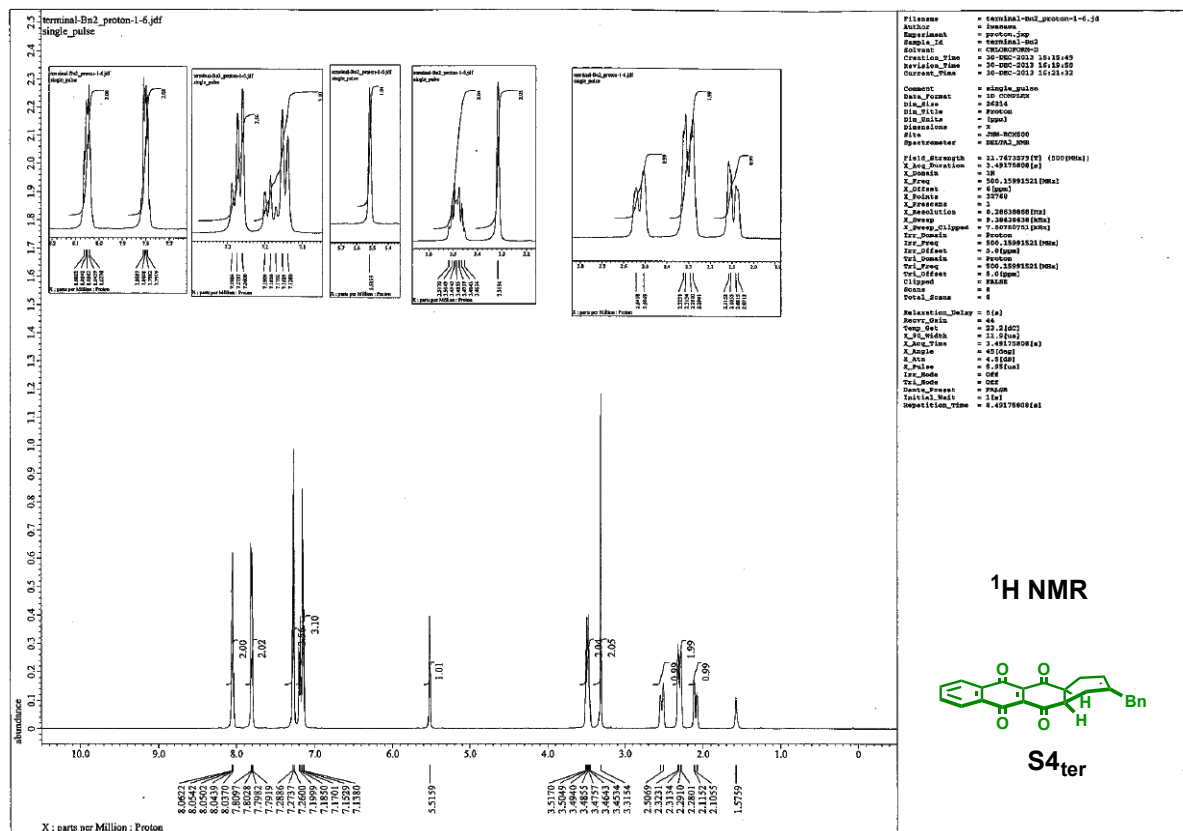
Physical data of **S4_{ter}**

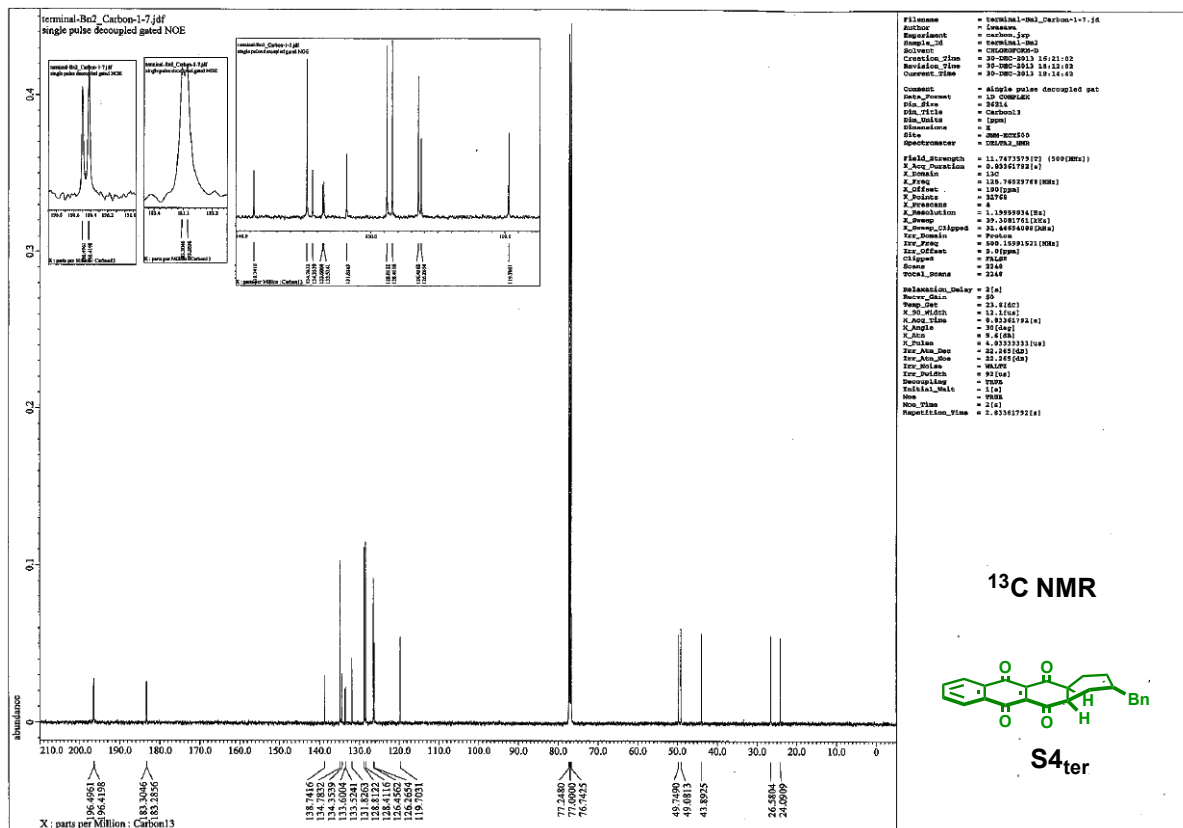
¹H NMR (500 MHz, CDCl₃): δ 8.06-8.04 (m, 2H), 7.81-7.79 (m, 2H), 7.28 (d, *J* = 7.5 Hz, 2H), 7.18 (t, *J* = 7.5 Hz, 2H), 7.15 (d, *J* = 7.5 Hz, 1H), 5.52 (br, 1H), 3.45-3.52 (m, 2H), 2.05 (s, 2H), 2.51-2.54 (m, 1H), 2.30 (dd, *J* = 16.5, 4.9 Hz, 2H), 2.09 (dd, *J* = 16.5, 4.9 Hz, 1H).

¹³C NMR (125 MHz, CDCl₃): δ 196.5, 196.4, 183.3, 183.3, 138.7, 134.8, 134.4, 133.6, 133.5, 131.8, 128.8, 128.4, 126.5, 126.3, 119.7, 49.7, 49.1, 43.9, 26.6, 24.1.

HRMS (FAB⁺, NBA): *m/z* Calcd. for C₂₅H₂₀O₄: 384.1362., Found: 384.1359 [M+2H]⁺. The peak derived from reduction product was observed in MS analysis.

IR (ATR): 1707, 1665, 1592, 1492, 1453, 1279, 1222, 1180 cm⁻¹.





Condition: Table 2 entry 9

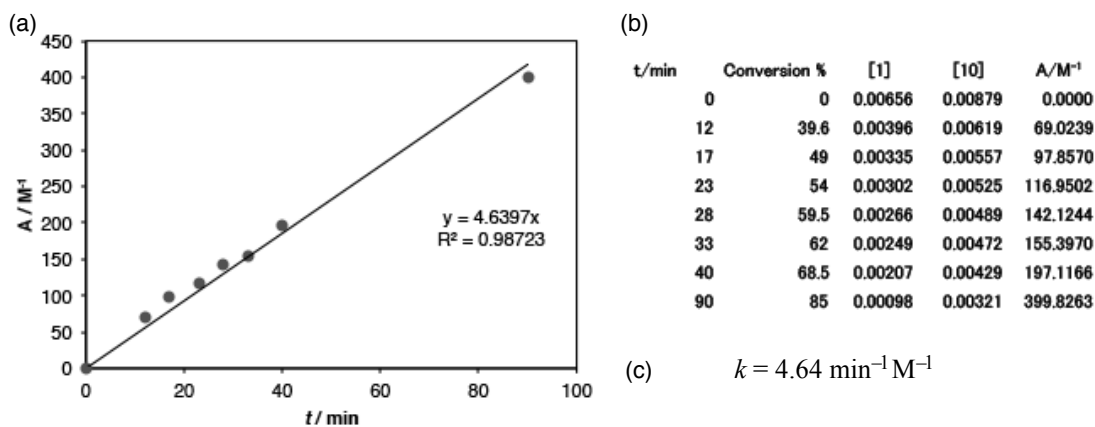


Fig. S21 (a) Second-order plot (A / M^{-1} vs. t / min) (b) table of time dependence of conversion, $[1]$, $[10]$ and A and (c) reaction rate

Condition: Table 2 entry 10

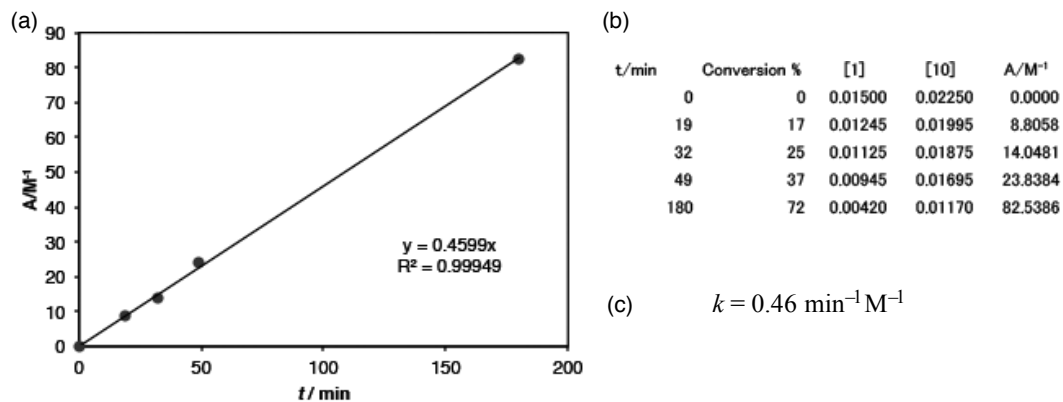
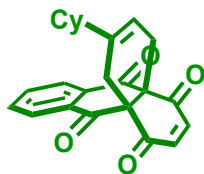


Fig. S22 (a) Second-order plot (A / M^{-1} vs. t / min) (b) table of time dependence of conversion, [1], [10] and A and (c) reaction rate



Physical data of **S5_{int}**

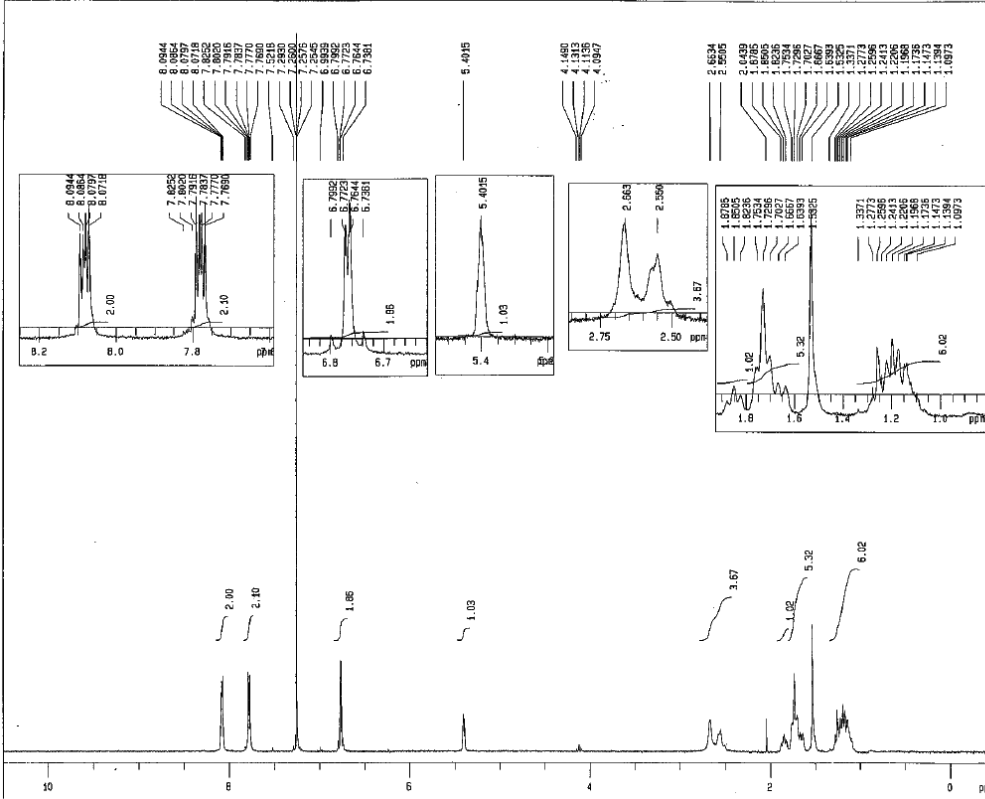
¹H NMR (500 MHz, CDCl₃): δ 8.09-8.07 (m, 2H), 7.82-7.77 (m, 2H), 6.77 (m, 2H), 5.40 (br, 1H), 2.66 (br, 2H), 2.55 (br, 2H), 1.85 (t, $J = 14.0$ Hz, 1H), 1.75-1.64 (m, 4H), 1.28-1.10 (m, 6H).

¹³C NMR (125 MHz, CDCl₃): δ 193.6, 191.8, 139.6, 139.3, 135.1, 133.2, 127.9, 127.8, 114.9, 65.5, 65.5, 65.5, 64.9, 45.0, 31.4, 29.3, 27.7, 26.5, 26.2.

HRMS (FAB⁺, NBA): m/z Calcd. for C₂₄H₂₃O₄: 375.1596., Found: 375.1605 [M+H]⁺.

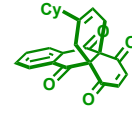
IR (ATR): 2925, 2851, 1711, 1683, 1593, 1448, 1424, 1258, 1238 cm⁻¹.

internal-cyhex (Mn-692-D)



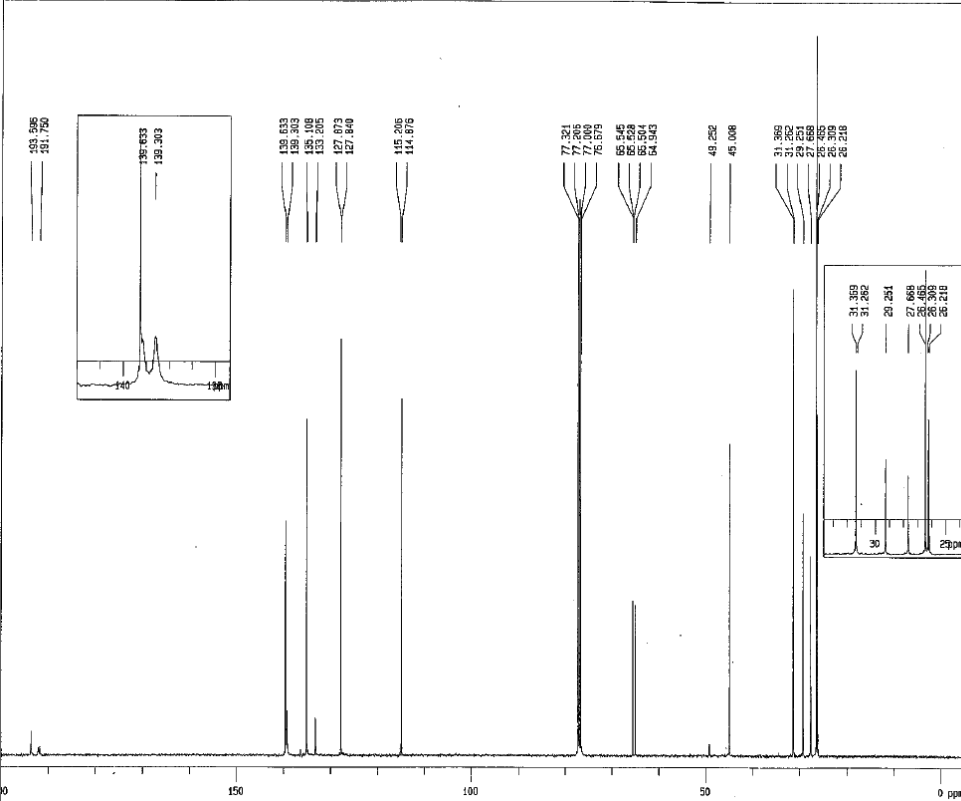
Date : Wed Dec 25 16:55:00 2013
 FileName : .LoadingID.mdata
 Comment : internal-cyhex M6
 SI:cellhistory :
 SNAME : non
 POINT : 32768 points
 SAMPLE : 32768 points
 FREQ : 7517.7 Hz
 FILTER : 550 Hz
 DELAY : 20.6 usec
 DEADT : 72.7 usec
 INTVL : 126.3 usec
 TIMES : 16 times
 DUMMY : 1 times
 PD : 3.0000 sec
 ACQTM : 4138.9588 msec
 PREDL : 0.01000 msec
 INVT : 1000.0000 msec
 RESOL : 0.24 Hz
 FWH : 6.50 usec
 OBUS : 1H
 OBFSD : 395.75 MHz
 OBFSE : 134436.00 Hz
 PRG : 31
 SCANS : 16 times
 SLVNT : CDCl3
 SPINNING : 12.7 Hz
 TEMP : 27.3 C

¹H NMR



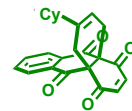
S5int

internal-cyhex

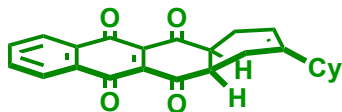


Date : Thu Dec 26 07:54:50 2013
 FileName : .LoadingID.mdata
 Comment : internal-cyhex
 SI:cellhistory :
 SNAME : bcc
 POINT : 32768 points
 SAMPLE : 32768 points
 FREQ : 26881.7 Hz
 FILTER : 13450 Hz
 DELAY : 14.9 usec
 DEADT : 19.0 usec
 INTVL : 37.2 usec
 TIMES : 7500 times
 DUMMY : 1 times
 PD : 3.0000 sec
 ACQTM : 1218.9588 msec
 PREDL : 0.01000 msec
 INVT : 1000.0000 msec
 RESOL : 0.32 Hz
 FWH : 6.55 usec
 OBUS : 13C
 OBFSD : 20.45 MHz
 OBFSE : 104750.00 Hz
 PRG : 35
 SCANS : 7500 times
 SLVNT : CDCl3
 SPINNING : 13 Hz
 TEMP : 28.2 C

¹³C NMR



S5int



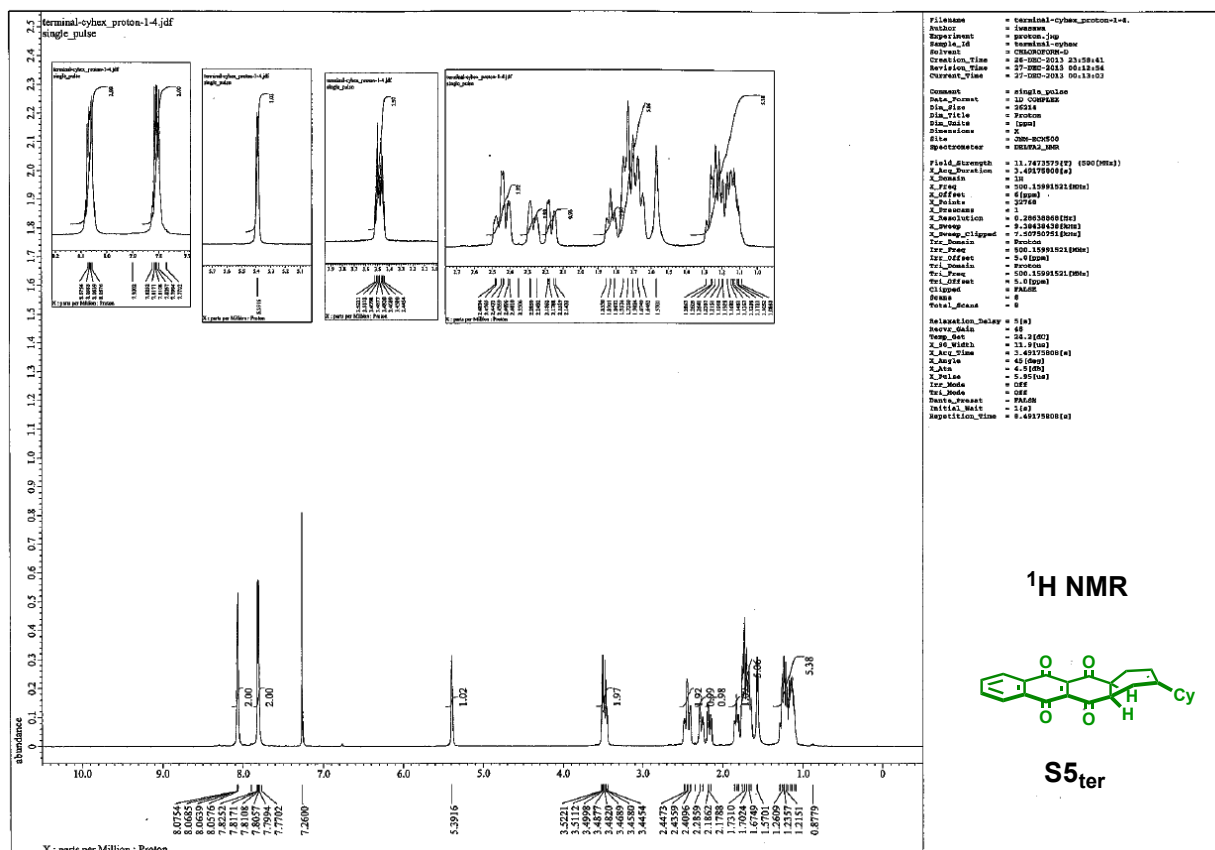
Physical data of **S5_{ter}**

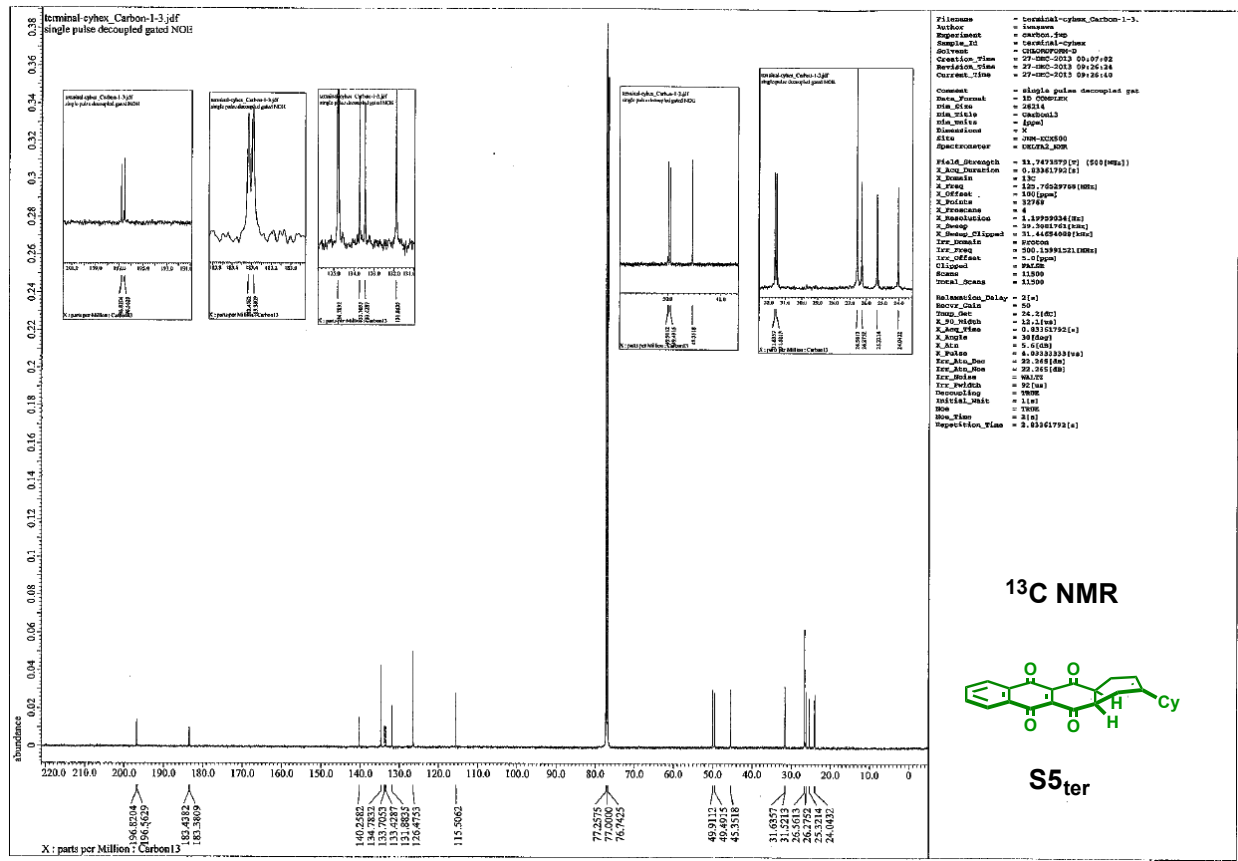
¹H NMR (500 MHz, CDCl₃): δ 8.07-8.06 (m, 2H), 7.82-7.77 (m, 2H), 5.39 (br, 1H), 3.52-3.45 (m, 2H), 2.44 (dt, *J* = 18.6, 4.3 Hz, 2H), 2.27 (d, *J* = 18.6 Hz, 1H), 2.17 (dd, *J* = 18.6 Hz, 1H), 1.83 (t, *J* = 11.5 Hz, 1H), 1.76-1.65 (m, 5H), 1.29-1.09 (m, 5H).

¹³C NMR (125 MHz, CDCl₃): δ 196.8, 196.6, 183.4, 183.4, 140.3, 134.8, 133.7, 133.4, 131.9, 126.5, 115.5, 49.9, 49.5, 45.4, 31.6, 31.5, 26.6, 26.3, 25.3, 24.0.

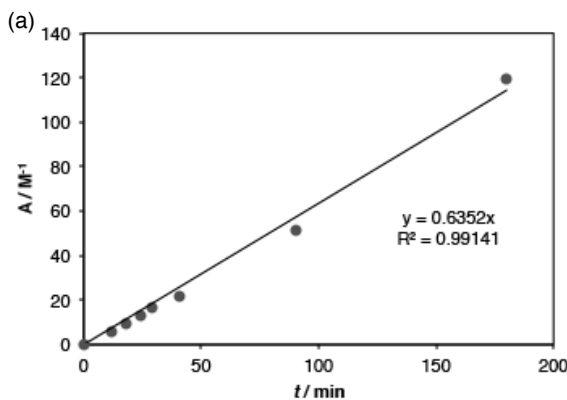
HRMS (FAB⁺, NBA): *m/z* Calcd. for C₂₄H₂₄O₄: 375.1674., Found: 376.1646 [M+2H]⁺. The peak derived from reduction product was observed in MS analysis.

IR (ATR): 1707, 1665, 1592, 1492, 1453, 1279, 1222, 1180 cm⁻¹.





Condition: Table 2 entry 11



(b)

t/min	Conversion %	[I]	[11]	A/M ⁻¹
0	0	0.00656	0.01037	0.0000
12	6	0.00617	0.00998	6.0853
18	9	0.00597	0.00978	9.3699
24	12	0.00578	0.00958	12.8336
29	15	0.00558	0.00939	16.4918
41	19	0.00532	0.00912	21.7023
90	37	0.00413	0.00794	51.2942
180	61	0.00256	0.00637	119.2066

(c) $k = 0.64 \text{ min}^{-1} \text{ M}^{-1}$

Fig. S23 (a) Second-order plot (A / M^{-1} vs. t / min) (b) table of time dependence of conversion, [I], [11] and A and (c) reaction rate

Condition: Table 2 entry 12

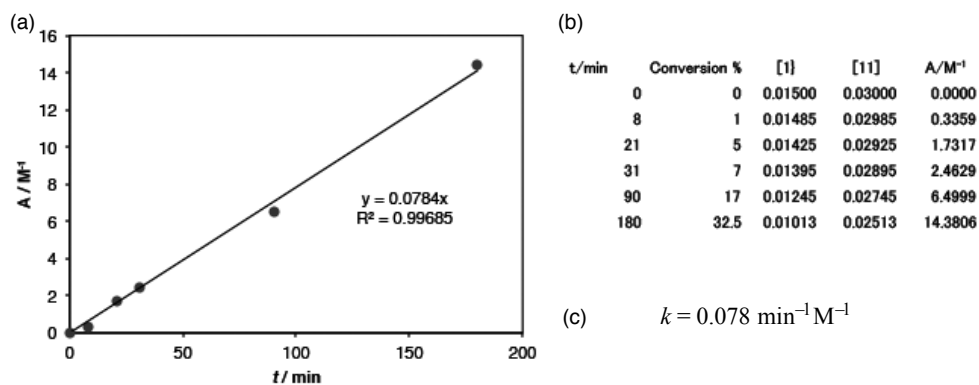
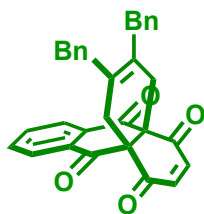


Fig. S24 (a) Second-order plot (A / M^{-1} vs. t / min) (b) table of time dependence of conversion, [1], [11] and A and (c) reaction rate



Physical data of **S6_{int}**

¹H NMR (500 MHz, CDCl₃): δ 8.05-8.04 (m, 2H), 7.77-7.74 (m, 2H), 7.28 (d, $J = 7.5$ Hz, 4H), 7.19 (t, $J = 7.5$ Hz, 2H), 7.12 (d, $J = 7.5$ Hz, 4H), 6.71 (br, 2H), 3.57 (q, $J = 12.9$ Hz, 4H), 2.59 (br, 4H).

¹³C NMR (125 MHz, CDCl₃): δ 193.4, 191.7, 139.4, 138.5, 135.1, 133.1, 128.5, 128.4, 127.9, 127.7, 126.3, 65.4, 38.7, 31.7.

HRMS (FAB⁺, NBA): m/z Calcd. for C₃₂H₂₄O₄: 472.1675., Found: 472.1699 [M]⁺.

IR (ATR): 2920, 1710, 1684, 1593, 1494, 1260, 1074 cm⁻¹.

ITC study revealed that the association constants of adducts **S1_{int}**, **S4_{int}** and **S6_{int}** were almost 0 M⁻¹. The binding behavior of **[2+2]_{crown}** containing K⁺ with **S6_{int}** was also examined by ¹H NMR study. **[2+2]_{crown}** (2.0 mM), 2 equivalents of KOTf (4.0 mM), and 1 equivalent of **S6_{int}** (2.0 mM) were mixed in CDCl₃/CD₃CN (0.8 mL, 1:1) and ¹H NMR spectrum was measured at 303 K. No obvious shift of proton signals of **S6_{int}** was observed, compared with the signal of free **S6_{int}** (Fig. S25a,b).

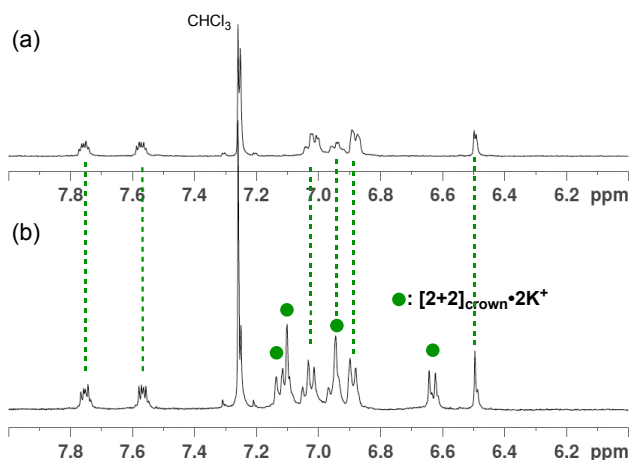
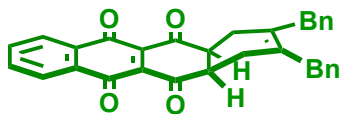


Fig. S25 Partial ¹H NMR spectra (400 MHz, CDCl₃/CD₃CN (1:1)) of (a) **S6_{int}** and (b) a mixture of **[2+2]_{crown}** (2.0 mM), **S6_{int}** (2.0 mM), and KOTf (4.0 mM).



Physical data of **S6_{ter}**

¹H NMR (500 MHz, CDCl₃): δ 8.06-8.04 (m, 2H), 7.82-7.79 (m, 2H), 7.29 (t, *J* = 7.2 Hz, 4H), 7.16-7.20 (m, 6H), 3.60-3.51 (q, *J* = 14.3 Hz, 4H), 3.48 (t, *J* = 4.1 Hz, 2H), 2.43 (dd, *J* = 16.9, 4.1 Hz, 2H), 2.20 (dd, *J* = 18.0, 4.1 Hz, 2H).

¹³C NMR (125 MHz, CDCl₃): δ 196.5, 183.3, 139.1, 134.8, 133.6, 131.8, 128.6, 128.4, 128.2, 126.5, 126.2, 49.8, 38.8, 28.3.

HRMS (FAB⁺, NBA): *m/z* Calcd. for C₃₂H₂₆O₄: 474.1831., Found: 474.1815 [M+2H]⁺. The peak derived from reduction product was observed in MS analysis.

IR (ATR): 1717, 1706, 1666, 1594, 1285 cm⁻¹.

Condition: Table 2 entry 13

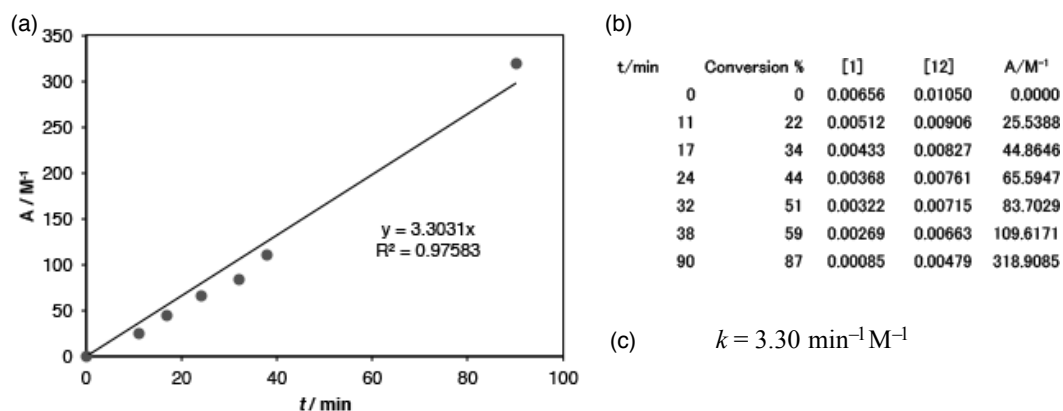


Fig. S26 (a) Second-order plot (A / M^{-1} vs. t / min) (b) table of time dependence of conversion, [1], [12] and A and (c) reaction rate

Condition: Table 2 entry 14

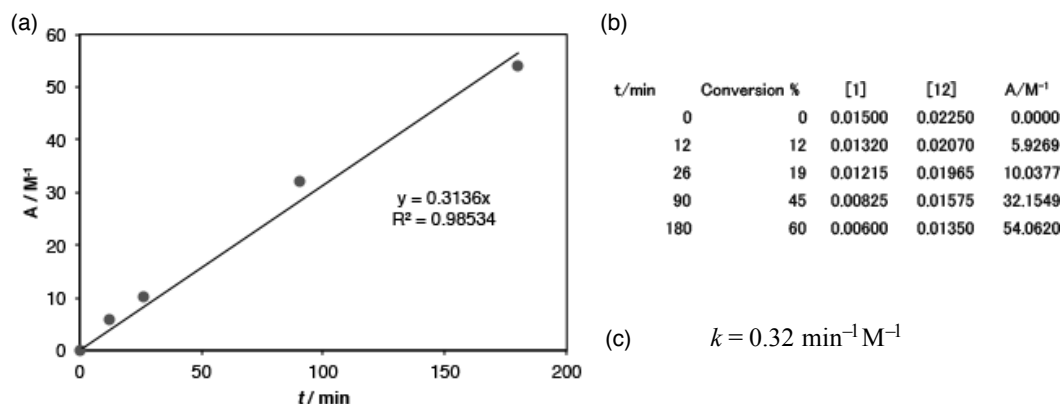
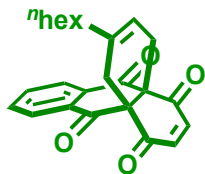


Fig. S27 (a) Second-order plot (A / M^{-1} vs. t / min) (b) table of time dependence of conversion, [1], [12] and A and (c) reaction rate



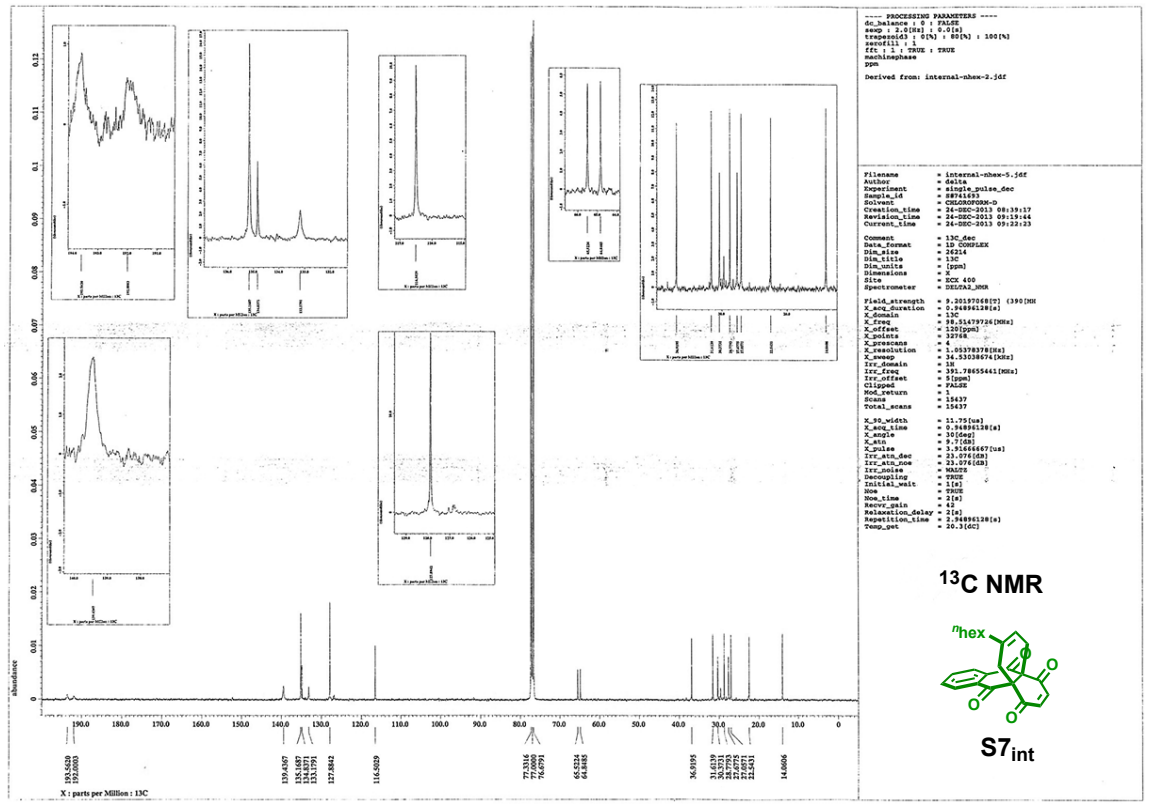
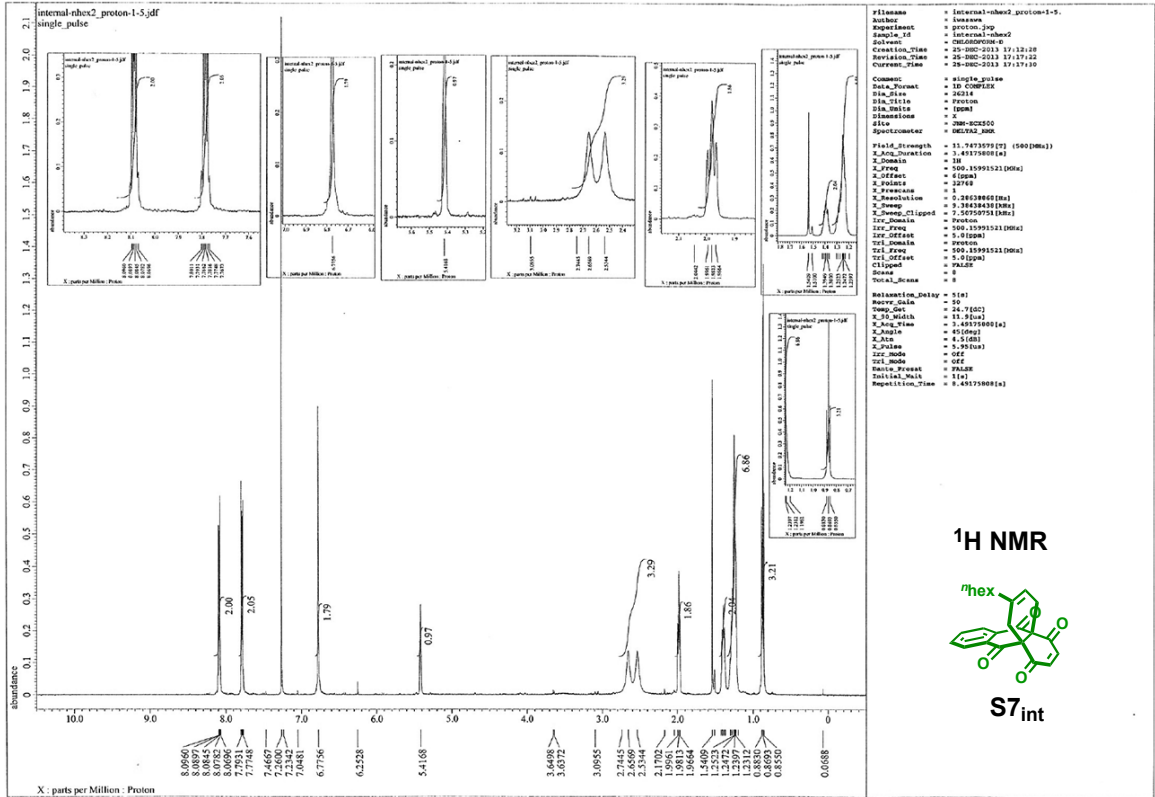
Physical data of **S7_{int}**

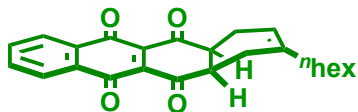
¹H NMR (500 MHz, CDCl₃): δ 8.10-8.07 (m, 2H), 7.80-7.77 (m, 2H), 6.77 (br, 2H), 5.42 (br, 1H), 2.66 (br, 2H), 2.53 (br, 2H), 1.98 (t, $J = 7.45$ Hz, 2H), 1.39-1.38 (m, 2H), 1.25-1.23 (m, 6H), 0.87 (t, $J = 7.2$ Hz, 3H).

¹³C NMR (125 MHz, CDCl₃): δ 193.6, 192.0, 139.4, 135.2, 134.8, 133.2, 127.9, 116.5, 65.5, 64.8, 36.9, 31.6, 30.4, 28.8, 27.7, 27.1, 22.5, 14.1.

HRMS (FAB⁺, NBA): m/z Calcd. for C₂₄H₂₄O₄: 376.1675., Found: 376.1648 [M]⁺.

IR (ATR): 2926, 2856, 1712, 1679, 1592, 1466, 157, 1427, 1365, 1257, 1084, 1067 cm⁻¹.





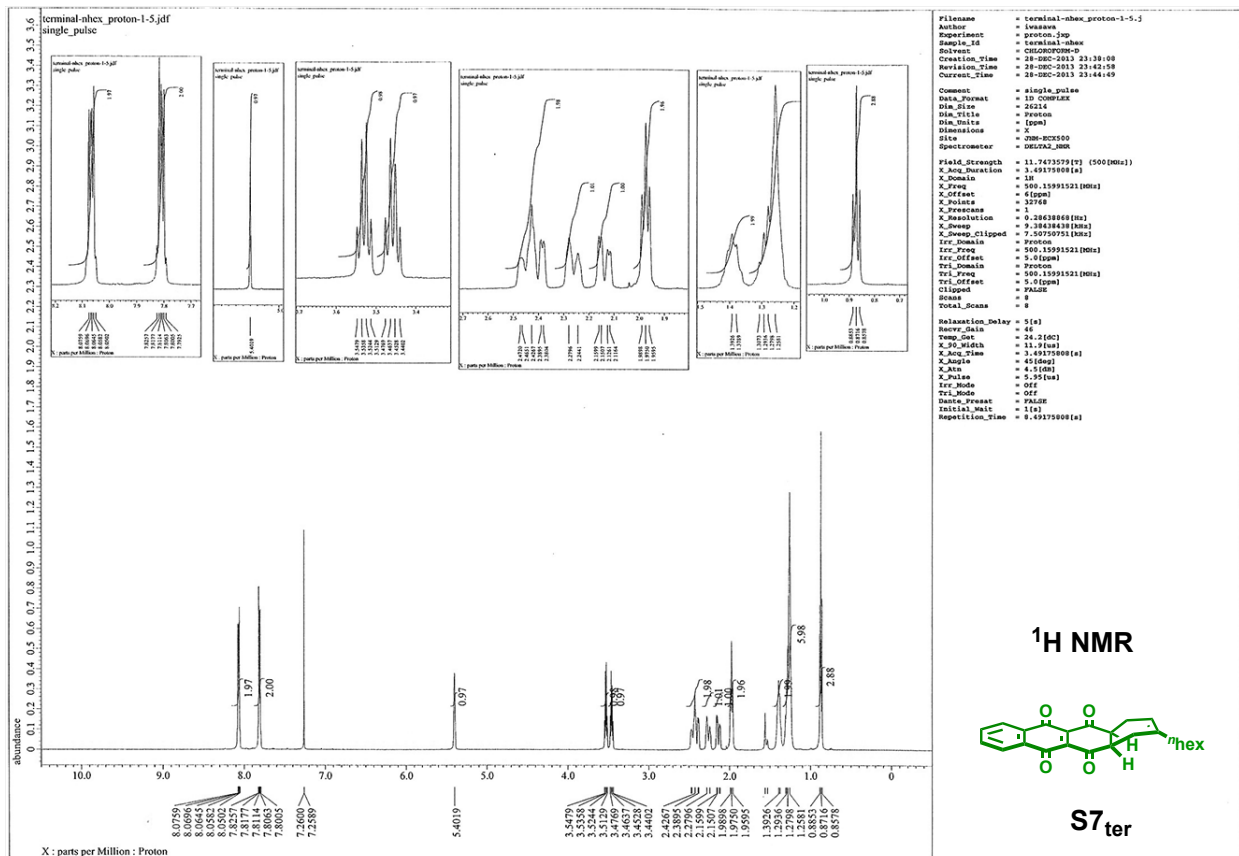
Physical data of **S7_{ter}**

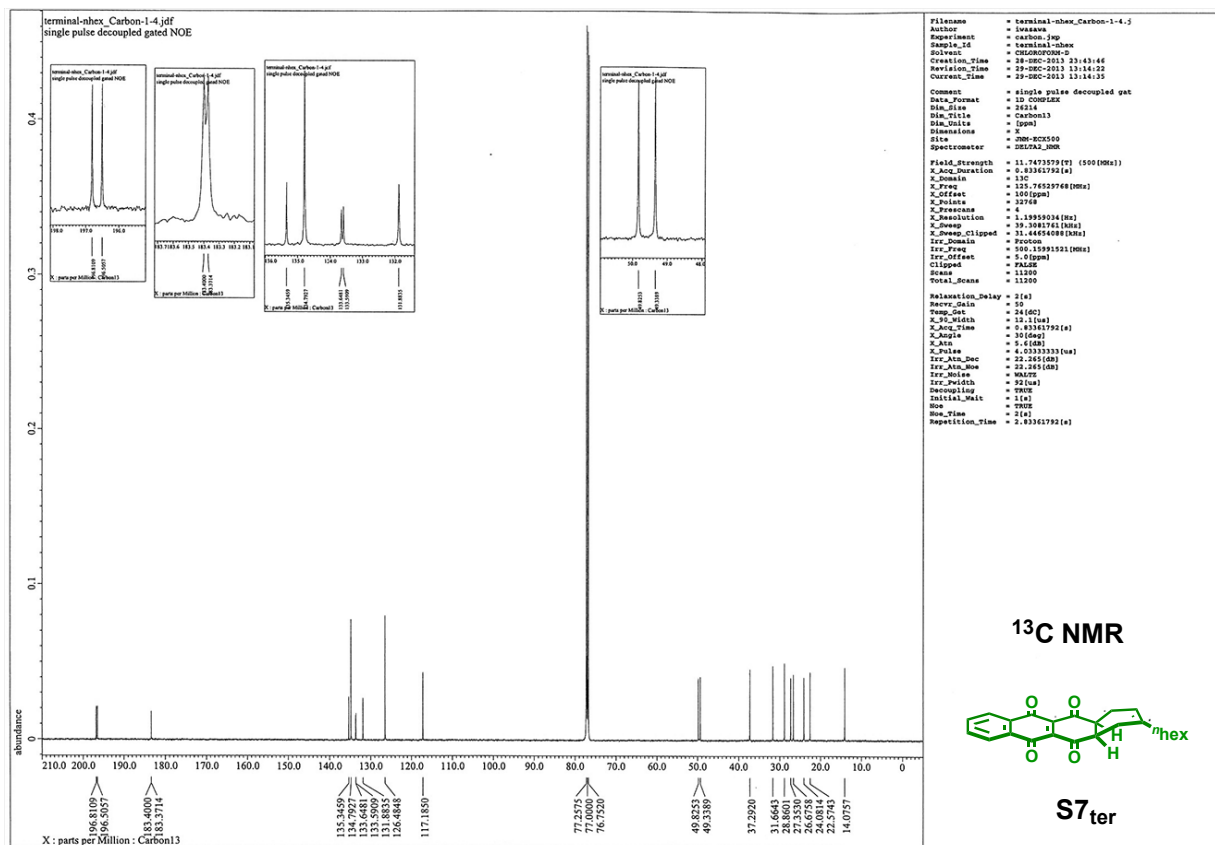
¹H NMR (500 MHz, CDCl₃): δ 8.08-8.05 (m, 2H), 7.83-7.80 (m, 2H), 5.40 (br, 1H), 3.53 (q, *J* = 5.5 Hz, 1H), 3.45 (q, *J* = 5.5 Hz, 1H), 2.47-2.38 (m, 2H), 2.28-2.24 (m, 1H), 2.16-2.12 (m, 1H), 1.98 (t, *J* = 7.8 Hz, 2H), 1.39-1.38 (m, 2H), 1.31-1.26 (m, 6H), 0.87 (t, *J* = 7.2 Hz, 3H).

¹³C NMR (125 MHz, CDCl₃): δ 196.8, 196.5, 183.4, 183.4, 135.3, 134.8, 133.6, 133.6, 131.9, 126.5, 117.2, 49.8, 49.3, 37.3, 31.7, 28.9, 27.4, 26.7, 24.1, 22.6, 14.1.

HRMS (FAB⁺, NBA): *m/z* Calcd. for C₂₄H₂₆O₄: 378.1831., Found: 378.1856 [M+2H]⁺.

IR (ATR): 1717, 1706, 1668, 1593, 1287 cm⁻¹.



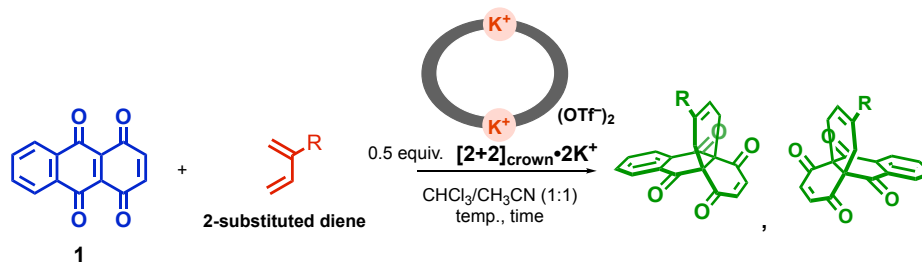


4-2-2. The Enantioselective Diels-Alder Reaction of **1** with 2-Substituted 1,3-Butadienes

The enantioselectivities of the reaction of **1** and various 2-substituted 1,3-butadienes in the presence of chiral host catalyst $[2+2]_{\text{crown}} \cdot 2\text{K}^+$ were examined (Table S1). Chirality induction was slightly observed (up to 19% ee). It also suggested that $[2+2]_{\text{crown}}$ framework recognized the substituent of dienes and the reaction proceeded inside the host.

Typical experiment: **1** (10.5 μmol), 2-substituted 1,3-butadiene, $[2+2]_{\text{crown}}$ (5.25 μmol), and KOTf (10.5 μmol) were dissolved in 0.8 mL of $\text{CHCl}_3/\text{CH}_3\text{CN}$ (1:1) in a test tube and the solution was stirred at -10°C for 3h. The reaction mixture was evaporated, dissolved in dichloromethane and washed with water. The organic layer was concentrated under reduced pressure, followed by purification by GPC to afford the product. The enantiomeric excess (*ee*) of the product was determined by HPLC using Chiralpak IF column (DAICEL, 4.6 mm ϕ x 250 mm) [EtOAc/hexane (20:80)]; flow rate 1.0 mL/min, UV detector 254 nm (Fig. S28).

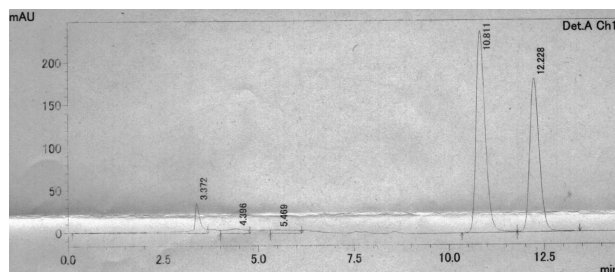
Table S1 The enantioselective Diels-Alder reaction of **1** with 2-substituted 1,3-butadienes in the presence of $[2+2]_{\text{crown}} \cdot 2\text{K}^+$



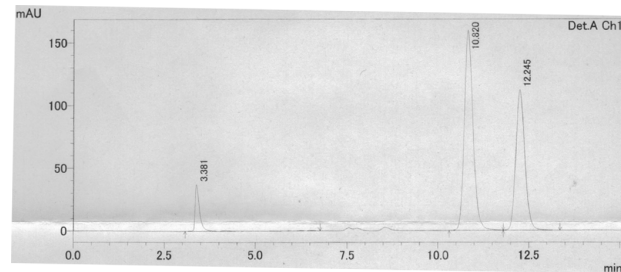
entry	diene	temp.	time	ee %
1		rt	3 h	11% ee
2	3 equiv.	-10 °C	3 h	15% ee
3		-40 °C	3 h	19% ee
4 ^a		rt	3 h	12% ee
5 ^b		rt	24 h	11% ee
6		2.5 equiv.	-10 °C	3 h
7 ^c	-10 °C		3 h	15% ee
8	1.5 equiv.		-40 °C	3 h
9	2.5 equiv.	-10 °C	3 h	9% ee
10	2.5 equiv.	-10 °C	3 h	1% ee
11	2.5 equiv.	-10 °C	3 h	0.5% ee

^a KPF₆ was employed. ^b Solvent was CH₃CN only. ^c 1 equiv. [2+2]crown•2K⁺ and 2 equiv. KOTf were employed.

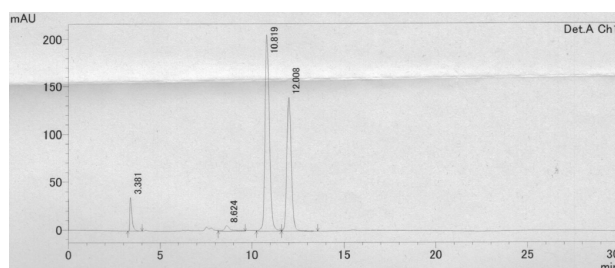
entry 1



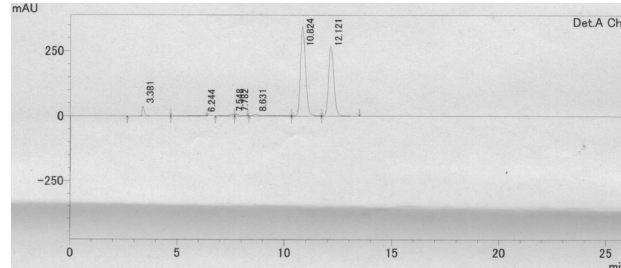
entry 2



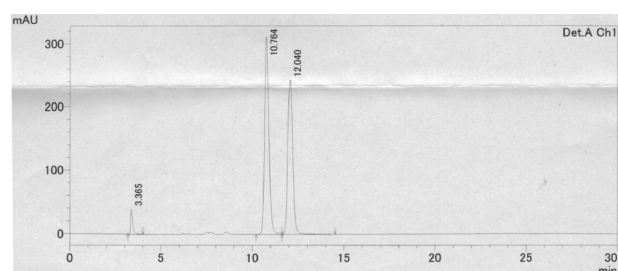
entry 3



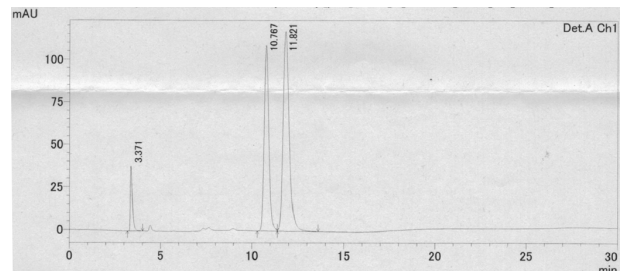
entry 4



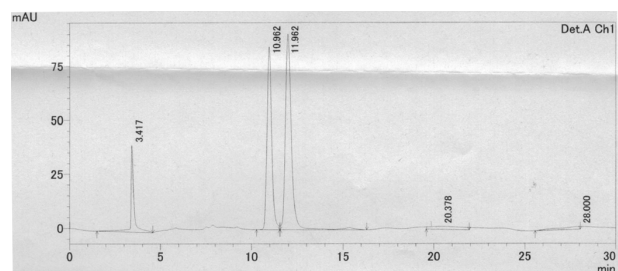
entry 5



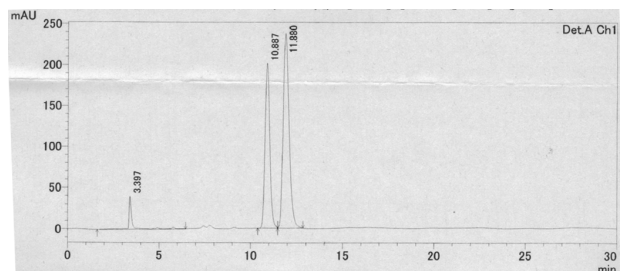
entry 6



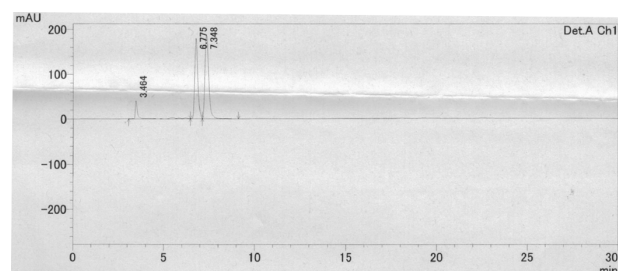
entry 7



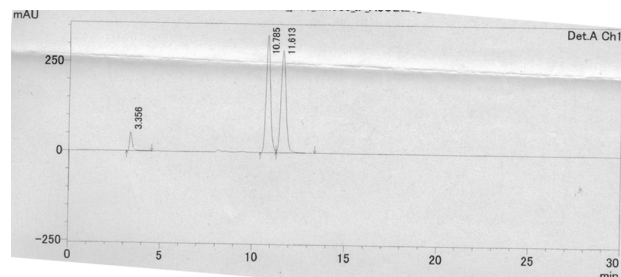
entry 8



entry 9



entry 10



entry 11

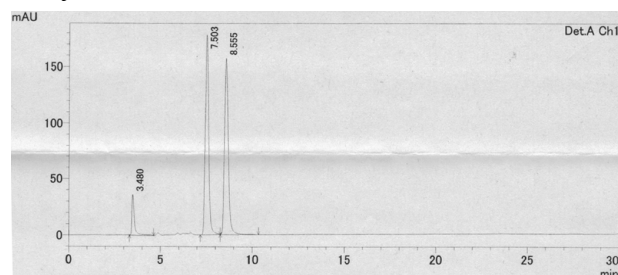
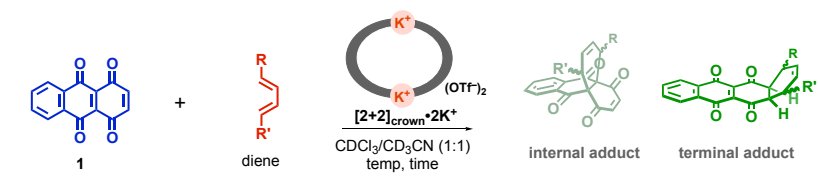


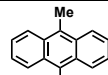
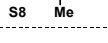
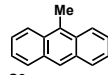

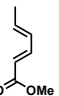
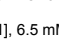
Fig. S28 HPLC charts

4-3. The Diels-Alder Reaction of **1** with 1-Mono and 1,4-Di-substituted 1,3-Butadienes

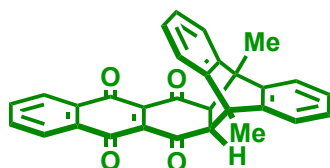
The limitation of applicable diene in this system was also assessed with 1-mono, and 1,4-di-substituted 1,3-butadienes **S8**, **S9**, and **S10** (Table S1). In the reaction with these dienes, the acceleration of the reaction was not observed clearly, and terminal adduct was obtained as major product regardless of whether the catalyst was used. This result indicates that substituents at 1- or 1,4-position of 1,3-butadienes are too much steric hindrance for this reaction.

Table S2 The Diels-Alder reaction of 1 and S8, S9 or S10 in the presence or absence of [2+2]_{crown}•2K⁺ ^a



Entry	Diene	[2+2] _{crown} •2K ⁺	Temp.	Time	Yield ^b	
					Internal	Terminal
1	1.5 equiv. 	1.0 equiv.	-10 °C	4 h	none	45%
2	S8 	none	-10 °C	4 h	none	34%
3	1.5 equiv. 	1.0 equiv.	27 °C	1.5 h	none	68%
4	S9 	none	27 °C	1.5 h	trace	61%
5	3.0 equiv. 	1.0 equiv.	60 °C	4 h	none	44%
6	S10 	none	60 °C	4 h	trace	14%

^a Reaction conditions: [1], 6.5 mM; [KOTf], 13 mM; 0.8 mL CDCl₃/CD₃CN (1:1). ^b NMR yield.



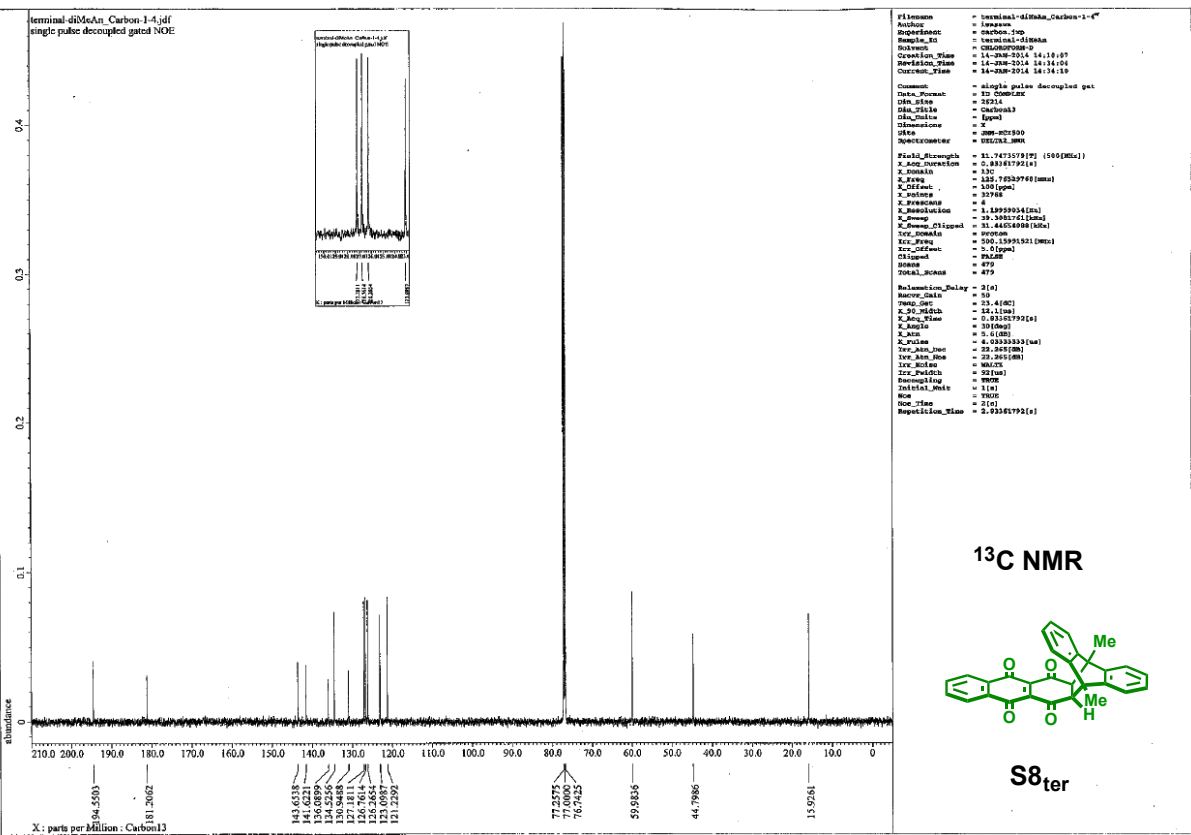
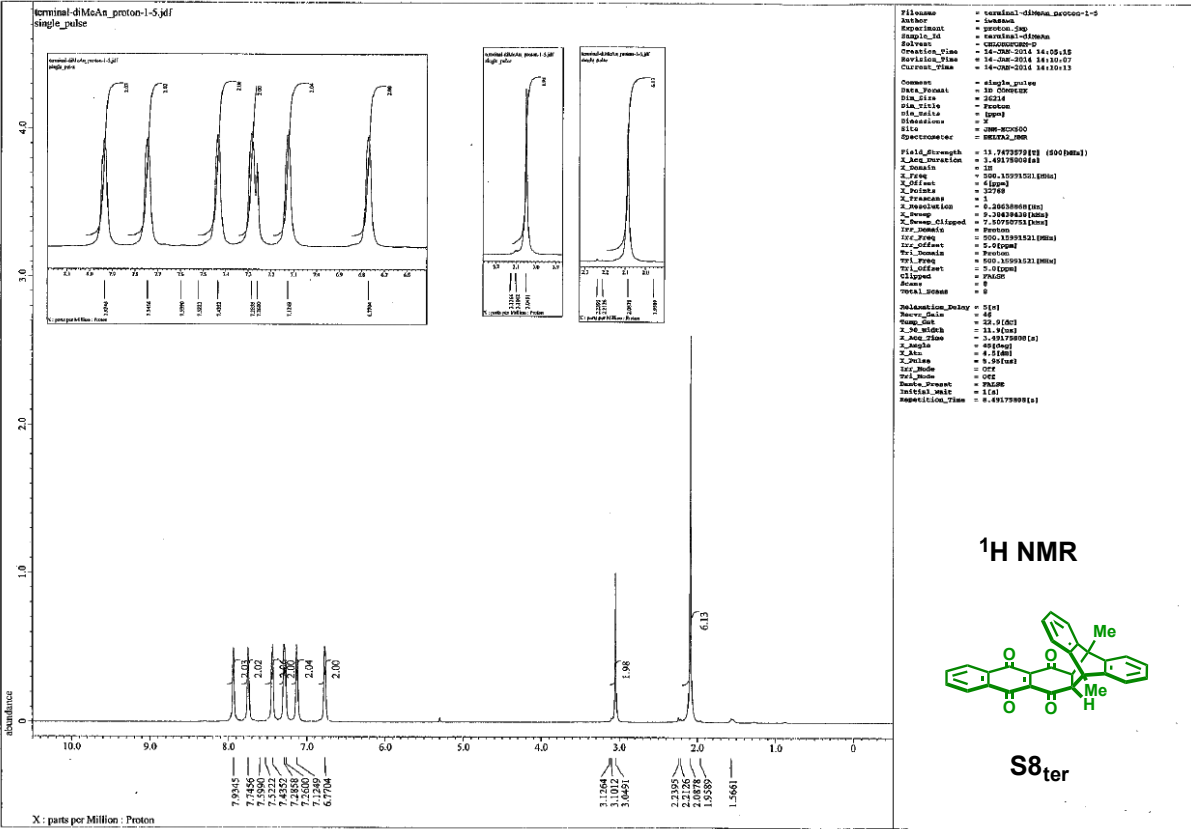
Physical data of **S8_{ter}**

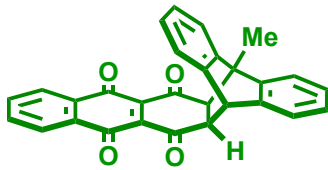
¹H NMR (500 MHz, CDCl₃): δ 7.93 (br, 2H), 7.75 (br, 2H), 7.44 (br, 2H), 7.29 (br, 2H), 7.12 (br, 2H), 6.77 (br, 2H), 3.04 (s, 2H), 2.09 (s, 6H).

¹³C NMR (125 MHz, CDCl₃): δ 194.6, 181.2, 143.7, 141.6, 136.1, 134.5, 130.9, 127.2, 126.8, 126.3, 123.1, 121.2, 60.0, 44.8, 15.9.

HRMS (FAB⁺, NBA): *m/z* Calcd. for C₃₀H₂₁O₄: 445.1440, Found: 445.1460 [M+H]⁺.

IR (ATR): 1710, 1661, 1590, 1454, 1386, 1291, 1272, 1191, 908 cm⁻¹.





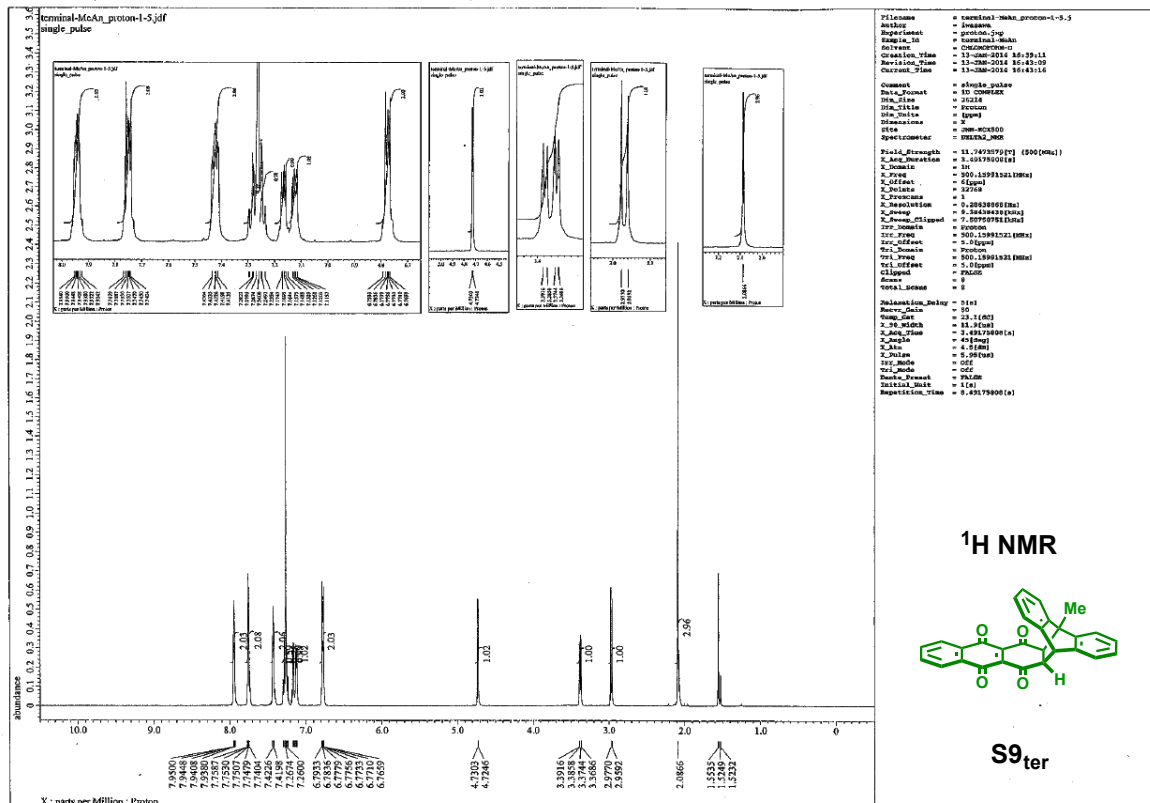
Physical data of **S9_{ter}**

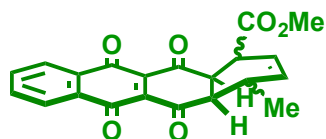
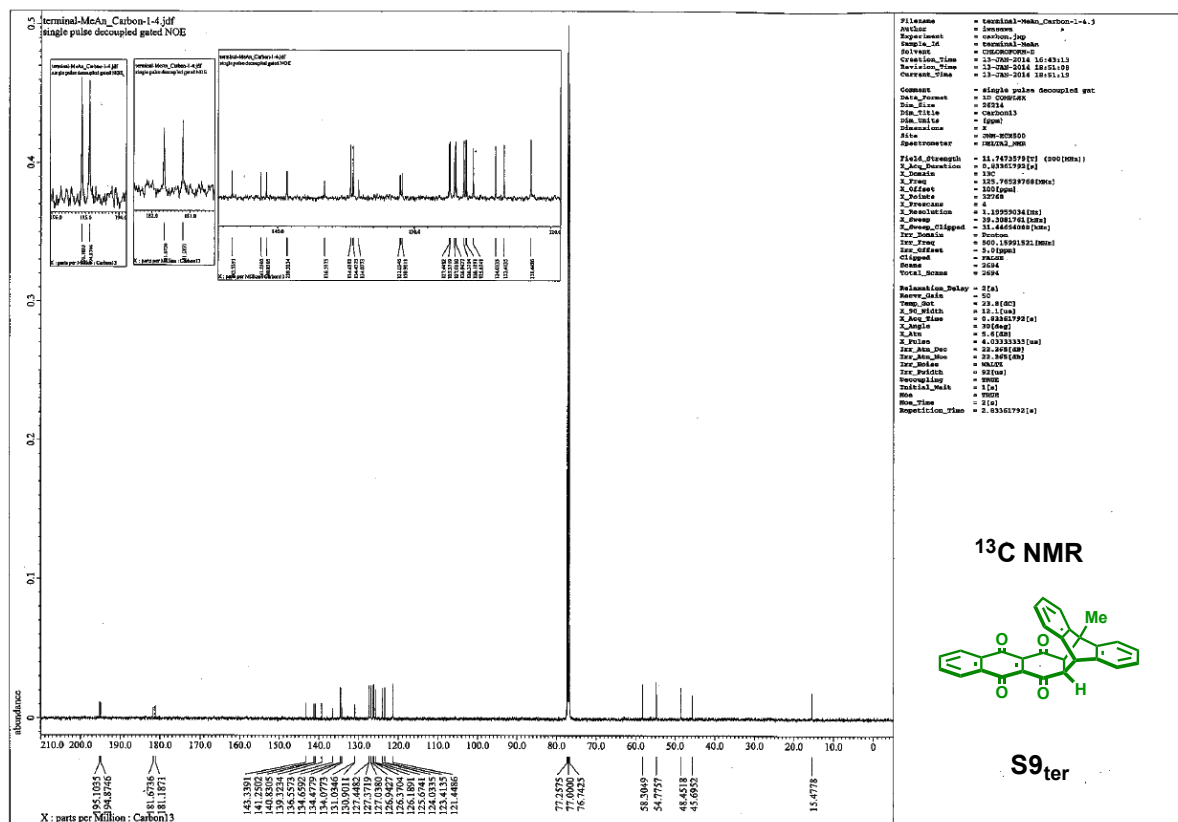
¹H NMR (500 MHz, CDCl₃): δ 7.95-7.92 (m, 2H), 7.77-7.74 (m, 2H), 7.41-7.44 (m, 2H), 7.28-7.23 (m, 2H), 7.17-7.15 (m, 1H), 7.13-7.12 (m, 1H), 6.79-6.77 (m, 2H), 4.73 (d, *J* = 2.9 Hz, 1H), 3.38 (dd, *J* = 8.8 Hz, 1H), 2.97 (d, *J* = 8.8 Hz, 1H), 2.09 (s, 3H).

¹³C NMR (125 MHz, CDCl₃): δ 195.1, 194.9, 181.7, 181.2, 143.3, 141.3, 140.8, 139.3, 136.6, 134.7, 134.5, 134.1, 131.0, 130.9, 127.4, 127.4, 127.0, 126.9, 126.4, 126.2, 125.7, 124.0, 123.4, 121.4, 58.3, 54.8, 48.5, 45.7, 15.5.

HRMS (FAB⁺, NBA): *m/z* Calcd. for C₂₉H₁₉O₄: 438.1284, Found: 431.1298 [M+H]⁺.

IR (ATR): 1705, 1660, 1591, 1455, 1387, 1286, 1272, 1173 cm⁻¹.





Physical data of **S10_{ter}**

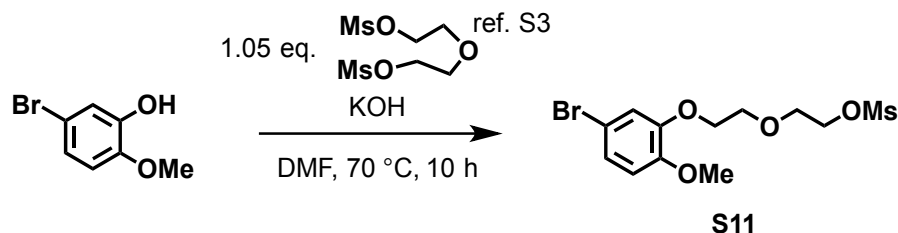
¹H NMR (500 MHz, CDCl₃): δ 8.09-8.05 (br, 2H), 7.84-7.80 (br, 2H), 6.18-6.15 (m, 1H), 5.71-5.75 (m, 1H), 4.10-4.09 (m, 1H), 3.75 (s, 3H), 3.63 (t, *J* = 6.9 Hz, 1H), 3.34-3.31 (m, 1H), 2.82-2.77 (m, 1H), 0.95 (d, *J* = 7.5 Hz, 3H).

¹³C NMR (125 MHz, CDCl₃): δ 196.8, 194.6, 182.7, 136.2, 134.9, 134.8, 133.9, 132.0, 131.7, 130.8, 126.5, 121.5, 52.4, 52.1, 49.1, 40.0, 31.0, 17.7.

HRMS (FAB⁺, NBA): *m/z* Calcd. for C₂₁H₁₈O₆: 336.1103, Found: 336.1125 [M+2H]⁺. The peak derived from reduction product was observed in MS analysis.

IR (ATR): 1710, 1668, 1591, 1435, 1277, 1191, 908 cm⁻¹.

5. Experimental Procedure and Characterization of New Compounds



To a DMF (100 mL) solution of 5-Bromo-2-methoxyphenol (5.42 g, 26.7 mmol) was added KOH (1.57 g, 27.9 mmol) and the mixture was heated at 70 °C for 1 h. After cooling at room temperature, to this solution was added a DMF (60 ml) solution of bis-[2-(methylsulfonyl)oxyethyl]ether (10.5 g, 40.1 mmol). After the mixture was heated at 70 °C for 10 h, the reaction mixture was quenched with water. The organic materials were extracted with ethyl acetate three times, and the combined extracts were washed with brine, and dried over MgSO₄. After removal of the solvent under reduced pressure, the residue was purified by silica gel column chromatography (*n*-hexane/ethyl acetate = 1:1), and white solid of **S11** was obtained (4.77 g, 48% yield).

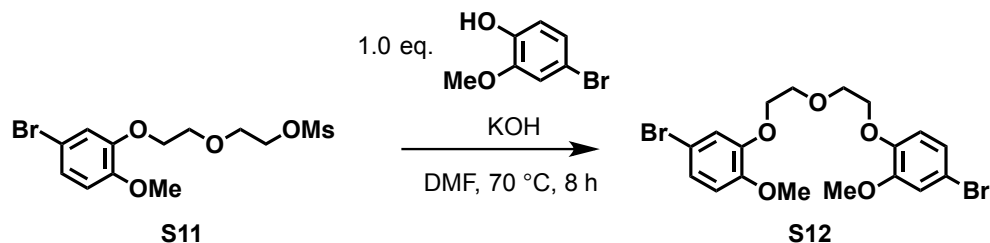
Physical data of **S11**

¹H NMR (500 MHz, CDCl₃): δ 7.05 (dd, *J* = 8.5, 2.1 Hz, 1H), 7.01 (d, *J* = 2.1 Hz, 1H), 6.74 (d, *J* = 8.5 Hz, 1H), 4.39-4.41 (m, 2H), 4.14-4.16 (m, 2H), 3.88-3.90 (m, 2H), 3.83-3.85 (m, 2H), 3.82 (s, 3H), 3.06 (s, 3H).

¹³C NMR (125 MHz, CDCl₃): δ 148.8, 148.8, 124.2, 117.0, 113.0, 112.5, 69.6, 69.2, 68.7, 56.0, 37.7.

HRMS (FAB⁺, NBA): *m/z* Calcd. for C₁₂H₁₇O₆BrS: 367.9929., Found: 367.9420 [M]⁺.

IR (ATR): 1586, 1507, 1350, 1254, 1224, 1173, 1129, 1023, 1016, 959, 812 cm⁻¹.



To a DMF (33 mL) solution of 4-Bromo-2-methoxyphenol (2.71 g, 12.7 mmol) was added KOH (712 mg, 12.7 mmol) and the mixture was heated at 70 °C for 1 h. After cooling at room temperature, to this solution was added a DMF (37 ml) solution of **S11** (4.71g, 12.7 mmol). After the mixture was heated at 70 °C for 8 h, the reaction mixture was quenched with water. The organic materials were extracted with ethyl acetate three times, and the combined extracts were washed with brine, and dried over MgSO₄. After removal of the solvent under reduced pressure, the residue was purified by silica gel column chromatography (*n*-

hexane/ethyl acetate = 2:1), and white solid of **S12** was obtained (4.83 g, 81% yield).

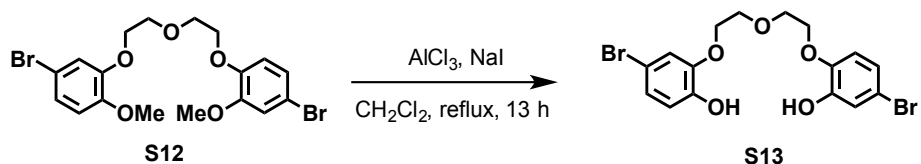
Physical data of **S12**

^1H NMR (500 MHz, CDCl_3): δ 7.04-7.01 (m, 2H), 6.99-6.96 (m, 2H), 6.78 (d, $J = 8.3$ Hz, 1H), 6.72-6.71 (m, 1H), 4.17-4.15 (m, 4H), 3.94-3.91 (m, 4H), 3.82 (s, 3H), 3.80 (s, 3H).

^{13}C NMR (125 MHz, CDCl_3): δ 150.4, 149.0, 148.9, 147.5, 123.9, 123.3, 117.0, 115.2, 115.2, 113.4, 113.0, 112.5, 69.8, 69.7, 68.9, 68.8, 56.1, 56.0.

HRMS (FAB $^+$, NBA): m/z Calcd. for $\text{C}_{19}\text{H}_{20}\text{O}_5\text{Br}_2$: 473.9677., Found: 473.9672 [M] $^+$.

IR (ATR): 1588, 1505, 1399, 1358, 1325, 1253, 1227, 1184, 1123, 1020, 965, 853, 841 cm^{-1} .



To a CH_2Cl_2 (100 mL) solution of **S12** (2 g, 4.2 mmol) was added AlCl_3 (3.36 g, 25.2 mmol) and NaI (6.29 g, 42 mmol). After the mixture was refluxed for 13 h, the reaction mixture was quenched with water. The organic materials were extracted with ethyl acetate three times, and the combined extracts were washed with brine, and dried over MgSO_4 . After removal of the solvent under reduced pressure, the residue was purified by silica gel column chromatography (*n*-hexane/ethyl acetate = 3:2), and colorless oil of **S13** was obtained (1.56 g, 83% yield).

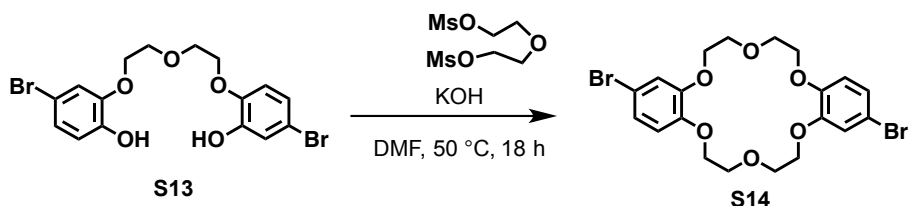
Physical data of **S13**

^1H NMR (500 MHz, CDCl_3): δ 7.13 (d, $J = 2.6$ Hz, 1H), 7.07-7.04 (m, 2H), 6.94 (dd, $J = 8.6, 2.6$ Hz, 1H), 6.86 (d, $J = 8.6$ Hz, 1H), 6.79 (d, $J = 8.6$ Hz, 1H), 4.19-4.15 (m, 4H), 3.87-3.83 (m, 4H).

^{13}C NMR (125 MHz, CDCl_3): δ 148.5, 146.7, 146.4, 145.1, 126.2, 123.0, 119.5, 119.1, 117.8, 117.5, 115.7, 111.2, 70.3, 69.9, 69.4, 69.4.

HRMS (FAB $^+$, NBA): m/z Calcd. for $\text{C}_{16}\text{H}_{16}\text{O}_5\text{Br}_2$: 445.9344., Found: 445.9335 [M] $^+$.

IR (ATR): 3392, 1490, 1455, 1362, 1259, 1216, 1115, 1050, 941, 870, 792 cm^{-1} .



To a DMF (70 mL) solution of **S13** (1.5 g, 3.34 mmol) was added KOH (0.39 g, 3.51 mmol) and the mixture was heated at 70 $^\circ\text{C}$ for 1 h. After cooling at room temperature, to this solution was added a DMF (60 mL) solution of bis[2-(methylsulfonyl)oxyethyl]ether (0.92 g, 3.51 mmol). After the mixture was heated at 70 $^\circ\text{C}$

for 10 h, the reaction mixture was quenched with water. The precipitate was filtered and washed with water and ethyl acetate, and dried to afford the white solid **S14** (1.28 g, 74% yield).

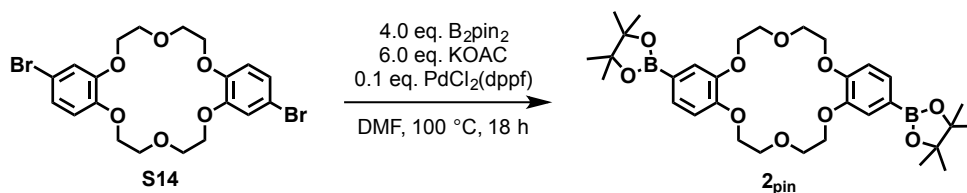
Physical data of **S14**

^1H NMR (500 MHz, CDCl_3): δ 7.00 (dd, $J = 6.7, 2.3$ Hz, 1H), 6.97 (d, $J = 2.3$ Hz, 1H), 6.73 (d, $J = 6.7$ Hz, 2H), 4.14-4.12 (m, 8H), 4.00-3.99 (m, 8H).

^{13}C NMR (125 MHz, CDCl_3): δ 149.5, 148.0, 123.8, 116.8, 114.9, 113.1, 69.9, 69.7, 69.0.

HRMS (FAB $^+$, NBA): m/z Calcd. for $\text{C}_{20}\text{H}_{22}\text{O}_6\text{Br}_2$: 513.9763., Found: 513.9756 [M] $^+$.

IR (ATR): 1506, 1252, 1227, 1134, 997, 931, 864 cm^{-1} .



To a DMF (27 mL) solution of **S14** (1.24 g, 2.39 mmol) was added $\text{PdCl}_2(\text{dppf})$ (174 mg, 0.239 mmol), B_2pin_2 (2.42 g, 9.57 mmol) and KOAc (1.40 g, 14.34 mmol). After the mixture was heated at 100 $^\circ\text{C}$ for 18 h, the reaction mixture was quenched with water. The organic materials were extracted with CH_2Cl_2 three times, and the combined extracts were washed with water five times and brine, and dried over MgSO_4 . After removal of the solvent under reduced pressure, the residue was purified by GPC to afford the desired product **2pin** (658 mg, 45% yield).

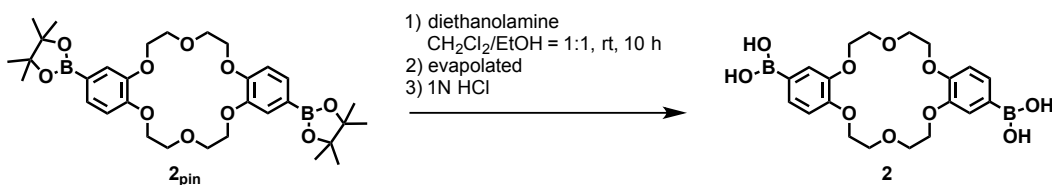
Physical data of **2pin**

^1H NMR (400 MHz, CDCl_3): δ 7.38 (dd, $J = 8.1, 1.2$ Hz, 2H), 7.27 (d, $J = 1.2$ Hz, 2H), 6.86 (d, $J = 8.1$ Hz, 2H), 4.23-4.21 (m, 2H), 4.17 (m, 2H), 4.06-4.04 (m, 2H), 4.02-4.00 (m, 2H), 1.32 (s, 24H).

^{13}C NMR (125 MHz, CDCl_3): δ 151.5, 148.1, 128.9, 121.3, 119.2, 112.6, 83.6, 70.0, 69.9, 69.0, 68.5, 24.9.

HRMS (FAB $^+$, NBA): m/z Calcd. for $\text{C}_{32}\text{H}_{46}\text{O}_{10}\text{Br}_2$: 612.3277., Found: 612.3274 [M] $^+$.

IR (ATR): 1601, 1520, 1419, 1353, 1300, 1258, 1217, 1138, 1060, 970 cm^{-1} .



To a $\text{CH}_2\text{Cl}_2/\text{EtOH}$ (9:1) (35 mL) solution of **2pin** (350 mg, 0.57 mmol) was added diethanolamine (0.35 mL, 3.42 mmol). After stirred at room temperature for 10 h, solvent was removed under reduced pressure. 1N HCl (10 mL) were added to the residue and stirred for 2 h, white precipitate was obtained by filtration. The precipitate was washed with water and CH_2Cl_2 , **2** (185 mg, 72% yield) was obtained.

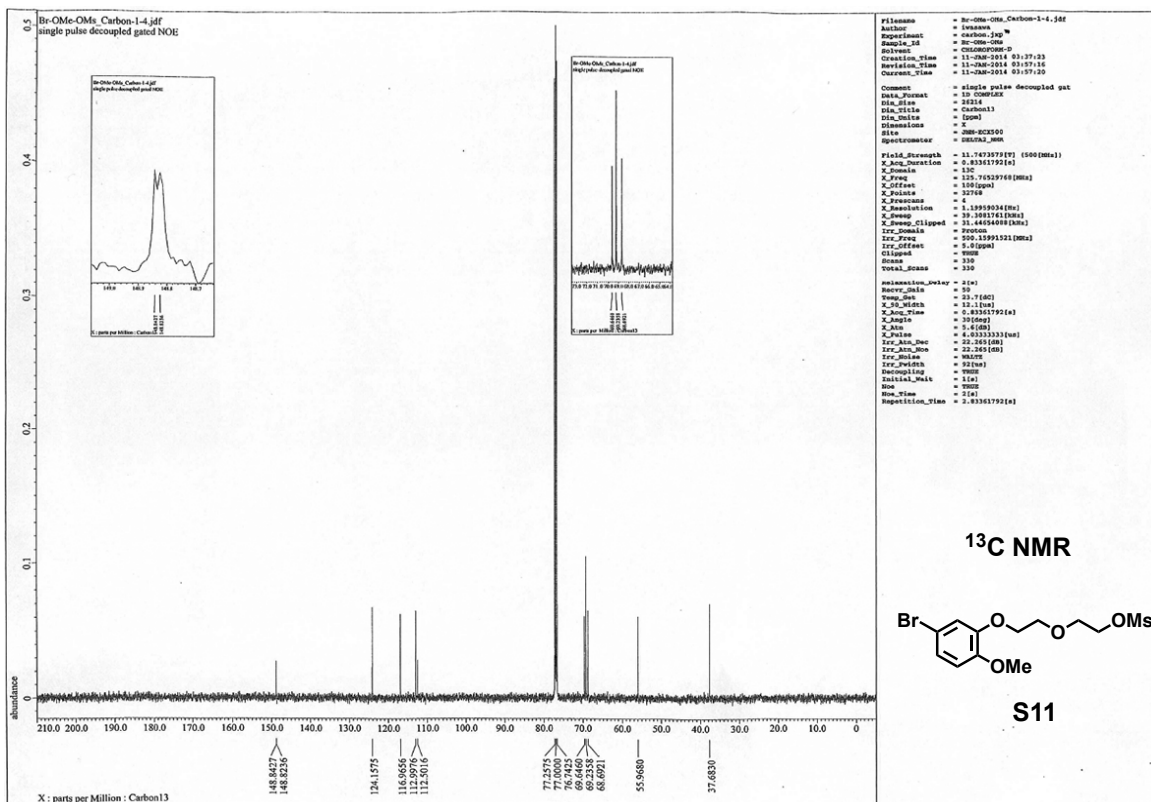
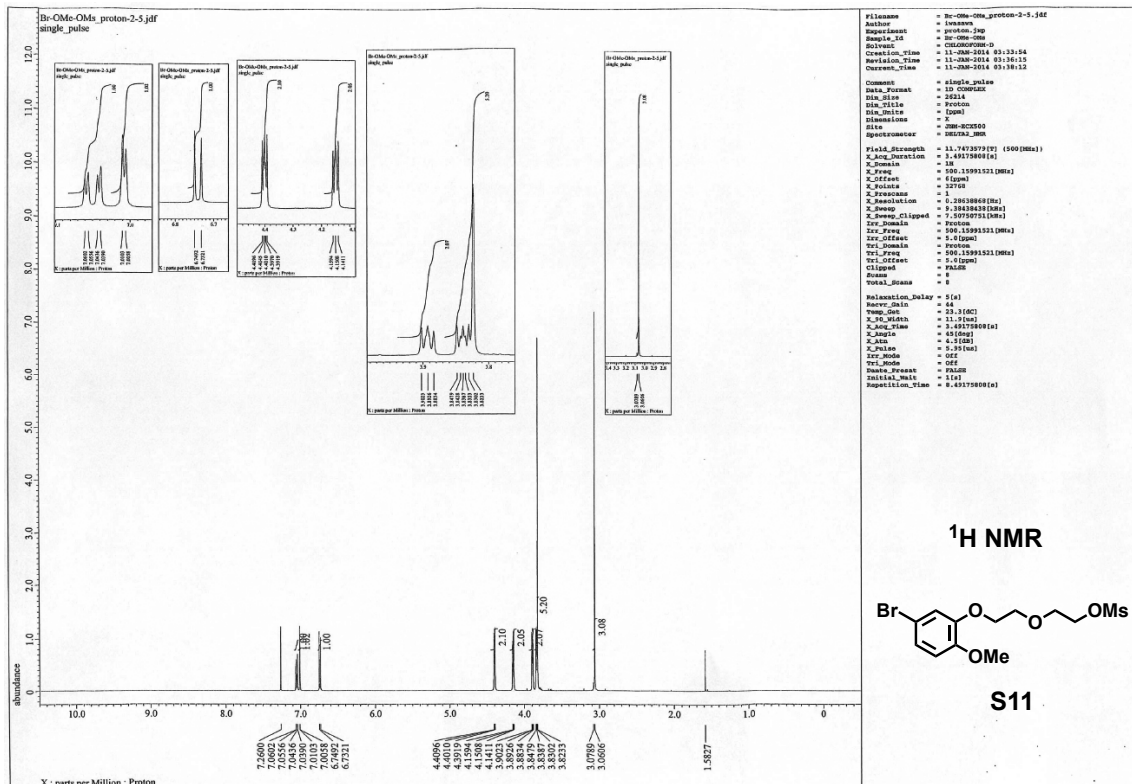
Physical data of **2**

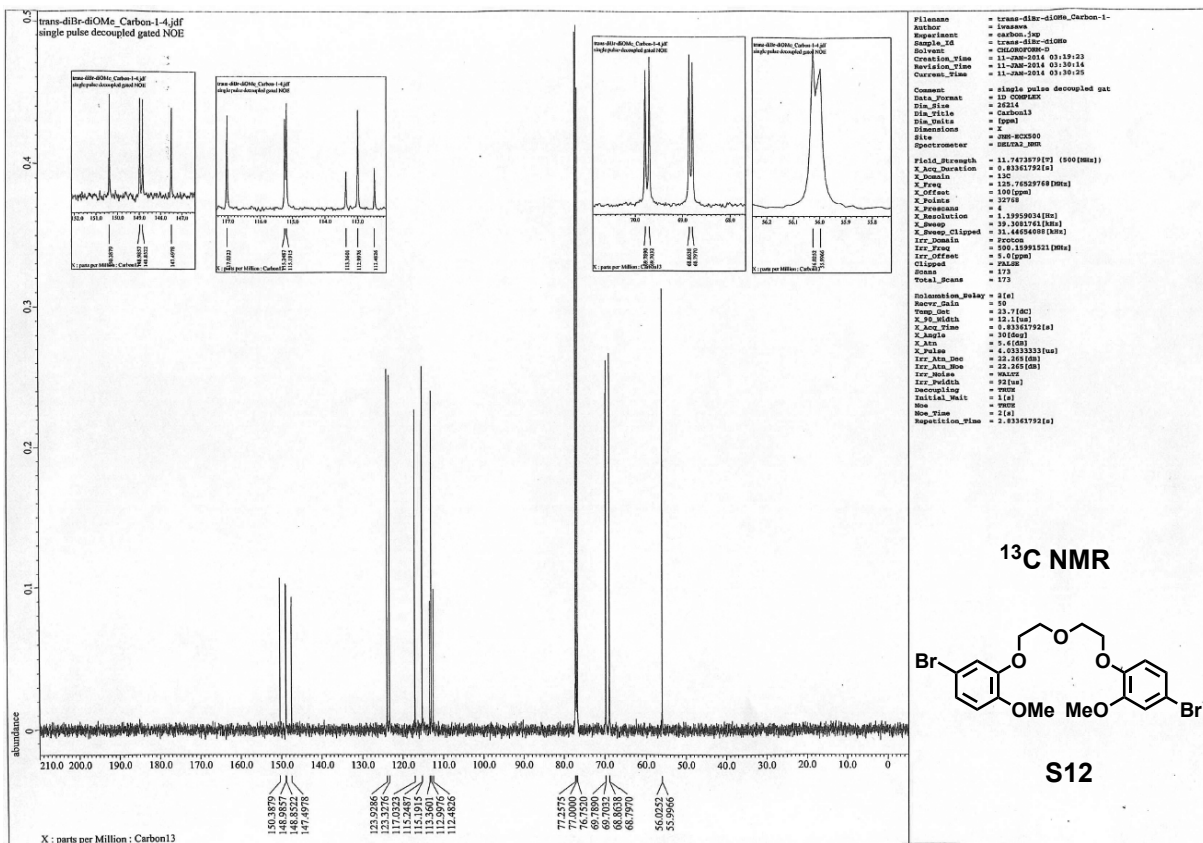
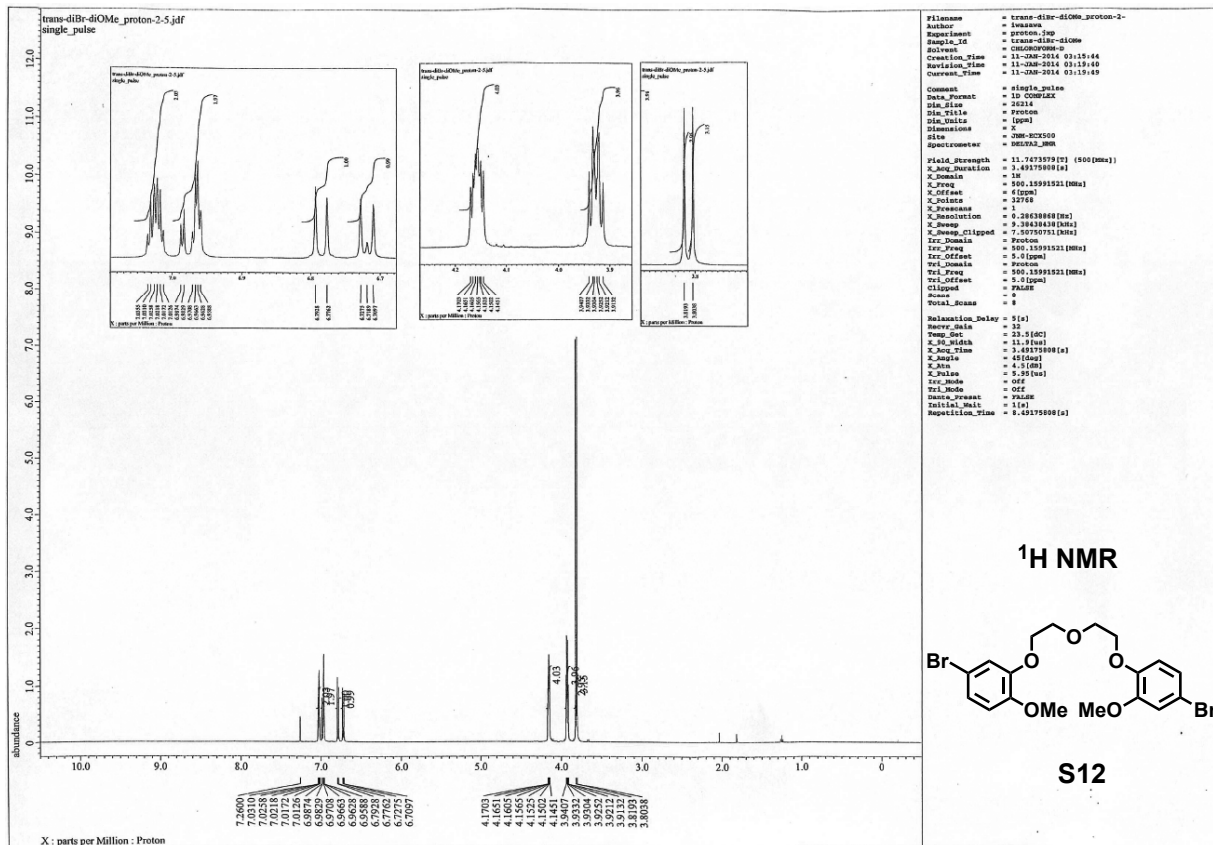
^1H NMR (500 MHz, DMSO- d_6): δ 7.85 (s, 4H), 7.36-7.35 (m, 4H), 6.90 (d, $J = 8.3$ Hz, 2H), 4.07 (br, 8H), 3.84 (br, 8H).

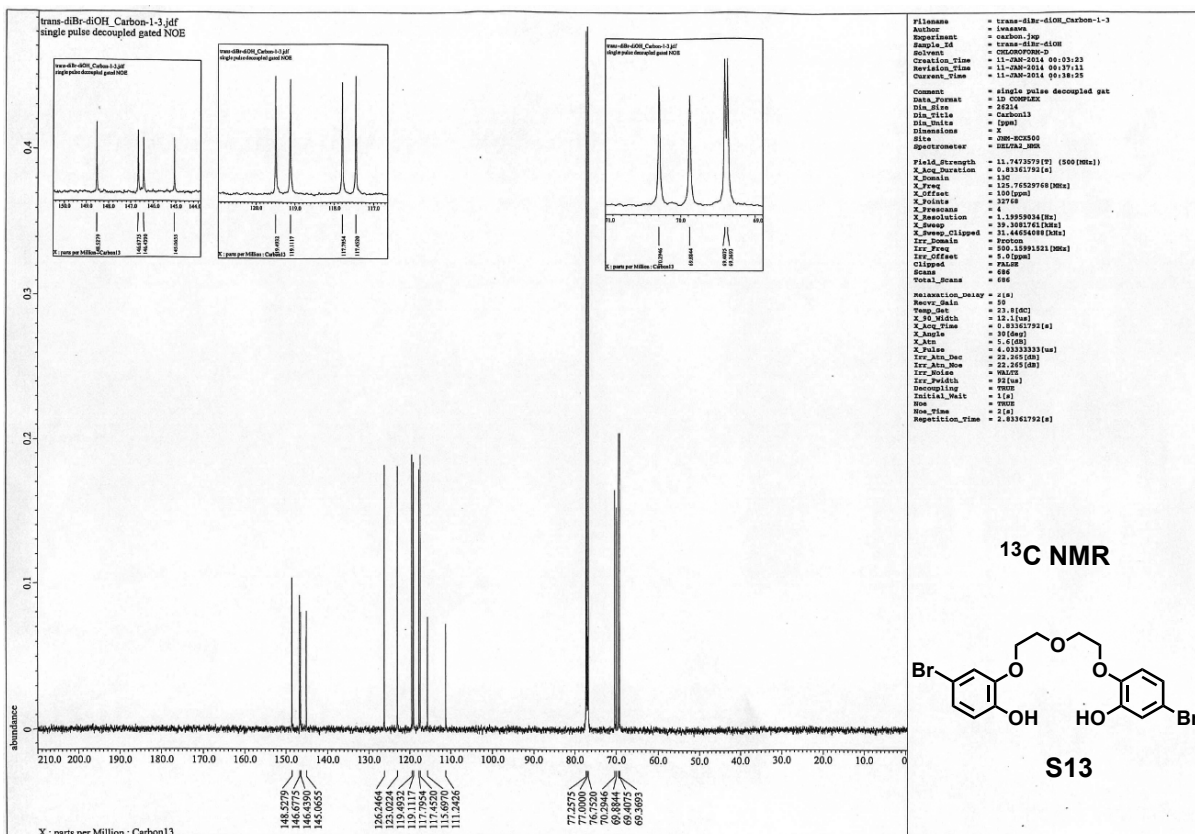
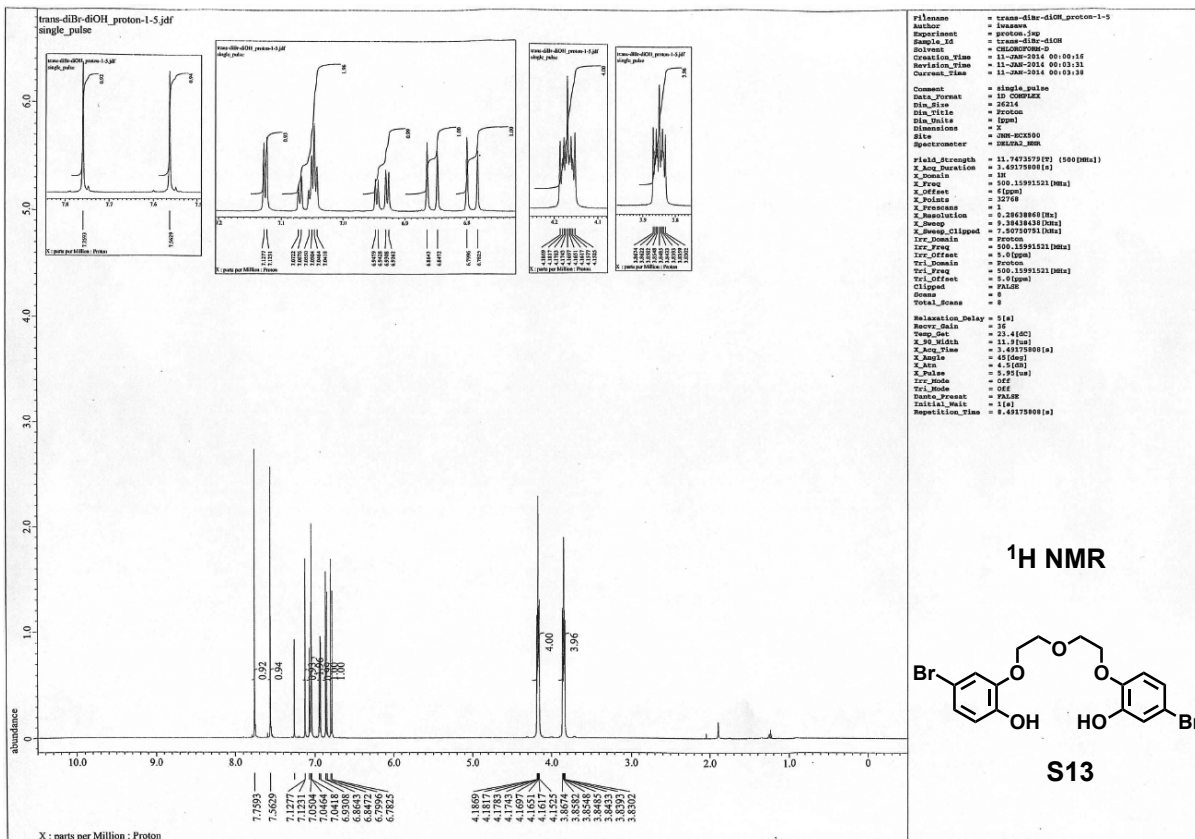
^{13}C NMR (125 MHz, DMSO- d_6): δ 149.7, 147.0, 127.6, 125.7, 117.6, 111.4, 69.0, 68.9, 67.5, 67.4.

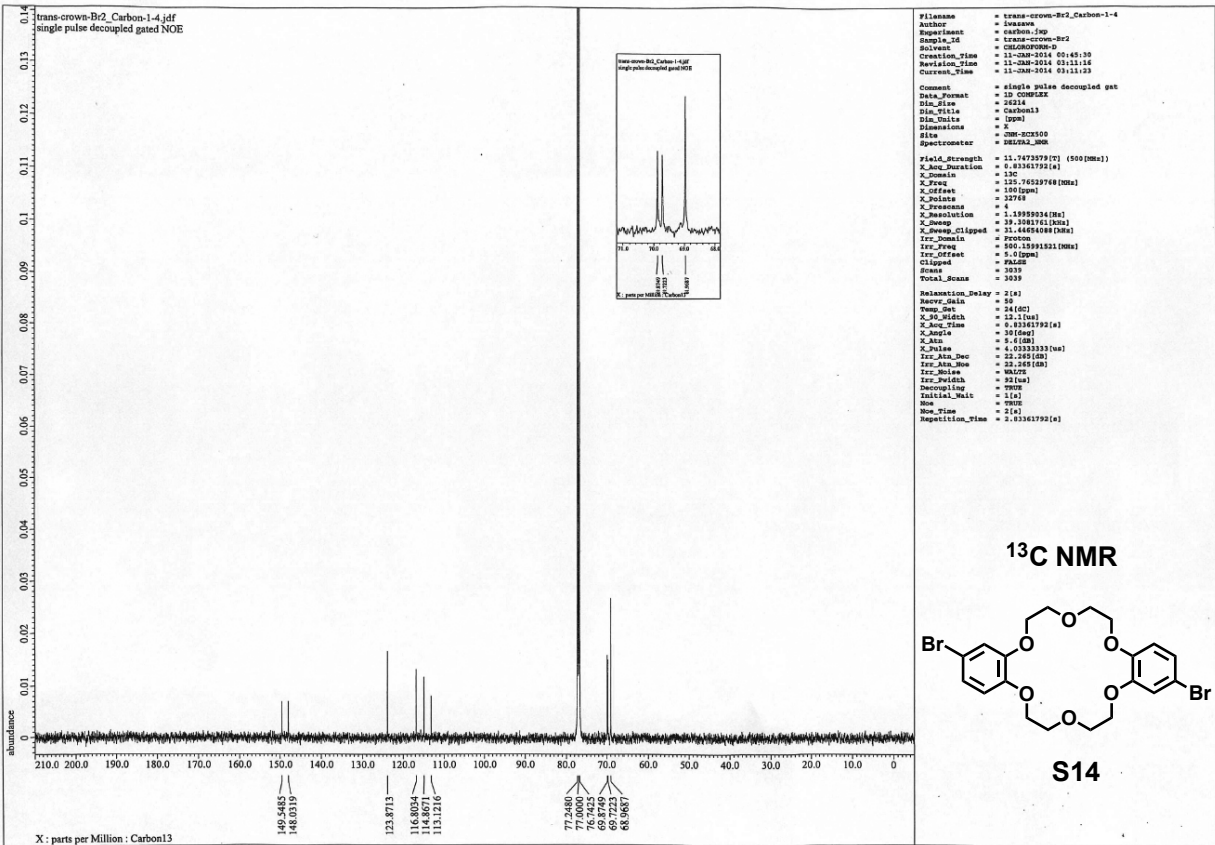
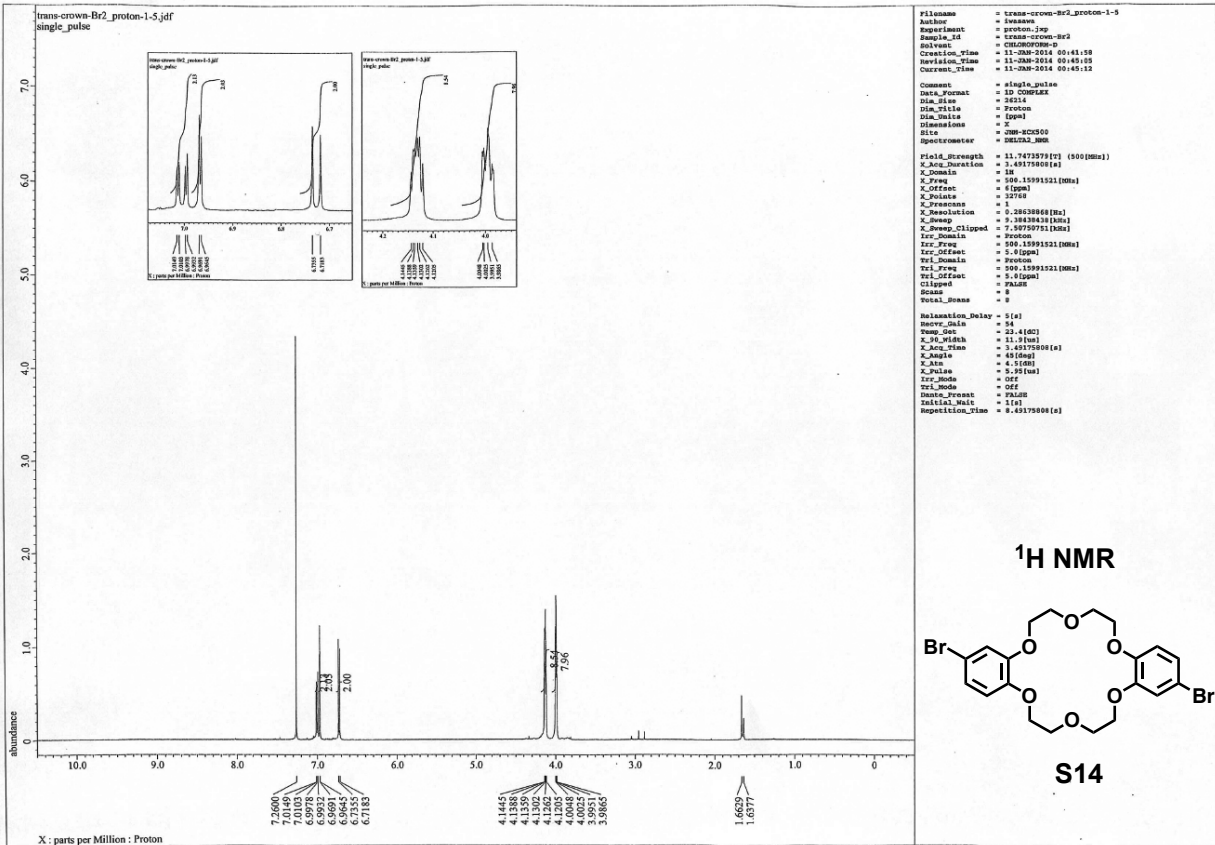
IR (ATR): 3363, 1601, 1519, 1420, 1388, 1349, 1315, 1257, 1227, 1157, 1121, 1087, 1052, 988, 942 cm^{-1} .

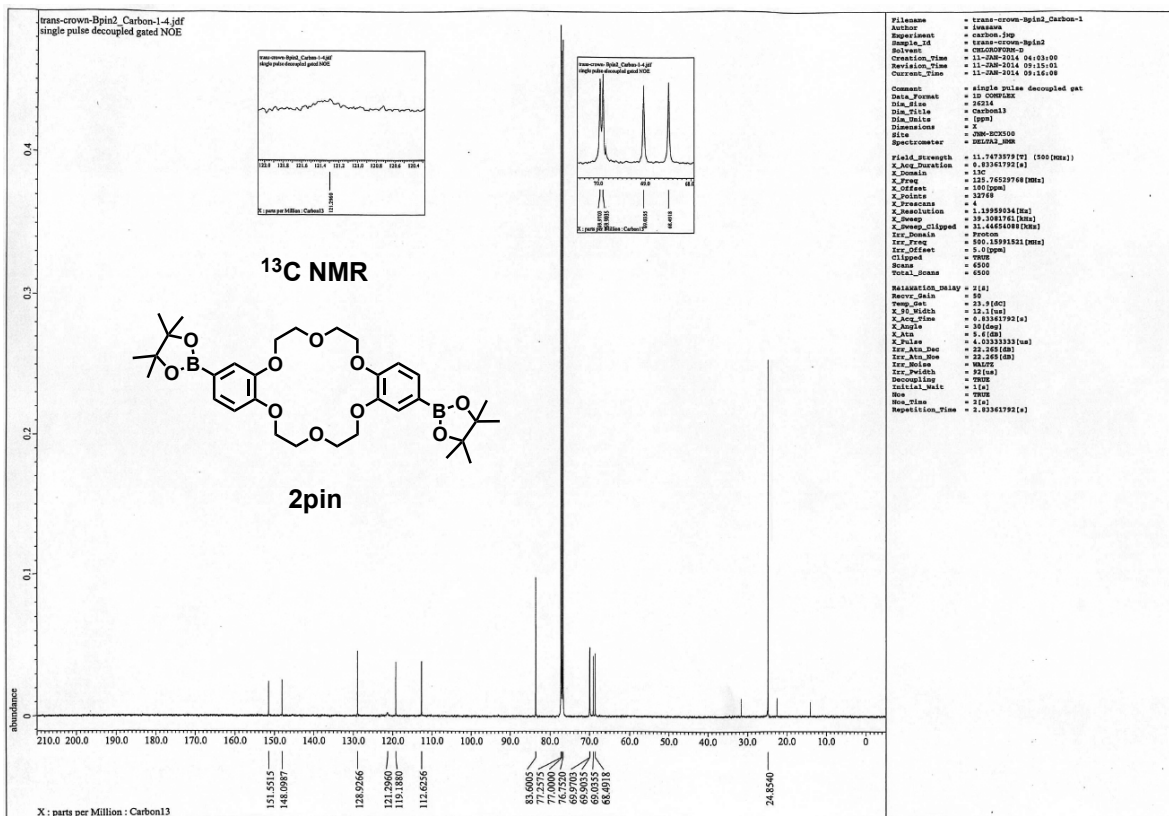
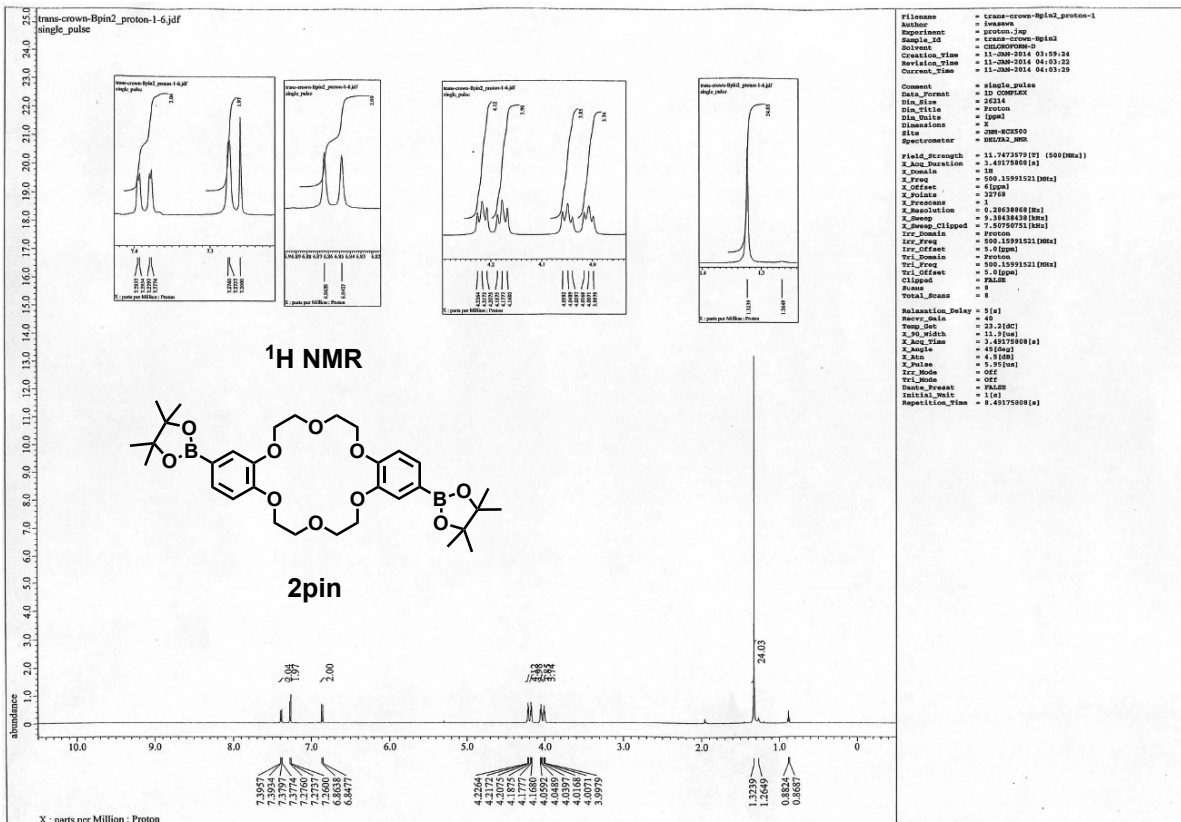
6. ¹H and ¹³C NMR Spectra of New Compounds

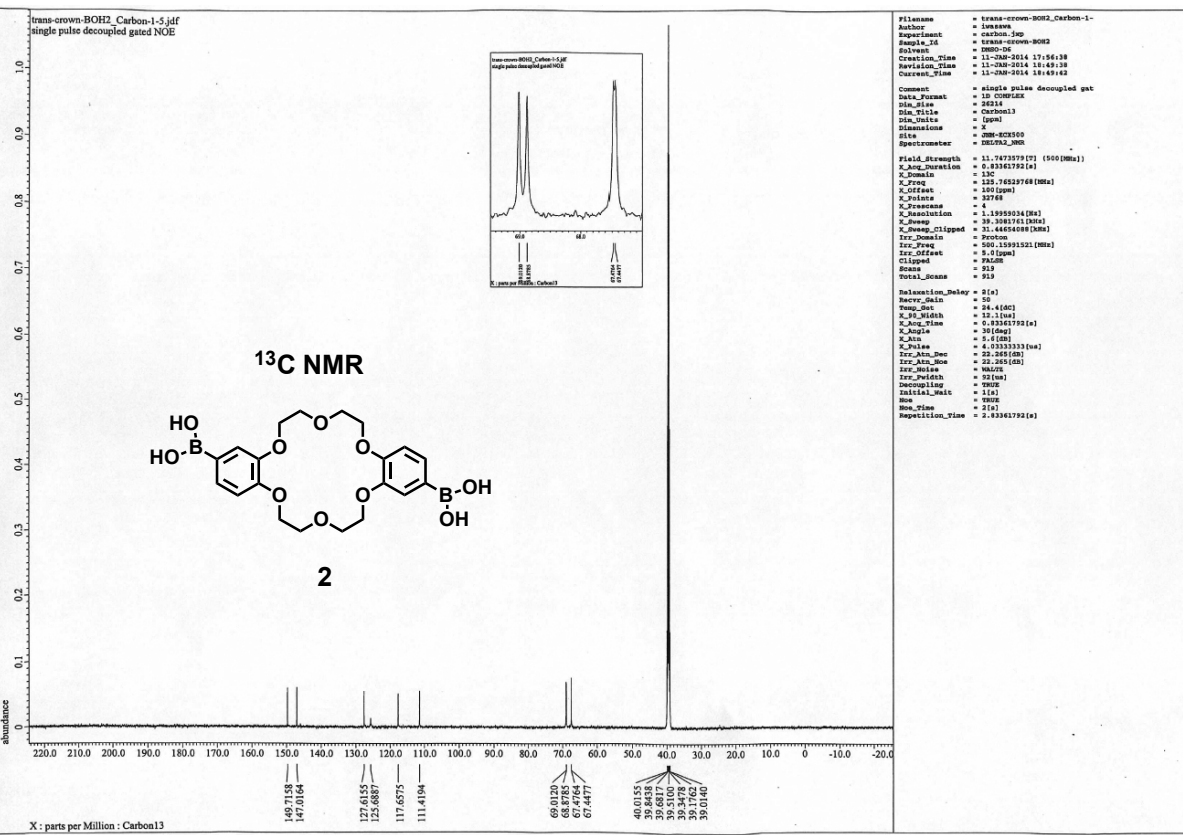
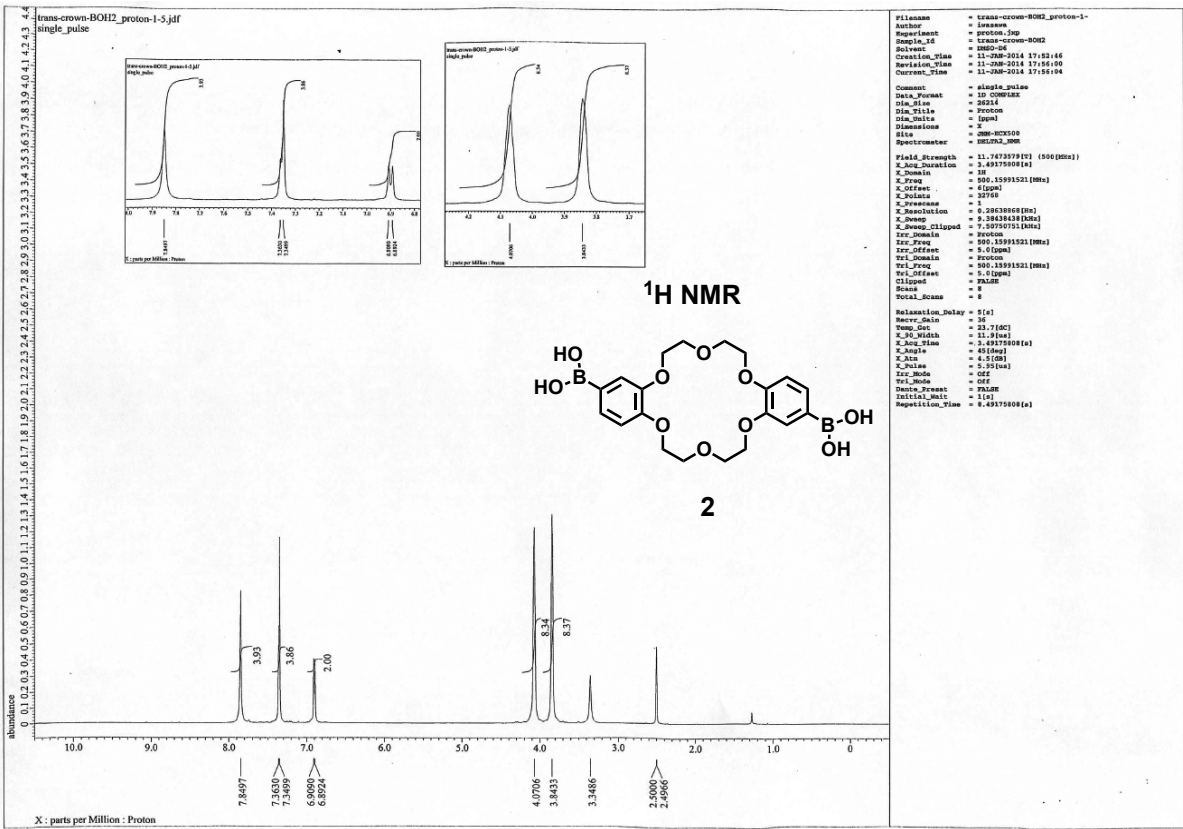












7. X-ray Crystallographic Analysis of a racemic crystal of [2+2]_{crow}

Single crystals, suitable for X-ray diffraction analysis, were obtained as racemic crystals from the mixture of equimolar amounts of macrocyclic boronic esters constructed by using **2** and (+)-tetrol or (-)-tetrol, respectively. Racemic crystals of [2+2]_{crow} were obtained by vapor diffusion method using a dichloromethane solution as a good solvent, and pentane as a poor solvent.

The single crystal X-ray diffraction data were collected on a Rigaku R-AXIS II with IP area detector using CuK α ($\lambda = 1.54186 \text{ \AA}$). The structure was solved by direct methods by *SHELXS*. The cage molecular structure of [2+2]_{crow} was obtained. The five dichloromethane molecules were included by [2+2]_{crow} (the site occupancy factors were 0.8, 0.8, 0.7, 0.4 and 0.65, respectively). And a dichloromethane molecule was outside the cage (the site occupancy factor is 0.4). The refinement was performed by full-matrix least squares using *SHELXL*-2014. Crystal structure of [2+2]_{crow}: C₇₂ H₈₀ B₄ O₂₀, 3.75(C H₂ Cl₂) $M_r = 1627.07$, Monoclinic, $P2_1/c$, $a = 18.3378(10) \text{ \AA}$, $b = 20.9587(10) \text{ \AA}$, $c = 22.0613(12) \text{ \AA}$, $\beta = 91.6688(18)^\circ$, $V = 8475.4(8) \text{ \AA}^3$, $D_{\text{calc}} = 1.275 \text{ g cm}^{-3}$, $T = 93(2) \text{ K}$, no. of unique reflections = 15473, $R_{\text{int}} = 0.1521$, no. of parameters = 1042, no. of restraints = 60, $R_1 = 0.1203$, $wR_2 = 0.3170$, $S = 0.893$ for 15473 reflections, max/min. residual density 0.757/-0.264 e \AA^{-3} . CCDC reference number 1541693.

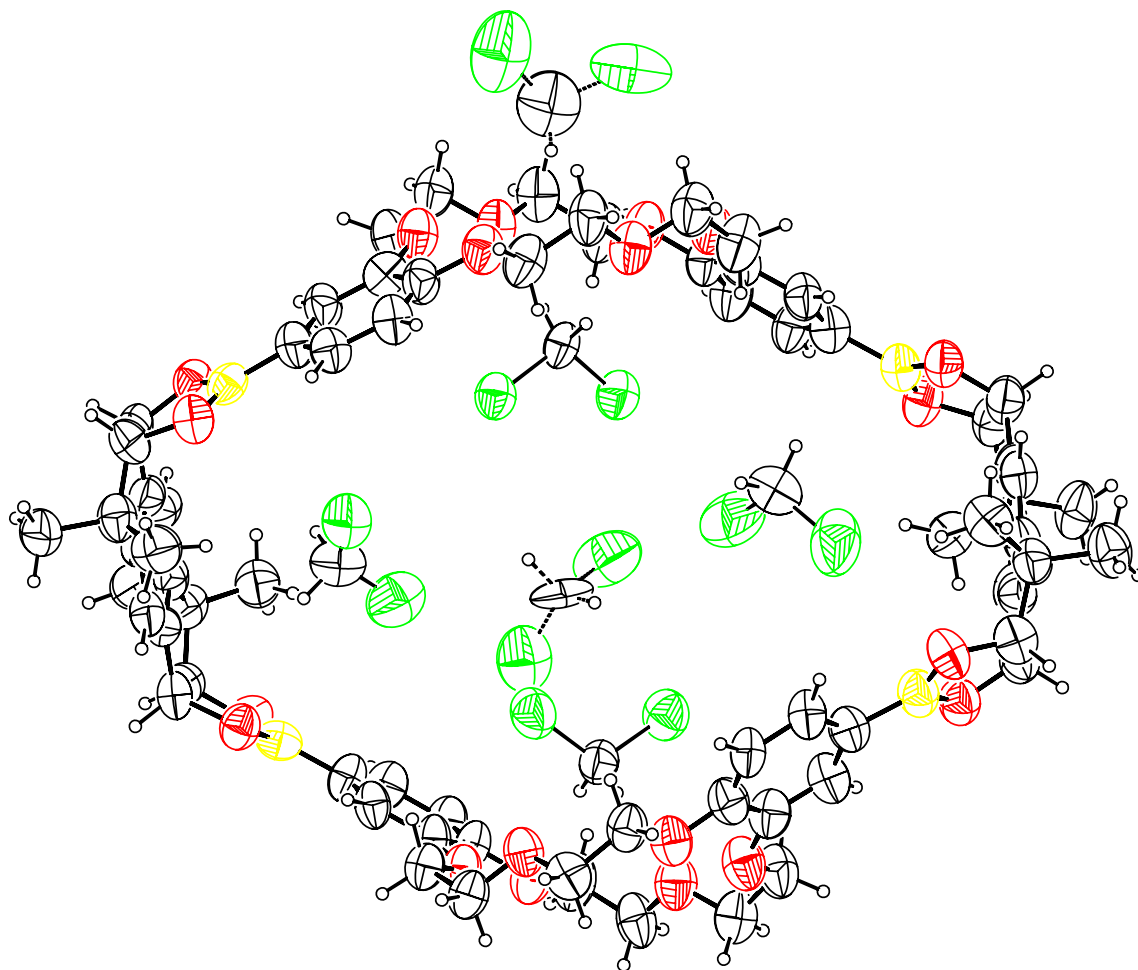


Fig. S29 ORTEP drawing (30% probability ellipsoids) of $[2+2]_{\text{crown}}$.

Table S3 Crystal data and structure refinement for [2+2]_{crwn}.

Empirical formula	C ₇₂ H ₈₀ B ₄ O ₂₀ , 3.75(CH ₂ Cl ₂)	
Formula weight	1627.07	
Temperature	93(2) K	
Wavelength	1.54186 Å	
Crystal system	Monoclinic	
Space group	<i>P</i> 2 ₁ / <i>c</i>	
Unit cell dimensions	<i>a</i> = 18.3378(10) Å. <i>b</i> = 20.9587(10) Å <i>β</i> = 91.6688(18)°. <i>c</i> = 22.0613(12) Å.	
Volume	8475.4(8) Å ³	
<i>Z</i>	4	
Density (calculated)	1.275 Mg/m ³	
Absorption coefficient	2.828 mm ⁻¹	
<i>F</i> (000)	3398	
Crystal size	0.150 x 0.110 x 0.090 mm ³	
Theta range for data collection	3.203 to 68.247°.	
Index ranges	-22 ≤ <i>h</i> ≤ 22, -25 ≤ <i>k</i> ≤ 24, -26 ≤ <i>l</i> ≤ 26	
Reflections collected	78205	
Independent reflections	15473 [<i>R</i> (int) = 0.1521]	
Completeness to theta = 67.686°	99.9 %	
Absorption correction	Semi-empirical from equivalents	
Max. and min. transmission	0.785 and 0.482	
Refinement method	Full-matrix least-squares on <i>F</i> ²	
Data / restraints / parameters	15473 / 60 / 1042	
Goodness-of-fit on <i>F</i> ²	0.893	
Final <i>R</i> indices [<i>I</i> > 2σ(<i>I</i>)]	<i>R</i> ₁ = 0.1203, <i>wR</i> ₂ = 0.3170	
<i>R</i> indices (all data)	<i>R</i> ₁ = 0.2748, <i>wR</i> ₂ = 0.4130	
Extinction coefficient	n/a	
Largest diff. peak and hole	0.757 and -0.264 e.Å ⁻³	

8. References

- S1) S. J. Bingham and J. H. P. Tyman, *J. Chem. Soc., Perkin Trans. 1*, 1997, 3637–3642.
- S2) (a) H. Sakurai, N. Iwasawa and K. Narasaka, *Bull. Chem. Soc. Jpn.*, 1996, **69**, 2585–2594; (b) S. Ito, K. Ono and N. Iwasawa, *J. Am. Chem. Soc.*, 2012, **134**, 13962–13965.
- S3) A. M. Ingham, C. Xu, T. W. Whitcombe, C. Xu, J. N. Bridson and A. McAuley, *Can. J. Chem.*, 2002, **80**, 155–162.
- S4) S. Sen, S. Singh and S. M. Sieburth, *J. Org. Chem.*, 2009, **74**, 2884–2886.